

FUEL AND MATERIAL BEHAVIOUR

(Session 8)

Chairperson

W. GOLL
Germany

INTEGRITY ASSESSMENT OF CANDU SPENT FUEL DURING INTERIM DRY STORAGE IN MACSTOR

J.W. LIAN
Atomic Energy of Canada Limited
Chalk River
Ontario
Canada

Abstract

This paper presents an assessment of the integrity of CANDU spent fuel during dry storage in MACSTOR. Based on review of the safety requirements for sheath integrity during dry storage, a fuel temperature limit for spent CANDU fuel stored in MACSTOR is specified. The spent fuel conditions prior to, and during dry storage are assessed. The safety margin for spent CANDU fuel stored in MACSTOR is assessed against various failure mechanisms using the probabilistic estimation approach derived from US LWR fuel data set.

1. INTRODUCTION

The high capacity Modular Air Cooled STORage (MACSTOR) system is an advanced storage system developed by Atomic Energy of Canada Limited (AECL) for the dry storage of spent fuel from CANDU[®] power reactors. A proven safe, efficient, flexible and economical technology, MACSTOR is selected for use in Canada, Romania, Korea and China for the construction of large-scale above-ground dry storage facilities for CANDU[®] spent fuel. The constructed capacity of these projects represents a significant share of the total worldwide dry storage capacity.

A typical CANDU fuel bundle is shown in Figure 1. Each of the 37 fuel elements contains natural UO₂ pellets in a Zircaloy-4 sheath, which forms the primary containment barrier for the fission products within the spent fuel.

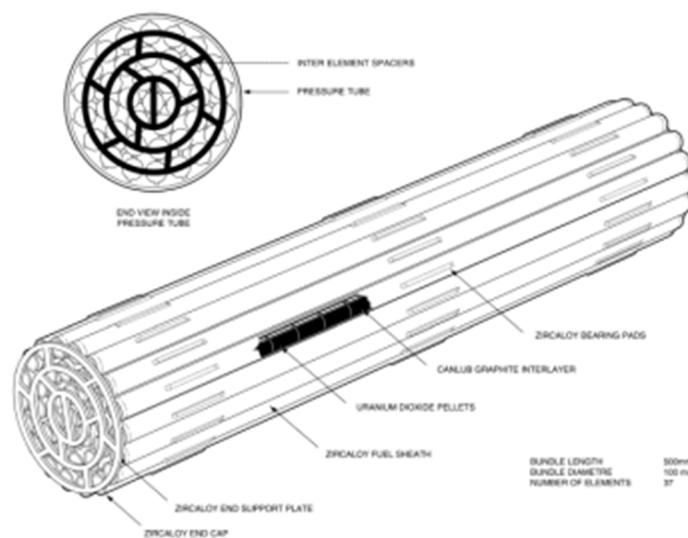


FIG. 1. A typical CANDU-6 fuel bundle.

The MACSTOR is a concrete monolith used to store fuel baskets filled with spent fuel bundles from the nuclear reactors. As shown in Figs 2–3, the fuel baskets are stored in storage cylinders laid in rows of ten, each storage cylinder holding ten fuel baskets¹. The storage module is cooled by air that is passively driven through a number of air inlets and outlets located on the longitudinal sides of the module.

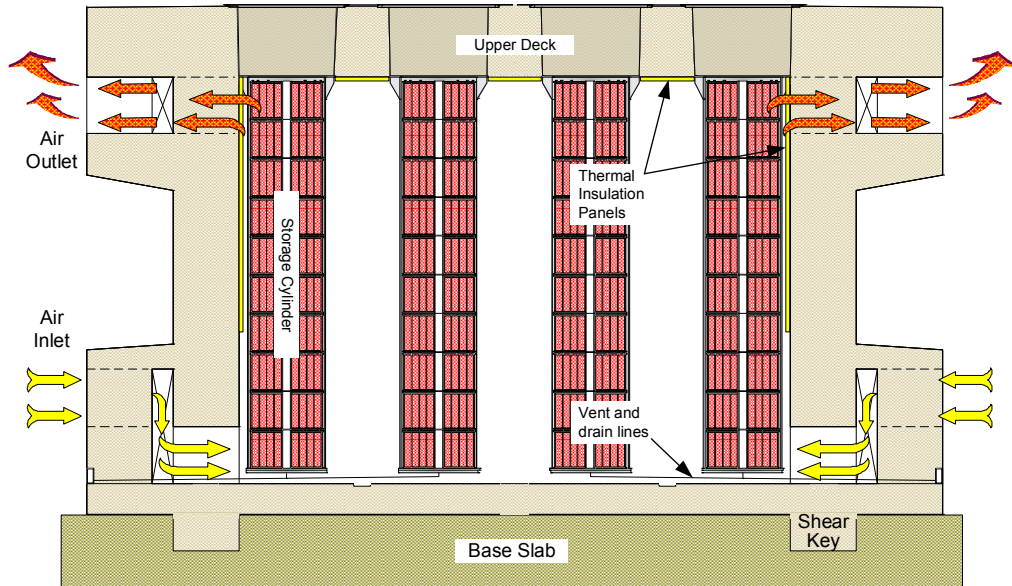


FIG. 2. Elevation view of a typical MACSTOR-400 module.



FIG. 3. MACSTOR-400 module at Qinshan, China.

¹ There are two sizes of MACSTOR modules. The MACSTOR-400 has 40 storage cylinders laid in four rows of ten each, holding a total of 400 fuel baskets per module. The smaller size, the MACSTOR-200 has 20 storage cylinders laid in two rows of ten for a total of 200 fuel baskets per module.

The fuel baskets, constructed of type 304L stainless steel, can each hold 60 fuel bundles. Once loaded in the storage pool, the fuel basket is drained, dried and weld sealed. The cover gas for the fuel bundles is air. After a storage cylinder is filled with 10 fuel baskets, a permanent shield plug is installed and seal welded. The weld-sealed baskets and storage cylinder provide a double containment system to the fuel bundle. The storage cylinders are equipped with a monitoring system, allowing monitoring for presence of humidity and absence of contamination in the storage cylinder internal air.

2. CANDU SPENT FUEL CHARACTERISTICS

The fuel management strategy for dry storage of fuel bundles adopted by CANDU stations is to maintain known or suspected damaged fuel in the pool and to only proceed with dry storage of intact fuel bundles. One of the fundamental safety requirements for the safe storage of the spent fuel is to ensure that the fuel sheath will be protected during storage against degradation that leads to gross failure of the spent fuel sheath. Factors that are critical to the performance of the spent fuel during dry storage include the characteristics of the spent fuel prior to dry storage, the maximum temperature and environment conditions of the spent fuel during the dry storage.

2.1. Characteristics of spent fuel prior to dry storage

2.1.1. *Burnup distribution of spent fuel bundles*

The average discharge burnup of the CANDU fuel bundle may reach 7,800 MWd/MtU. In the thermal analysis for MACSTOR, worst-case loading conditions with high-burnup fuel bundles (i.e., a bundle with burnup value exceeding 12,000 MWd/MtU) are assumed. Typically, over 99–99.9% of the bundles have burnup below 12,000 MWd/MtU.

2.1.2. *Heat release of fuel bundles*

The heat release of a fuel bundle decreases with time from the disintegration of its radionuclides. The decay heat data for a reference average burnup spent CANDU fuel bundle and a reference high-burnup bundle over time are shown in Table 1.

TABLE 1. REFERENCE HEAT DECAY WITH TIME FOR FUEL BUNDLES

Years of cooling (Completed)	Heat release average burnup bundle (7,800 MWd/MtU) (Watts)	Heat release high burnup bundle (12,000 MWd/MtU) (Watts)
6	6.08	9.76
8	4.89	7.62
10	4.43	6.81

2.1.3. *Fuel sheath stress*

The CANDU fuel element sheath is a closed thin-walled cylinder with an internal diameter of 12.24 mm and a wall thickness of 0.42 mm. At 40°C, a typical CANDU fuel element would have an internal pressure <0.2 MPa [1]. When the spent fuel is stored underwater, the sheath temperature would not exceed 40°C, and hence the hoop stress of the sheath can be estimated as being less than 2.92 MPa.

2.1.4. *Fission gas release*

To assess the fraction of fission gas released to the void inside the spent fuel, puncture tests on 33 fuel elements from 14 bundles were performed, and the fission gas was collected and analyzed [1]. The release fraction of stable xenon, which is representative of other stable or long-lived volatile fission products, was typically below 3%.

2.2. Operating conditions during dry storage

During dry storage, the higher fuel temperature would result in a series of changes in operating conditions significant to sheath integrity. Therefore, the “worst” conditions that would result in the maximum fuel temperature during dry storage should be assessed.

2.2.1. *Maximum fuel temperature during dry storage*

The following “worst” conditions are used for the calculation of the bounding fuel temperature during dry storage over the service life of the module:

First year of dry storage when the heat release rate of the spent fuel in the module is the highest;

The first summer is assumed to experience the warmest days of the summer recorded for the site when the ambient air temperature and the solar heat input to the module would be the highest;

Although less than 1% of CANDU spent fuel bundle may reach a burnup of 12,000 MWd/MtU, the following conservative fuel loading conditions are assumed:

- A hot basket would be loaded with seven high burnup bundles in a cluster each having a high heat release of 9.76 W, in addition to 53 average bundles;
- A hot cylinder would be loaded with three hot baskets at the top three positions of the cylinder, in addition to the other seven average baskets;
- The centre of the module would contain four hot storage cylinders forming a cluster.

Using the above “worst” conditions, the calculated maximum fuel temperature of the warmest bundle stored in a MACSTOR system located in warmer climate is typically below 150°C. A maximum fuel temperature of 150°C is used in the sheath integrity assessment in this paper².

² It should be emphasized that the use of fuel temperature of 150°C in this assessment is very conservative. Over the service life the fuel stored in a typical MACSTOR-400 module only reaches an average

2.2.2. Maximum internal gas pressure and sheath hoop stress during dry storage

As a typical CANDU fuel element would have an internal pressure <0.2 MPa at 40°C. Using the ideal gas law, the maximum internal gap pressure inside this fuel element and the sheath hoop stress at 150°C would be 0.27 MPa and 3.95 MPa, respectively.

3. SAFETY REQUIREMENT FOR SHEATH INTEGRITY DURING DRY STORAGE

3.1. IAEA safety requirements for sheath integrity

The following safety requirements related to the fuel sheath integrity during storage are specified in the IAEA Safety Series No. 116 [2]:

The spent fuel cladding shall be protected during storage against degradation that leads to gross ruptures, or the fuel shall otherwise be contained in such a manner that degradation of the fuel during storage will not pose operational safety problems (Article 223).

The heat removal capability shall be such that the temperature of all fuel (and fuel cladding) in a storage facility does not exceed the maximum temperature recommended or approved by the national nuclear Regulatory Body for the type and condition of fuel to be stored (Article 225).

3.2. US NRC safety requirements for sheath integrity

The United States Nuclear Regulatory Commission (US NRC) imposes a more quantitative acceptance criterion on the sheath integrity during storage of spent nuclear fuel as below [3]:

For each fuel type proposed for storage, the DCSS³ should ensure a very low probability (e.g., 0.5 percent per fuel rod) of cladding breach during long-term storage.

As the design life of the dry storage system in the US is restricted to 20 years [3], the above criteria can be conservatively translated as a sheath failure rate of 1.0 percent per fuel rod in 100 years of storage, which is used in this paper as the target failure limit for the CANDU spent fuel during dry storage.

3.3. Fuel temperature limits for intact CANDU fuel stored in MACSTOR

To provide a qualitative assessment of sheath integrity of the spent CANDU fuel during dry storage in MACSTOR, in terms of maximum fuel temperature limits associated with Zircaloy sheath failure probabilities, the EPRI-NP-6387 document [4] is used as the basis for the assessments in this paper.

The Reference [4] establishes the maximum allowed fuel temperatures during dry storage corresponding to different allowed sheath failure probabilities for spent fuel rods from pressurized light water reactors (LWR) during 100 years of dry storage, based on a database of LWR fuel rods. For storage in air, the main results of EPRI-NP-6387 are:

temperature of approximately 85°C. For assessing sheath degradation over the entire service life of the module, using a time-averaged fuel temperature would be more realistic.

³ DCSS stands for Dry Cask Storage System in Reference [3].

Creep-rupture and external oxidation should not cause failure at storage temperatures below 300°C;

For storage temperatures below 300°C, stress-corrosion cracking (SCC) is the limiting mode, but is unlikely to occur to any large extent in dry storage fuel;

Fatigue is not a limiting failure mechanism for stored fuel sheath;

Splitting of sheath by UO₂ oxidation is a limiting mode only with defected fuel.

In comparison with the CANDU spent fuel, the LWR spent fuel is characterized with much higher fuel burnup, larger fission product inventory and higher release rate to the void. Therefore, for a given storage temperature the LWR fuel is expected to be more susceptible to sheath failure than the CANDU fuel during dry storage. This is because:

The LWR fuel sheath would be exposed to higher concentration of the corrosive fission gas, and

The LWR fuel sheath would be subjected to a much higher driving force (hoop stress) for sheath failure.

Therefore, the failure probabilities derived in [4] for LWR fuel is conservative for the CANDU fuel.

The fuel temperature limit for dry storage of intact spent CANDU fuel in MACSTOR is 300°C. As shown in [4], with a fuel temperature below 300°C, the failure modes of creep rupture and external oxidation would not play any significant role, and the limiting failure mode would be SCC. Corresponding to a fuel temperature of 300°C, reference [4] shows a failure rate of about 0.1% per rod over 100 years of dry storage, which is 10 times smaller than the target criteria of 1.0% per fuel rod in 100 years of storage.

Note that the failure rate of 0.1% per rod over 100 years is predicted for the LWR fuel, and is based on LWR fuel database. The actual failure rate for the CANDU fuel corresponding to 300°C would be even lower; hence additional conservatism is provided.

4. SHEATH INTEGRITY ASSESSMENT

4.1. Sheath failure by creep rupture and by external oxidation

Below a storage temperature of 300°C, the creep rate and the external oxidation rate of the Zircaloy sheath are so low that the probability of sheath failure by creep rupture and by sheath oxidation would be very small [4]. With a maximum fuel temperature of 150°C and a time-averaged temperature below 85°C, the spent CANDU fuel stored in MACSTOR would have a negligible probability of sheath failure by creep rupture and external oxidation.

4.2. Sheath failure by SCC

At storage temperatures below 300°C, SCC is the limiting failure mode for the Zircaloy sheath during dry storage.

For a maximum fuel temperature of 150°C, the probability of sheath failure for the LWR fuel in 100 years dry storage is estimated to be about 0.01% per rod [4]. This failure rate is 100 times lower than the target criteria of 1.0% per fuel rod in 100 years of storage. For the spent CANDU fuel stored in MACSTOR, the failure rate would be even lower due to the conservatism applied.

4.3. Failure by fatigue

The spent fuel sheath may fail by fatigue if it is subjected to a very large number of repeated cyclic loading. For the spent fuel in dry storage, the only credible situations that could result in cyclic loading are:

During fuel transportation, or

During an earthquake when in dry storage.

Evaluation of the sheath behaviour under these two conditions [4] concluded that large incipient cracks are stable under the dynamic stresses calculated during transportation or a magnitude 6.75 earthquake. Furthermore, the number of cycles required for any realistically sized crack to grow to failure exceeded the anticipated number of cycles by a factor of 200 or greater. Reference [4] concluded that fatigue is not a limiting failure mechanism for stored fuel sheath.

Therefore for the spent CANDU fuel stored in MACSTOR, fatigue is not considered as a credible failure mode for the fuel sheath.

4.4. Failure by UO₂ oxidation

When air is used as cover gas, the UO₂ pellets in a failed Zircaloy sheath could split the sheath open if oxidation at elevated temperatures were allowed to convert UO₂ to U₃O₈. However, oxygen can enter the fuel rod only through an existing defect; failure cannot be initiated by this mechanism for an intact fuel rod. Therefore UO₂ oxidation is not considered a credible failure mechanism for the *intact* spent CANDU fuel stored in MACSTOR.

Although, the transfer to dry storage of known defected fuel bundles is not purposely made, there remains a possibility that a bundle with a small undetected rod failure is transferred to dry storage. The low operating temperatures of the MACSTOR module still ensure that such a bundle would not further deteriorate during storage [5].

5. SAFETY MARGIN ASSESSMENT

A maximum allowable fuel temperature of 300°C is specified for the dry storage of spent CANDU fuel in MACSTOR. At 300°C, the sheath failure rate by SCC is about 0.1% per rod in 100 years of storage, which is 10 times lower than the target criteria of 1.0% per fuel rod in 100 years of storage. Hence this maximum allowable fuel temperature of 300°C leaves significant safety margin.

Under the credible most severe conditions, a few individual fuel bundles stored in MACSTOR may reach a maximum temperature of 150°C for a short period of time. Therefore, there is a 150°C temperature margin against the temperature limit. Assuming conservatively that the fuel rods stay at 150°C all the time, the failure rate, according to [4],

would be about 0.01% per rod in 100 years, which is 100 times lower than the target criteria of 1.0% per fuel rod in 100 years of storage.

The fuel operating temperature over the service life of the facility decreases with time as the fuel slowly reduces its heat release. Over the period, and considering the daily and seasonal temperature variations, the average fuel temperature is approximately 85°C, providing a very large temperature margin of 215°C. Using this time-averaged fuel temperature of 85°C would result in a more realistic failure rate of 0.001% per rod in 100 years, which is 1000 times lower than the target criteria of 1.0% per fuel rod in 100 years of storage.

As has been demonstrated in Section 3.3, the spent CANDU fuel is less susceptible to SCC than the LWR fuel; hence the actual failure rate for the CANDU fuel would be even lower than the value quoted above.

Therefore, it can be concluded that:

- The temperature of the fuel stored in MACSTOR would have at least 150°C of margin against an already very conservative temperature limit, and
- The failure rate of the spent CANDU fuel stored in MACSTOR would be at least three orders of magnitude lower than the target limit based on the US NRC document NUREG-1536 for dry storage of spent LWR fuel in the US.

6. DISCUSSION AND CONCLUSION

The above sections have demonstrated that:

- The characteristics of the spent CANDU fuel would inherently dictate that it will be more robust during dry storage than the spent LWR fuel due to:
 - Lower heat release rate and lower operating temperature;
 - Lower sheath stress;
 - Lower concentration of the corrosive fission gas.
 Hence the failure rate estimation in Reference [4], which was derived based on LWR characteristics, would be conservative for the spent CANDU fuel;

The design of the MACSTOR ensures the spent fuel will be stored at low storage temperature such that there would be ample safety margin even when the results of Reference [4] are conservatively applied to the CANDU fuel;

Under the credible most severe conditions, there would be a temperature margin of at least 150°C, against a conservative temperature limit of 300°C. Therefore the following IAEA requirement:

“The heat removal capability shall be such that the temperature of all fuel (and fuel cladding) in a storage facility does not exceed the maximum temperature recommended or approved by the national nuclear Regulatory Body for the type and condition of fuel to be stored.” is met;

Under the credible most severe conditions, the predicted failure rate of the spent CANDU fuel stored in MACSTOR would be three orders of magnitude lower than the target criteria based on [3] for LWR spent fuel. There is no identifiable degradation mechanism that could lead to gross rupture of the sheath. Even in the very unlikely event of a fuel failure, two more

barriers, namely the fuel basket and the storage cylinder, would ensure that the fission product released from the fuel be contained. Therefore the following IAEA requirement:

“The spent fuel cladding shall be protected during storage against degradation that leads to gross ruptures, or the fuel shall otherwise be contained in such a manner that degradation of the fuel during storage will not pose operational safety problems.” is met.

In conclusion, intact fuel bundles will be safely stored in the MACSTOR with ample safety margin.

REFERENCES

- [1] WASYWICH, K.M., “Examination of Spent CANDU Fuel following 27 Years of Pool Storage”, EPRI report, TR-100674, Electric Power Research Institute, (1992).
- [2] INTERNATIONAL ATOMIC ENERGY AGENCY, “Design of Spent Fuel Storage Facilities”, IAEA Safety Series No. 116, International Atomic Energy Agency, (1994).
- [3] U.S. NUCLEAR REGULATORY COMMISSION, “Standard Review Plan for Dry Cask Storage Systems, Final Report”, USNRC document NUREG-1536, U.S. Nuclear Regulatory Commission, (1997).
- [4] MILLER, A.K., et al., “Estimates of Zircaloy Integrity During Dry Storage of Spent Nuclear Fuel”, EPRI (Electric Power Research Institute) EPRI-NP-6387/1989 (1989).
- [5] BEAUDOIN, R., “Evaluation of Safety Margins during Dry Storage of CANDU Fuel in MACSTOR/KN-400 Module”, Canadian Nuclear Society, 6th International Conference on Simulation Methods in Nuclear Engineering 2004, (2004).

CHALLENGE TO OVERCOME THE CONCERN OF SCC IN CANISTER DURING LONG-TERM STORAGE OF SPENT FUEL

T. SAEGUSA*, J. TANI**, T. ARAI**, M. WATARU*, H. TAKEDA*, K. SHIRAI*

* Civil Engineering Laboratory, CRIEPI
Abiko, Chiba

** Materials Science Laboratory, CRIEPI
Yokosuka, Kanagawa
Japan

Abstract

In order to put the concrete cask in practical use in Japan (an island country), stress corrosion cracking (SCC) of canister must be coped with. It is required to take measures for one or two of the three factors, i.e. welding residual stress, material, and environment, to cope with the SCC that may result in loss of the containment function of the canister. Prevention of loss of containment due to SCC of a canister was evaluated either by a method of comparing the amount of salt on the canister surface during storage with the minimum amount of salt to initiate rust and SCC or by a method of comparing the wetting time of the canister surface under salty-air field environment with the lifetime of the SCC fracture of the canister material. Although the use of highly corrosion-resistance stainless steel is one solution, it brings about a cost rise of the concrete cask storage. In order to suppress the cost rise, it should be evaluated whether the measure against SCC of the normal stainless steel is possible by reducing welding residual stress. In addition, technology should be developed to reduce salt particles in the air flowing into the storage facility and concrete cask.

1. INTRODUCTION

In Japan, spent nuclear fuel exceeding the reprocessing capacity is being generated with progress of nuclear power generation, and the needs of spent fuel storage are growing more and more. Although the spent fuel storage by metal casks is putting in practical use until now, utilization of alternative storage method, i.e. the concrete cask is also needed from viewpoints of risk management of cask procurement and economical advantage. Since Japan is surrounded by the sea, stress corrosion cracking (SCC) of welded stainless steel canisters in the concrete cask storage system should be evaluated and coped with. The canister shall not lose its containment function due to SCC during long-term storage. The SCC occurs when a stainless steel with welding residual stress is exposed to salty air environment as shown in Figure 1. It is required to take measures for one or two of the three factors, i.e. welding residual stress, material, and environment, to cope with the SCC that may result in loss of the containment function of the canister. We evaluated prevention of loss of containment due to SCC of a canister either by comparing the amount of salt on the canister surface during storage with the minimum amount of salt to initiate rust and SCC, or by comparing the wetting time of the canister surface under field environment with the lifetime of the SCC fracture of the canister material. We found the use of highly corrosion-resistance stainless steel could prevent SCC. However, it brings about a cost rise of the concrete cask storage. In order to suppress the cost rise, we should develop alternative measure against SCC, possibly by reducing welding residual stress of the normal stainless steel canister. In addition, technology should be developed to reduce salt particles in the air flowing into the storage facility and concrete cask.

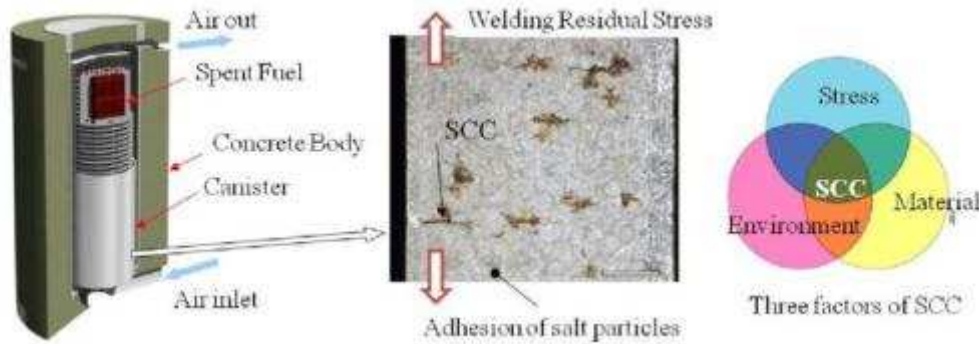


FIG. 1. Phenomenon of SCC in concrete cask storage.

2. METHOD [1]

2.1. SCC Evaluation based on critical salt concentration on canister surface

The SCC due to chloride is preceded by local corrosion such as pitting or crevice corrosion prior to initiation of cracking. In the atmospheric environment, this local corrosion accompanies rust formation on the surface. We could assume no SCC generates without rust formation on the surface by visual observation. Rust formation or SCC initiation will start when the surface chloride quantity (density) exceeds the critical value. Such critical chloride density will be obtained through parametric material testings as a function of chloride density on the surface of the canister material.

2.1.1. Materials [2][3]

Specimen materials were normal stainless steels (SUS 304L and SUS 316L) and highly corrosion-resistant stainless steels (SUS329J4L and YUS 270) as shown in Table 1.

TABLE 1. SPECIMEN MATERIALS FOR SCC TESTING

	C	Si	Mn	P	S
UNS S30403 (SUS304L)	<0.030	<0.75	<2.00	<0.045	<0.030
UNS S31260 (SUS329J4L)	<0.030	<0.75	<1.00	<0.030	<0.030
UNS S31254 (YUS270)	<0.020	<0.80	<1.00	<0.030	<0.010
	Cu	Ni	Cr	Mo	N
UNS S30403	–	8.00–12.00	18.00–20.00	–	<0.10
UNS S31260	0.20–0.80	5.50–7.50	24.00–26.00	2.50–3.50	0.10–0.30
UNS S31254	0.50–1.00	17.50–18.50	19.50–20.50	6.00–6.50	0.18–0.22

(wt%)

2.1.2. Rust Initiation Test [2–3]

Specimens made of the above materials were prepared with the size of 75 mm × 75 mm × 2 mm. The surface was polished with wet polishing paper number 600 and ultrasonically cleaned with acetone. The test conditions (temperature/relative humidity) were determined as follows:

50°C/35%RH, 60°C/25%RH, 70°C/15%RH, 80°C/15%RH.

According to the meteorological data in Japan, the highest absolute humidity will be 30g/m^3 . Such air with the humidity was assumed to enter to the canister surface whose temperature is between $50\text{--}80^\circ\text{C}$. With those conditions, relative humidity on the canister surface was calculated to result in the above test conditions.

Synthetic sea water with pH8.2 was sprayed on the specimen surface that was heated to approximately 80°C , according to the Methods of salt spray testing (JIS Z 2371 (2000)). The salt concentration on the surface was in a range of $0.1\text{--}10\text{ g/m}^3$.

We defined rust initiation is a phenomenon that the areal ratio of the rusted surface exceeded 0.02%. We referenced the Rating Number Method (Appendix 1 to JIS Z2371 (2000)).

2.1.3. SCC Initiation test [2–3]

Specimens made of SUS 329J4L and YUS270 in Table 1 were prepared with a size as shown in Fig. 2. The specimens were subjected to a constant load as shown in Fig. 3 and placed in a chamber of a constant temperature and humidity. Chlorides were sprayed on the stressed area of the specimens similarly at the rust initiation tests. Initiation of SCC was confirmed by a scanning microscope. We defined SCC initiation is a phenomenon that a cracking was found from pitting corrosion, etc.

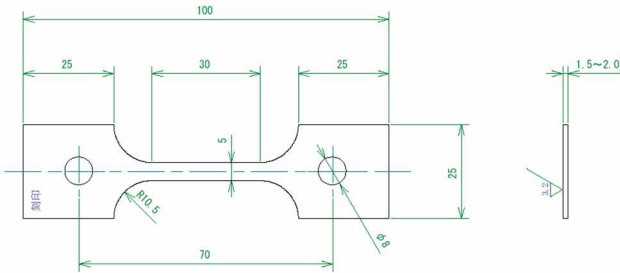


FIG. 2. Tensile specimen for SCC initiation test.

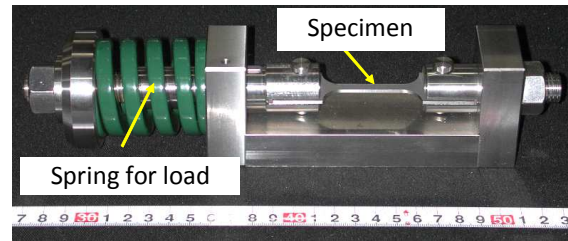


FIG. 3. Outlook of SCC initiation test device.

2.1.4. Salt deposition test [2, 4]

To evaluate the rust initiation and rust initiation, it is important to estimate the salt accumulation transported by salty cooling air on the metal canister surface. The cooling air goes up along the canister surface in the concrete cask. The salt particles in the air may collide with the surface by the diffusion and turbulence effect. To measure the deposition velocity, the CRIEPI performed two kinds of tests. One was a laboratory test and the other was a field test. From those tests, amount of salt deposition was estimated by the following equation.

$$Q = 5.07(t \times C/10000 \times 1.55)^{1/2} \quad (1)$$

where Q: amount of salt deposition, t: time (h), C: Salt concentration in the air ($\mu\text{g/m}^3$ as Cl).

Temperature dependence of the salt deposition was given by the following equation.

$$Q = \{5.07 - 0.022(T - 30)\} (t \times C/10000 \times 1.55)^{1/2} \quad (2)$$

where T: temperature of the canister surface ($^\circ\text{C}$)

Temperature decay of the canister with elapsed time was expressed by the following equation.

$$T = -0.575X + 89 \quad (3)$$

where X: time (year).

Using equations 1–3, salt deposition on a canister surface will be estimated as a function of time.

2.2. SCC Evaluation based on humid period of time during storage [5]

The SCC will not initiate on a dry surface of the canister. Moderate relative humidity (RH) is necessary to deliquesce (moisten) the chlorides adhering to the canister surface and to initiate crack as shown in Fig. 4. Therefore, the SCC initiates only during a humid period of time during storage. On the other hand, SCC failure time of canister material in the humid environment is experimentally obtained. We can evaluate if the canister material will initiate SCC during storage by comparing the humid period of time and the SCC failure time of the canister material.

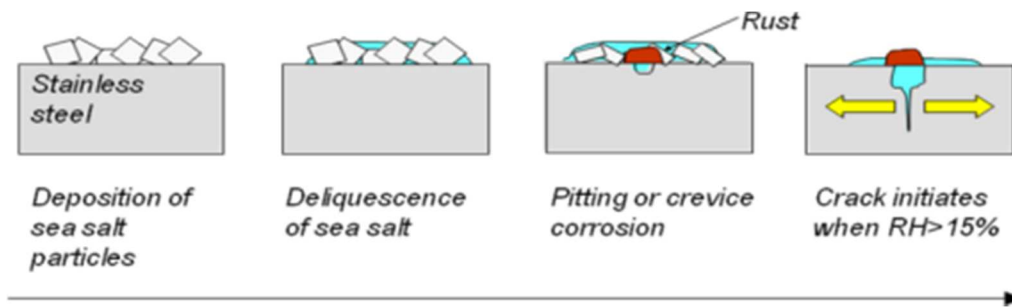


FIG. 4. Process of SCC initiation on canister surface during storage.

2.2.1. Estimation of humid period of time

The relative humidity at which the SCC can easily initiate (RHL) is dependent on the types of chlorides. The RH_L value for the synthetic sea salt is reportedly 15%. Relative humidity of the canister surface depends on the surface temperature and the absolute humidity of the environment. The canister surface temperature is calculated from decay heat analysis of the concrete cask system. The absolute humidity of the environment is estimated from the metrological record of the particular site. From these data, a period of time for crack initiation on the canister surface in a concrete cask at a particular site is calculated.

2.2.2. Experiment to obtain SCC failure time of canister material

The specimen materials were SUS304L, SUS329J4L and YUS270 shown in Table 1. The specimens shown in Fig. 2 and test device in Fig. 3 were used to obtain SCC failure time of the materials.

Applied stresses were $0.5\text{--}1.2 \times 0.2\%$ proof stress (610MPa at room temperature) of SUS329J4L, $0.5\text{--}1.5 \times 0.2\%$ proof stress (370MPa at room temperature) of YUS270, and $0.5\text{--}1.7 \times 0.2\%$ proof stress (284MPa at room temperature).

Synthetic sea water of 10 μ liter each was dropped repeatedly and dried (50 μ liter in total) on the specimen surface so that the surface concentration of the salt will be 10g/m².

The temperature was 80°C and the relative humidity was 35%.

2.3. Salt particle collection test

Sofar, the above mentioned tests aimed to solve the issue of SCC by the selection of highly corrosion resistant materials. Theoretically, the SCC issue could be prevented by dealing with either one of the three factors for SCC. However, it would be recommended to take another preventive measure to deal with the SCC. In addition to the measure of improving material, we have challenged to improve environment of concrete cask. The idea is to reduce salt concentration (particles) in the salty air. Fig. 5 is an example of salt particle collection device that is installed at the air-inlet of a storage building. The mechanism is to absorb salt particles on a water surface that is flowing on multiple layers of tray attached at the air-inlet of the storage building. The rainwater may be supplied naturally from the building roof and led to the trays. The salty air enters from the outdoor and flows on the surface of the watered trays. The salt particles in the salty air will be naturally absorbed into the rain water. We have made tested this salt particle collection device both in a laboratory and at outdoor near seashore. Fig. 6 shows types of the salt collection device, and Type-A (4 trays) and Type-C (8 trays) were employed both in the laboratory test and outdoor test.

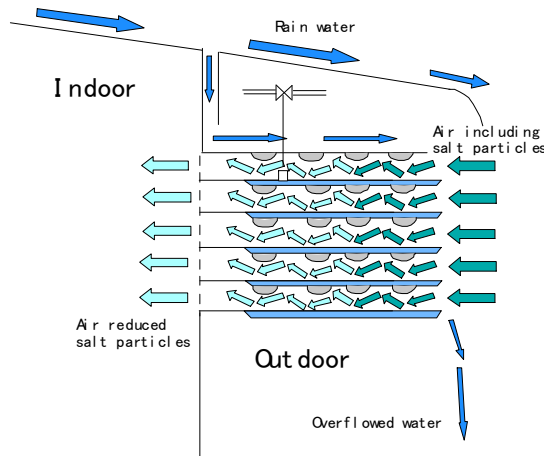


FIG. 5. Salt particle collection device.

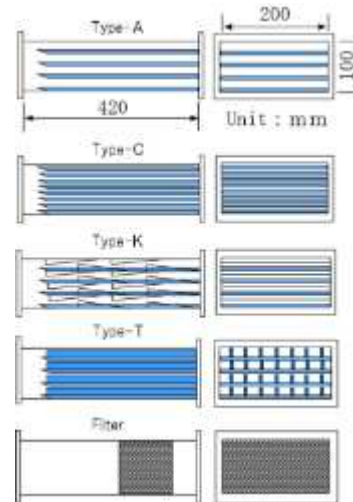


FIG. 6. Types of salt collection device.

3. RESULTS [1]

3.1. SCC Evaluation based on critical salt concentration on canister surface

3.1.1. Rust initiation and SCC initiation [2–3]

Fig. 7 shows threshold chloride density for rust initiation of various stainless steels. Fig. 8 shows threshold chloride density for SCC initiation of various stainless steels.

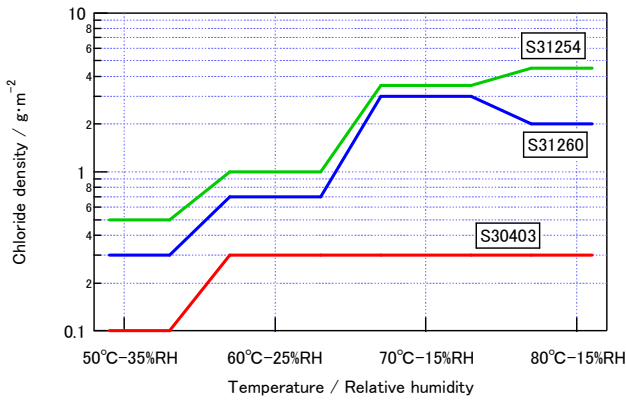


FIG. 7. Threshold chloride density for rust initiation of various stainless steels.

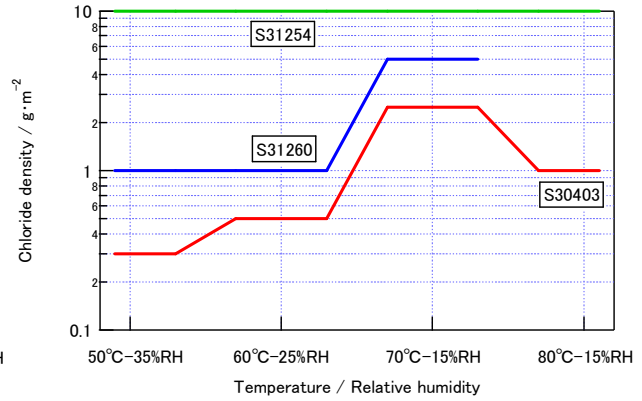


FIG. 8. Threshold chloride density for SCC initiation of various stainless steels.

3.1.2. Salt Deposition on canister surface[2,4]

Table 2 shows an example of calculated result on time to rust initiation and the time to SCC initiation for normal stainless steel (SUS 304L) and highly corrosion resistance stainless steels (SUS 329J4L and YUS 270). The minimum amount of salt for rust initiation and SCC initiation in Table 2 were experimentally obtained. The time to reach the minimum amount of salt for rust initiation and SCC initiation was obtained with an empirical equation for the salt deposition tests on a vertical surface of the heating canister in the concrete cask.

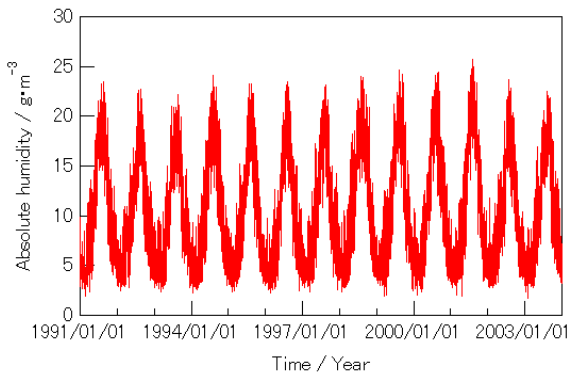


FIG. 9. Absolute humidity measurement at a central-east coast of the Japan island.

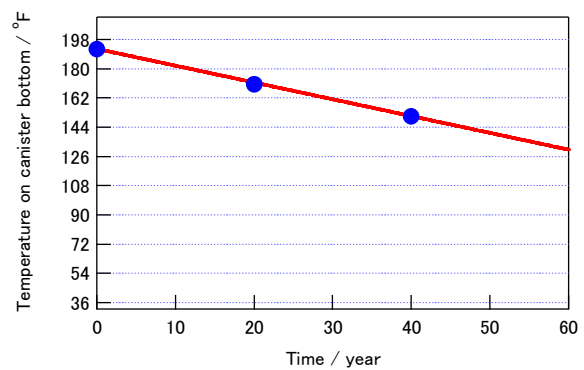


FIG. 10. Temperature decay on the canister bottom in the concrete cask.

TABLE 2. EXAMPLE OF CALCULATION OF TIME FOR RUST INITIATION AND SCC INITIATION IN CONVENTIONAL AND SCC RESISTANT STAINLESS STEELS

material	Minimum amount of salt for rust initiation (g/m ²)	Time to reach the minimum amount of salt for rust initiation (year)		Minimum amount of salt to initiate SCC (g/m ²)	Time to reach the minimum amount of salt for SCC initiation (year)	
		Salt concentration in air ^{*1} = 10μg/m ³	Salt concentration in air = 20μg/m ³		Salt concentration in air = 10μg/m ³	Salt concentration in air = 20μg/m ³
SUS 304L	0.1	40 y	22 y	0.3	250 y	130 y
SUS 329J4L ^{*2}	0.3	250 y	130 y	1	700 y and over	350 y and over
YUS 270 ^{*3}	0.5	700 y	350 y	10 and over	700 y and over	350 y and over
*1: A typical salt concentration in air at 400m from the sea is 16μg/m ³ .						
*2: Ni 18%, Cr 20%, Mo 6%, and Fe. *3: Equivalent to ASTM S31254. Ni 7%, Cr 26%, Mo 3%, and Fe.						

3.2. SCC Evaluation based on humid period of time during storage [5]

Fig. 9 shows absolute humidity at a central-east coast of the Japan Island measured from 1991–2003. Fig. 10 shows analytical result of temperature change on the canister bottom in the concrete cask system with elapsed time. From the results of Fig. 9 and Fig. 10, relative humidity at the bottom of the canister was obtained with elapsed time, as shown in Fig. 11. Fig. 11 indicated a humid period of time in which the relative humidity exceeds 15% is approximately 15,000 hours during the storage period of 60 years. Fig.12 shows results of SCC failure time of the canister materials.

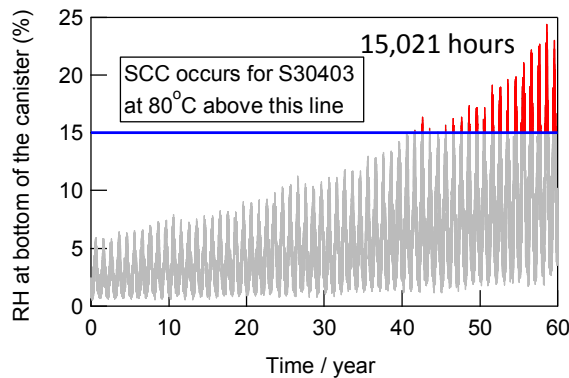


FIG. 11. Relative humidity change at the canister bottom with elapsed time indicating the humid period of time (15,012 hours).

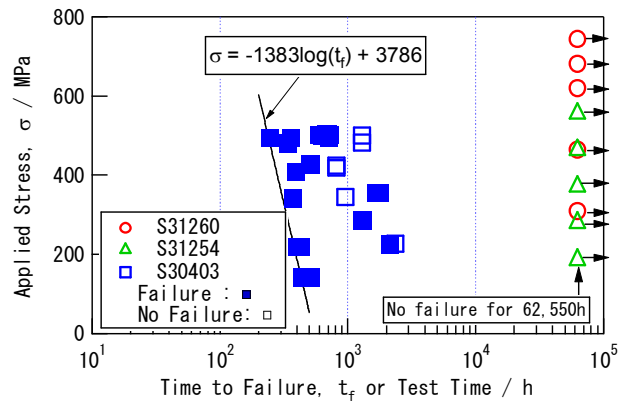


FIG. 12. SCC failure time of the canister materials indicating no failure of highly corrosion resistant materials for 62,550 hours.

3.3. Salt particle collection test [6]

We have started the salt particle collection performance tests to evaluate the effectiveness of such device from 2007. Fig.13 shows one of the results of the salt particle collection tests. The efficiency in the outdoor test became higher than in the indoor test. Specifically, the high efficiency was obtained with Type-C.

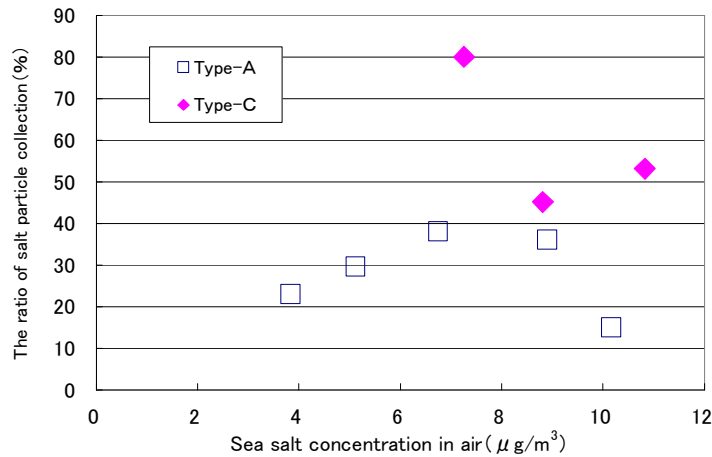


FIG.13. Relation between the sea salt concentration in air and the efficiency of salt particle collection.

4. DISCUSSION

Table 2 indicated the rust initiation and SCC initiation in the storage period of about 60 years would be prevented by the selection of highly corrosion resistance stainless steel. More realistic evaluation will be made based on the site specific conditions. Similarly, Fig. 10 and Fig. 11 indicated that SCC failure would be prevented by the selection of the highly corrosion resistant materials.

Although the above-mentioned measure against SCC by use of the highly corrosion resistance stainless steels is one solution, it brings about a cost rise. Authors are promoting a new research program on the alternative measure against SCC which will suppress the cost rise. That is, using a realistic environmental data (actual measurement of salt concentration in the air) and reducing the welding residual stress by Low Plasticity Burnishing method, the measure against SCC of SUS 304 steel will be demonstrated.

The effectiveness of the salt particle collection device is highly expected. To get more assurance it would be necessary to obtain more data.

5. CONCLUSION

The concern of SCC in the canister of the concrete cask during long-term storage of spent fuel on sites near seashore will be overcome by the selection of highly corrosion resistant materials.

In order to improve the economy of the preventive measures for SCC issues of the concrete cask storage, a new research program is going on by the use of normal stainless steel with reduced residual stress along the welding.

Reducing the salt concentration in the air can be expected by use of the salt particle collection device attached to air-inlet of storage building or to air-inlet of concrete casks.

ACKNOWLEDGEMENTS

This research was conducted partially under the contract of MITI/NISA of the Japanese Government.

REFERENCES

- [1] SAEGUSA, T. et al, Development of Concrete Cask Storage Technology for Spent Nuclear Fuel, CRIEPI Report N09 (May 2010), (In Japanese).
- [2] CRIEPI, Report of Investigation on Storage Technology of Recyclable Fuel Resource (Long-term Integrity of Storage Facility) to METI of the Japanese Government (March 2009) (In Japanese. Available at the METI library and the National Diet Library of Japan).
- [3] TANI, J., MAYUZUMI, M., HARA, N., Initiation and Propagation of Stress Corrosion Cracking of Stainless Steel Canister for Concrete Cask Storage of Spent Nuclear Fuel, Corrosion, Vol. 65, No.3, (2009) 187–194.
- [4] WATARU, M., et al, Research on Spent Fuel Storage in CRIEPI (Part 2 Concrete Cask), Proc. 2008EAFORM in Tokyo.
- [5] TANI, J., MAYUZUMI, M., Stress corrosion cracking of canister materials for storage of spent nuclear fuel (Vol.2) – An evaluation on the possibility of SCC initiation – CRIEPI Report Q08007 (2009) (in Japanese).
- [6] TAKEDA, H., et al, Development of Salt Particle Collection Device to Prevent SCC of Canisters, Proc. The 17th Int'l Conf. Nuclear Eng., ICONS 17, Brussels, Belgium (2009).

DEMONSTRATION TEST PROGRAM FOR LONG-TERM DRY STORAGE OF PWR SPENT FUEL

M. YAMAMOTO*, T. FUJIMOTO*, K. SHIGEMUNE*, H. MATSUO***, T. MATSUOKA****, D. ISHIKO****

*The Japan Atomic Power Company

Tokyo,

**The Kansai Electric Power Co., Inc.

Osaka,

***Kyusyu Electric Power Co., Inc.

Fukuoka

****Mitsubishi Heavy Industries, Ltd.

Kobe

Japan

Abstract

In Japan, interim storage in multipurpose dry metal casks for maximum 50 years is planned for management of spent fuel until reprocessing. In the interim storage, cladding integrity of spent fuel will be maintained and safety of transportation will be ensured after the storage based on the knowledge and experience concerning integrity of spent fuel during dry storage in Japan and overseas. To ensure safety of transportation after storage, some of Japanese electric companies (The Japan Atomic Power Company, The Kansai Electric Company and Kyusyu Electric Company (hereinafter called “the utilities”)) are planning to conduct a long-term storage test of PWR spent fuel assemblies, which have not been used for dry storage in Japan, in the similar environment to actual casks and to confirm maintenance of the spent fuel integrity. In this test, the utilities plan to install a compact test container in the research facility, store one or two spent fuel assemblies in inert atmosphere for up to 60 years. Also, they plan to analyze the internal gas periodically and confirm the fuel cladding integrity. This document introduces the backgrounds, the overall test plan and designing of the test container.

1. INTRODUCTION

Recyclable-Fuel Storage Center in Mutsu City, Aomori Prefecture, which is the first interim spent fuel storage facility in Japan, is preparing for maximum 50-year storage of spent fuel in dry metal casks for both transportation and storage. Spent fuel after confirming their integrity will be loaded and transported to the facility, and stored over the long term, maintaining its integrity based on research achievements in Japan and overseas. In addition, to reduce risk of radiation exposure to workers and waste materials, the interim storage facility has no hot cell, and the spent fuel will be confirmed for their integrity indirectly by monitoring casks during storage and transported after the storage without opening the cask lid.

Currently, spent fuel storage in dry metal casks is a proven method mainly in Europe and the United States based on numerous tests including demonstration tests. In Japan, long-term integrity of PWR spent fuel is investigated and interim storage is planned under the conditions maintaining fuel integrity. On the other hand, Nuclear Safety Commission of Japan (NSC) required the utilities to accumulate knowledge and experience on integrity of fuel and casks during dry storage, considering experience of spent fuel dry storage in Japan and the above facility features. Therefore, BWR fuel and its casks that are stored in Fukushima Daiichi (No.1) and Tokai Daini (No.2) reactor sites have been confirmed several times for their integrity during storage.

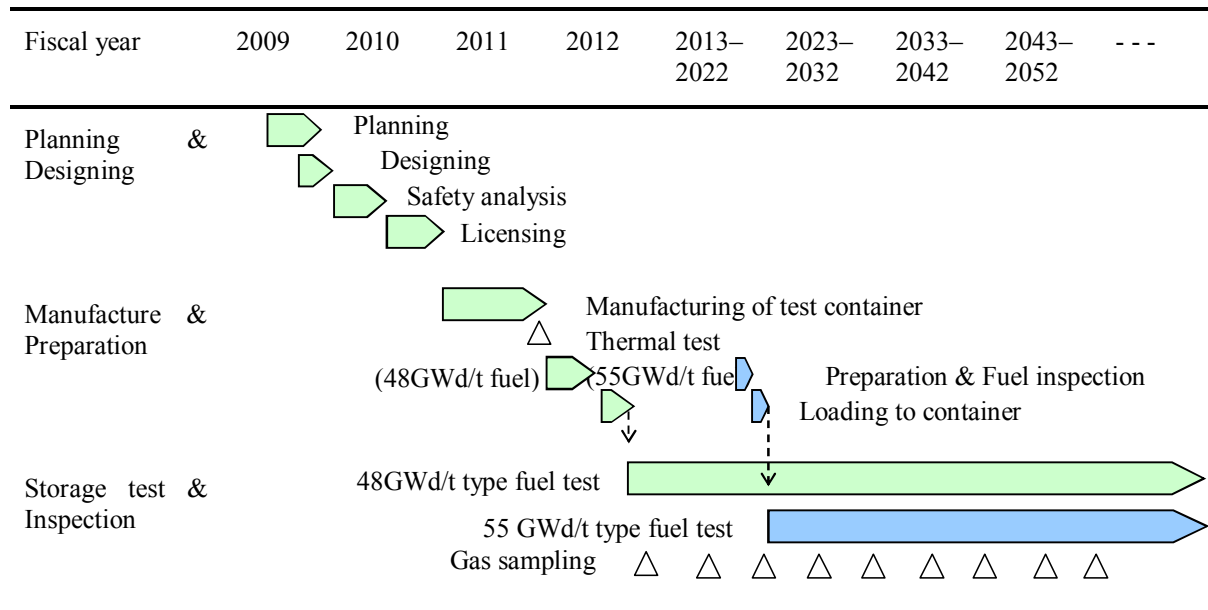
Under the circumstances, the utilities plan a long-term storage test for fuel integrity in domestic research facility (Nuclear Development Corporation (hereinafter called NDC)) to accumulate knowledge and experience on long-term integrity of PWR spent fuel during dry storage.

2. DEMONSTRATION TEST PROGRAM

2.1. Test overview and process

Integrity of 48GWd/t type spent fuel and 55GWd/t type spent fuel will be confirmed in the storage test. Now designing of a test container and preparation for a license are underway. The container will be manufactured in 2011 and storage test of 48 GWd/t type fuel will start in fiscal 2012. For the first 10 years, only 48 GWd/t type fuel will be loaded, and then 55 GWd/t type fuel will be added. The test is planned to continue for up to 60 years. In the storage test, appropriate test temperature and atmosphere in the container and no action of significant external force are confirmed by monitoring temperature and visual appearance of the test container and lid sealing performance. At the same time, the spent fuel integrity is confirmed by conducting internal gas sampling and Kr-85 analyses periodically (Table 1).

TABLE 1. TIME SCHEDULE OF DEMONSTRATION TEST OF PWR SPENT FUEL STORAGE



2.2. Fuel for test

Fuel specification assumed for tests is shown in Table 2. In September 1993, a 48 GWd/t type spent fuel assembly was unloaded from Kansai Electric Takahama Unit 3 and transported to hot laboratory in Tokaimura (NDC). A PIE test was conducted for some of the fuel rods and now it is stored in the pool of the facility. On the other hand, 55 GWd/t type fuel is also assumed and a proper spent fuel will be prepared for the test in the future.

TABLE 2. FUEL ASSEMBLIES ASSUMED FOR TESTS

Fuel for Test	Type 17×17 48GWd/t Fuel	type Type 17×17 55GWd/t type Fuel
Burnup (MWd/t)	42,800 (past record)	≤55,000 (assumption)
Cooling period (years)	19 (as of October, 2012)	10 or more (as of October, 2022)
Cladding material of fuel rods	Zircaloy-4	MDA or ZIRLO
Remarks	15 empty fuel rods*	Non

*Fuel rods used in PIE are never used for long-term storage tests.

2.3. Outline of container

To meet the test purpose, the test container must be designed to contain two Types of 17×17 PWR spent fuel for up to 60 years. Also, it must have a structure to establish temperature, pressure and atmosphere that can simulate spent fuel in actual metal casks with heat-transfer performance and to perform their monitoring. Furthermore, maintenance of sealing, subcritical and shielding performance is required for implementation of safe tests. Outline of the test container is shown in Figure 1.

Basket spacer is composed of boron containing aluminium alloy to maintain subcriticality. A container body mainly consists of an inner cylinder as a containment boundary, a thick mid-body for gamma-ray shielding and resin for neutron shielding. Since low heat load in the test container with up to two fuel assemblies loaded is one-tenth of an actual cask, a thermal insulator is placed between the inner cylinder and the mid-body as a temperature control component simulating actual cask temperature. For 10 years after the start of the test at loading only 48 GWd/t type fuel with lower heat load, another insulator is placed outside of the container to adjust its initial temperature.

The container has a single lid and double metal gaskets. Containment at lid containment boundary is confirmed by monitoring pressure of the space between the gasket springs.

2.4. Verification method of fuel integrity

Figure 2 shows a flow diagram of the fuel storage test. The following inspections of fuel integrity are conducted before, at the beginning of, and during the storage test.

2.4.1. Confirmation before storage tests

A spent fuel assembly during storage in the pool of hot laboratory is confirmed for its integrity before the dry storage test. It is confirmed by observing visual appearance of 4 outermost surfaces of the fuel assembly with an underwater camera.

2.4.2. Confirmation at beginning of storage tests

At loading of 48 GWd/t fuel into a test container and at additional loading of 55 GWd/t fuel, the fuel integrity after the loading operation is confirmed. No leak of the fuel rods is ensured by conducting gas sampling and analyses of Kr-85 and compositions as with confirmation during storage.

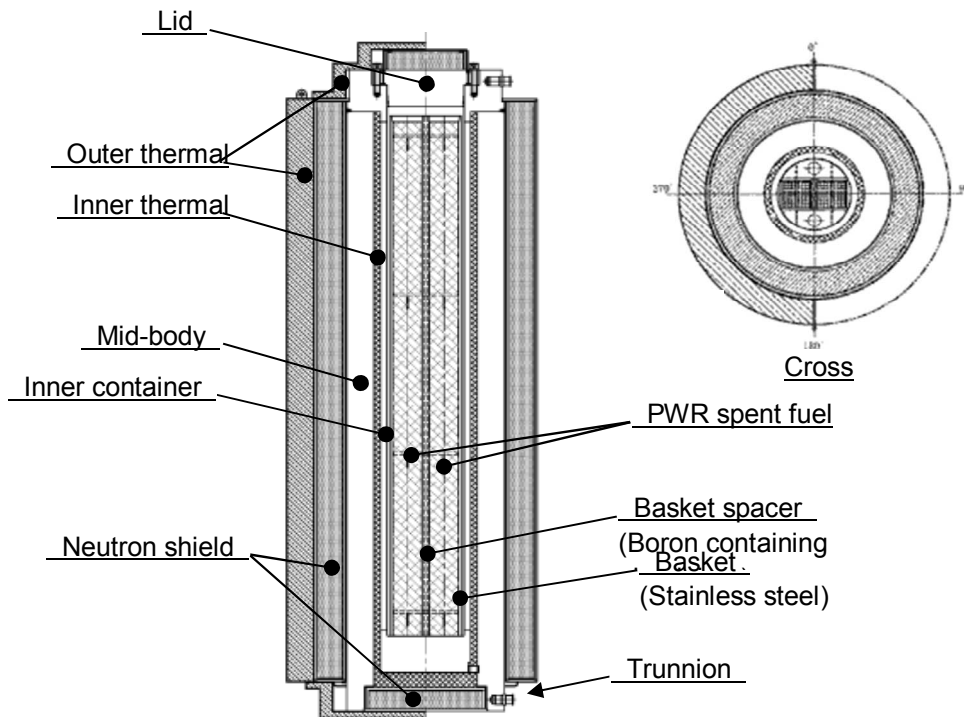


FIG. 1. Test container profile. Note: Outer thermal insulator installed at loading only 48 GWd/t F/A is removed when 55 GWd/t fuel assembly is added.

2.4.3. Confirmation during storage tests

The test condition is confirmed by analyses, gas sampling from inside of a test container and monitoring it from outside during storage until the completion of the test.

2.4.3.1. Gas sampling

For the purpose of detecting fuel rod failure, gas samples inside of a test container are taken periodically using a sampling pod (scheduled every 5 years) to conduct gas analyses. The gas sampling is conducted by connecting the previously-evacuated sampling pod to the lid port leading to inside of the test container through a valve. The sampled gas is analyzed for radioactive gas (detection of Kr-85) with a Ge semiconductor detector and components with a mass spectrometer. If any problems like significant increase of Kr-85 level are detected, the test will be suspended to evaluate effect on safety and investigate the cause. When examination of fuel integrity shows a possibility of fuel failure, the fuel will be investigated in detail.

2.4.3.2. Monitoring of containment

Monitoring of the following items are performed determining its frequency during the test.

(a) Temperature monitoring:

With the aim of estimating temperature history of fuel rods in the center of a fuel assembly, thermocouples are installed on the outer surface in the middle area of a test container to monitor temperature. Temperature of the fuel rods in the center of the fuel

assembly is calculated by inputting the outer surface temperature into a previously-verified assessment tool for temperature of the test container and fuel assemblies;

- (b) Confirmation of containment:
Pressure monitoring is performed using pressure gauges installed to a buffer tank leading to gap between double metal gaskets, which are pressurized with helium gas, to confirm maintenance of containment inside of the test container. At the same time, gas temperature is measured (Figure 3);
- (c) Confirmation of integrity:
Visual inspections are conducted to detect damage of the test container and to confirm its fixing condition that would have effect on the test;
- (d) Inspection of measuring equipment:
Thermocouples, temperature indicators, pressure gauges, etc. are calibrated or replaced with calibrated equipment to provide quality control of measuring equipment.

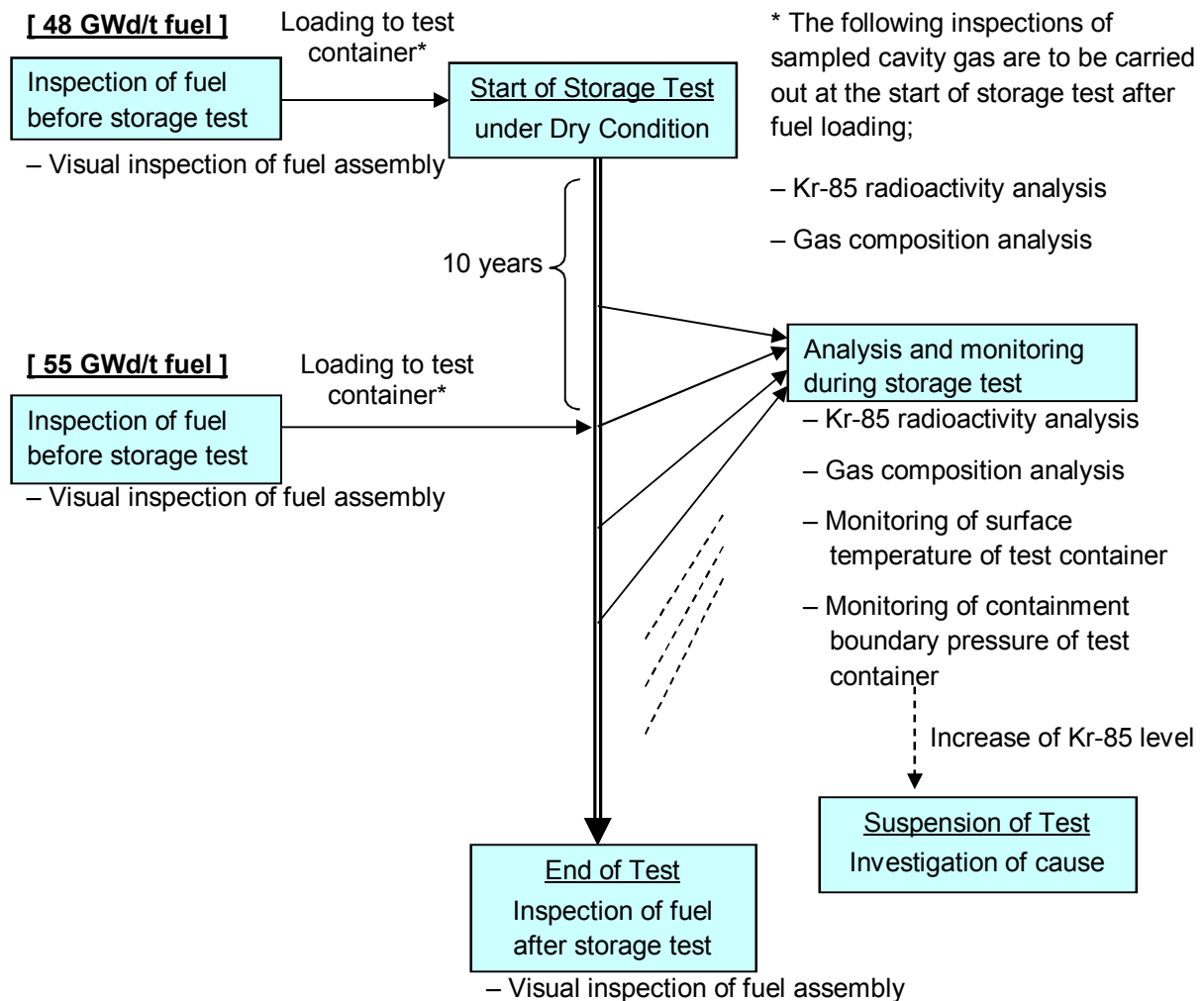


FIG. 2. Flow diagram of test programme.

2.4.4. Others

Japan Nuclear Energy Safety Organization (JNES) plans to participate in this test from a regulator's standpoint. This is intended for continuing examination and research required for evaluation of knowledge and experience accumulated by the utilities and consideration of safety of transportation. Therefore, we will discuss its details in the future.

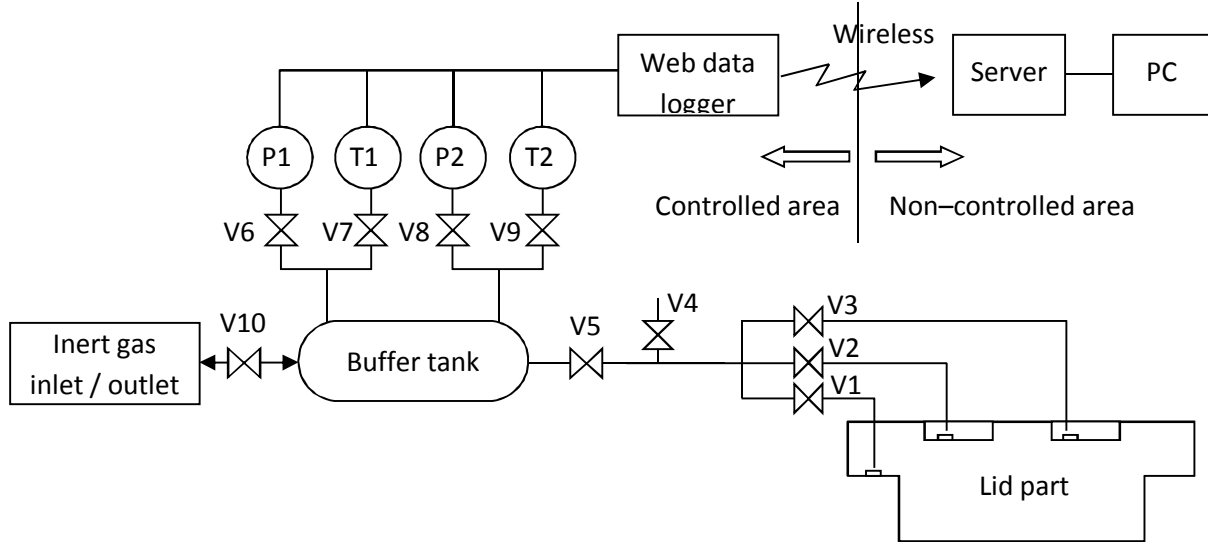


FIG. 3. Schematic drawing of pressure monitoring.

3. DESIGNING OF TEST CONTAINER

3.1. Organization of current knowledge and experience

Spent fuel assemblies after confirming their integrity are stored in metal casks with inert atmosphere. Thermal degradation, chemical degradation, etc. are assumed as factors affecting fuel integrity during storage. However, spent fuel integrity can be maintained if the fuel assemblies are stored maintaining inert atmosphere in cask cavity under appropriate temperature conditions without physical impact during handling. Spent fuel during storage without any physical impact can be evaluated as no damage on their integrity to thermal, chemical, radiation and mechanical degradation as shown in Table 3.

Integrity of spent fuel after storage can be confirmed by checking cask temperature, sealing performance and external force conditions during storage and cask handling.

In the United States, spent fuel dry storage test is being carried out in Idaho National Laboratory (INL) using CASTOR cask. PWR spent fuel assemblies brought from Surry Nuclear Power Plant, (15 × 15, of BU up to approx. 35,700 MWd/t, 2–4 years as cooling period before storage), were inspected when the above mentioned storage test period became approx. 15 years. As a result of radioactivity analysis of gas inside of the container, no Kr-85 or damage of fuel cladding tubes was detected. Furthermore, creep tests of cladding tubes, confirmation of hydride reorientation, measurement of hardening, observation of cross-sections, etc. ensure no damage or significant change in the cladding tubes due to aging degradation during storage (Ref. **Error! Reference source not found. Error! Reference source not found.**).

TABLE 3. EVALUATION OF DEGRADATION EVENTS

Conditions to be considered	Technical evidence	Actual condition of stored cask	Test conditions (target)
Thermal degradation	No embrittlement due to hydride reorientation, failure due to creep strain, recovery of irradiation hardening, or stress corrosion crack under 100 MPa or less circumferential stress at 275°C. Ref. [1]	Around 230°C (Gradually decrease with decrease in decay heat)	Around 230°C (Gradually decrease with decrease in decay heat)
Chemical degradation	Negligible oxidation/hydrogen absorption during storage (inert gas atmosphere) compared to that during in-core irradiation	He gas atmosphere Moisture: 10% or less	He gas atmosphere Moisture: 10% or less
Radiation degradation	Negligible neutron irradiation influence during storage. Saturation of mechanical strength due to neutron irradiation at relatively low burnup (around 5 GWd/t)	Burnup of stored fuel: Maximum 47 GWd/t	Burnup of contained fuel: 5 GWd/t or more
Mechanical degradation	Maintenance of integrity under normal test conditions of transport (free drop) (Acceleration: 20–45 G)	During storage: static position During earthquakes: Acceleration of 1 G	During storage: static position During earthquakes: Acceleration of 1 G

3.2. Simulated environment of actual casks

Simulated environment of a test container is discussed considering technical knowledge and experience under three conditions shown in Table 1 (thermal, chemical, and radiation degradation) and interim storage condition assumed for spent fuel under normal storage condition with actual metal casks.

3.2.1. Temperature

3.2.1.1. Target value of fuel maximum temperature

The maximum temperature of fuel cladding tubes during the storage test is set around the design value of actual casks since temperature simulation of actual casks is desirable.

Aging degradation that requires consideration of fuel cladding tube temperature includes recovery of irradiation effect, creep strain, hydride reorientation and stress corrosion crack. The creep strain and hydride reorientation require consideration of temperature and stress while the stress corrosion crack requires consideration of stress and environment. The threshold of recovery of irradiation effect is considered around 300°C while that with effect of hydride reorientation on mechanical properties of cladding tubes is 275°C and 100 MPa circumferential stress for 48 GWd/t fuel (Ref. [1]) and 250°C and 90MPa for 55 GWd/t fuel (Ref. **Error! Reference source not found.**). Temperature and stress below the threshold for hydride reorientation never causes any damage of cladding tubes or stress corrosion cracking due to creep strain during storage.

Therefore, limit temperature having no effect on fuel integrity during storage is respectively set as 275°C and 250°C for 48 GWd/t fuel and 55 GWd/t fuel. On the contrary, temperature at the beginning of storage of 48 GWd/t fuel is evaluated as approx. 230°C according to conservative analyses in the above interim storage facility.

Therefore, the target value of the fuel temperature in the long-term storage test is set as approx. 230°C for both 48 GWd/t fuel and 55 GWd/t fuel. In addition, 55 GWd/t fuel is inserted into a test container 10 years after start of the storage test of 48 GWd/t fuel, when heat load in the test container would be approx. 3 times higher. Although a thermal insulator of the container will be adjusted in loading 55 GWd/t fuel, temperature of 48 GWd/t fuel that gradually decreases with decay heat damping will increase again. The temperature of 55 GWd/t fuel is adjusted based on its actual fuel specification considering the temperature rise of 48 GWd/t fuel rods as well as the temperature limit for aging degradation.

Fuel temperature during tests is confirmed by temperature of the test container surface.

TABLE 4. LIMIT TEMPERATURE OF FUEL CLADDING TUBE

Fuel spec.	Limit temperature	Material of clad	Remarks
48 GWd/t	275°C	Zircaloy-4	Setting temperature based on effect of hydride reorientation with the lowest limit temperature of recovery of irradiation effect, creep and hydride orientation
55 GWd/t	250°C	MDA / ZIRLO	

TABLE 5. TARGET VALUE OF FUEL CLADDING TUBE MAX. TEMPERATURE AT BEGINNING OF TEST (STATIC STATE)

Fuel	Design value of actual cask (at environmental temperature)	Planned value of storage test (at environmental temperature)	Limit
48 GWd/t	Up to 230°C (at 45°C)	Approx. 230 (at 25°C)	$\leq 275^\circ\text{C}$
55 GWd/t	No assumption	Approx. 230 (at 25°C)	$\leq 250^\circ\text{C}$

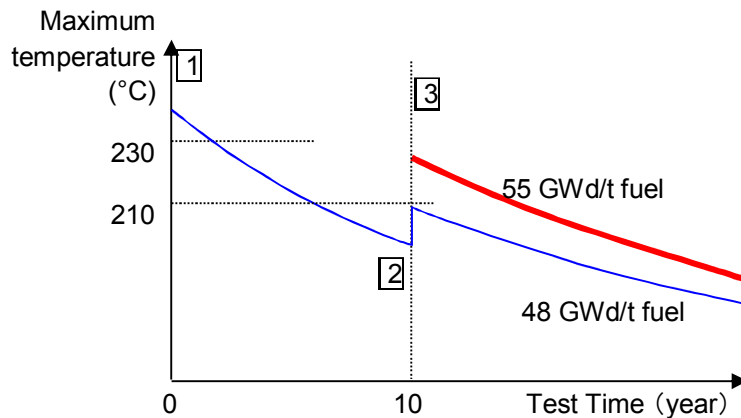


FIG. 4. Setting of fuel rod maximum temperature.

3.2.1.2. Thermal design of container

The test container has a thermal structure of removing heat by natural cooling without external power as with actual casks to simulate gradual temperature decrease easily in the test container and to avoid power supply troubles. Thermal design is the most important to the test container to simulate fuel temperature of actual metal casks. Therefore, its heat-transfer performance is verified by a heat-transfer test with a heater simulating actual fuel condition as well as FEM analyses for its designing. Table 6 shows heat load of the fuel in the test container.

TABLE 6. HEAT LOAD OF FUEL ASSEMBLIES IN TEST CONTAINER

	Beginning of test	Addition of 55 G fuel
Content	48 GWd/t fuel (cooling for 19 years)	48 GWd/t fuel (cooling for 29 years) and 55 GWd/t fuel (cooling for 10 years)
Heat load	547 W	1472 W (455+1017 W)

Since heat load at additional loading of 55 GWd/t fuel is relatively high (approx. 1.5 kW), temperature is controlled with only the thermal insulator inside of the container. Figure1 shows temperature distribution of the test container at additional loading of 55 GWd/t fuel. Large temperature difference of approx. 50°C is obtained due to temperature control effect of the insulator placed inside of the main body. Under the condition loading only 48 GWd/t fuel for the first 10 years, another insulator is placed outside of the container and low-pressure helium gas is applied as internal gas since the heat load is extremely low and simulation of actual cask internal temperature is difficult. This is intended to control thermal conduction of the gas and obtain large temperature difference inside of the test container as with the vacuum condition by setting internal gas as low pressure. The low pressure setting of internal gas, which causes no significant change in internal atmosphere, would not affect the simulation performance of chemical/thermal effect of actual casks on surface corrosion and temperature distribution.

Fuel temperature in the storage test is approx. 250°C for 48 GWd/t fuel and approx. 230°C for 55GWd/t fuel at the beginning of the test. The temperature at the beginning of the test for 48GWd/t fuel is evaluated under vacuum condition causing maximum temperature, and that in the storage tests will be below this value. After future examination, temperature control procedures due to gas pressure control will be determined. As mentioned above, both 48 GWd/t fuel and 55 GWd/t fuel meet the target value of the fuel temperature. Temperature increase in 48 GWd/t fuel at loading of 55 GWd/t fuel is within 10°C.

3.2.2. Test atmosphere

To meet the purpose of the long-term storage test, atmosphere in a test container around a fuel assembly must be specified. First, the test container is filled with inert gas (helium gas) having negative pressure as with actual metal cask cavity.

In addition, vacuum drying operation in the same procedure as actual casks is required at loading a fuel assembly before backfilling of inert gas. At the completion of the operation, amount of moisture is confirmed. Although internal surface area including the container inside and fuel assemblies is different from actual casks, residual moisture amount in both

cases has little effect on aging degradation of spent fuel in terms of corrosion of cladding tubes and hydrogen absorption.

Maintenance of inert atmosphere in the test container is confirmed during tests by monitoring pressure at lid containment boundary to confirm maintenance of sealing performance.

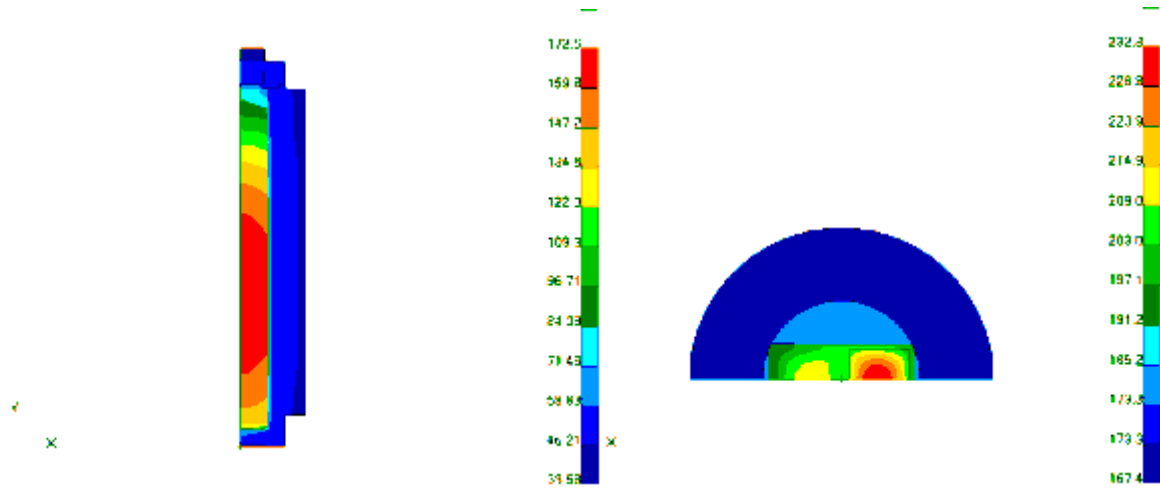


FIG. 6. Thermal analyses of test container (during loading of (48&55) GWd/t fuel assemblies).

3.2.3. Irradiation

Due to effect of neutron irradiation on mechanical properties of cladding tubes, mechanical strength shows saturation and ductility shows slow deterioration at low burnup with relatively low dose around 5GWd/t. Burnup of fuel assemblies used for the storage test is 42.8GWd/t and in-core irradiance is 10^{21} to 10^{22} n/cm². The mechanical properties of cladding tubes are located in this region. On the other hand, irradiation dose during storage is lower than 10^{16} n/cm² for actual casks and one digit smaller in the storage test. However, irradiation dose in the storage of actual casks and the storage test is extremely small compared to in-core irradiation and they are equal in terms of effect on mechanical properties of cladding tubes.

4. SUMMARY

Some Japanese utilities are planning to conduct a long-term storage test for up to 60 years for PWR fuel assemblies under the atmosphere simulating temperature and internal gas of actual casks to accumulate knowledge and experience on long-term integrity of PWR spent fuel during dry storage.

The storage test plan such as test methods and inspection items, and container design have been prepared. In the future, safety analyses, licensing and manufacturing of the test container are to be done, and the storage test of 48 GWd/t fuel will start at fiscal 2012.

Thermal design of the test container is important. Its temperature is controlled with thermal insulators and heat-transfer performance is confirmed by heat transfer tests at the completion of the container.

REFERENCES

- [1] JAPAN NUCLEAR ENERGY SAFETY ORGANIZATION, JNES technical report, 06Kirohou-0006, (2007), (in Japanese).
- [2] JAPAN NUCLEAR ENERGY SAFETY ORGANIZATION, JNES technical report, 08Kirohou-0006, (2009), (in Japanese).
- [3] IDAHO NATIONAL ENGINEERING AND ENVIRONMENTAL LABORATORY, Dry Cask Storage Characterization Project – Phase 1: CASTOR V/21 Cask Opening And Examination, INEEL/EXT-01-00183 Revision 1 (2001).
- [4] ARGONNE NATIONAL LABORATORY, Examination of Spent PWR Fuel Rods After 15 Years in Dry Storage, NUREG/CR-6831, ANL-03/17 (2003).

DEMONSTRATION DROP TEST AND DESIGN ENHANCEMENT OF THE CANDU SPENT FUEL STORAGE BASKET IN MACSTOR/KN-400

W.S. CHOI*, J.Y. JEON*, K.S. SEO*, J.E. PARK**

* Korea Atomic Energy Research Institute, Daejeon

** Korea Hydro & Nuclear Power Co. Ltd., Gyungju
Republic of Korea

Abstract

A dry interim storage facility named MACSTOR/KN-400 has been constructed at the Wolsung power plant in Korea. The MACSTOR/KN-400 has the separated 7 modules. There are 400 long slender cylinders in one module. In one cylinder, ten baskets where CANDU spent fuels are loaded are stacked and stored. For this MACSTOR/KN-400 facility, analyses and tests for the hypothetical accident conditions that might happen during moving and storing baskets into a cylinder were performed. In a demonstration test, one of test basket models did not satisfy one of the safety-related requirements. So, the revised basket designs were generated by the structural evaluation based on the finite element analyses and specimen tests. Among these revised designs, one design was chosen as the final revised design of the basket. The final revised design is the one that makes the largest reduction of plastic strain in the upper welding region. And it also is the one that makes the smallest design change from the previous basket design and the one easy to adopt the design change. Drop tests and leak tests of the final revised basket were performed and it satisfied all the performance requirements.

1. INTRODUCTION

The Wolsung dry storage facility named MACSTOR/KN-400 in Figure 1 is the one where CANDU type spent fuels are loaded in a basket and these ten baskets are stacked in a cylinder. Under the process of licensing this facility, KINS(Korea Institute of Nuclear Safety) recommended the demonstration drop test of this facility. KAERI(Korea Atomic Energy Research Institute) conducted this test with the support of KHNP (Korea Hydro & Nuclear Power Co.) Wolsung Power Plant. Analyses and tests for the hypothetical accident conditions that could occur in the process of stacking the baskets in a cylinder were performed. Two cases were considered for this hypothetical accident condition. One is for a basket dropping of a drop height of 7.5 m onto the cylinder bottom. The other is for a basket dropping with the same height onto the other basket stacked in a cylinder. Preliminary analyses are performed when a cylinder is hung in the air and when a cylinder is placed on a rigid surface, which show the latter condition is more severe than the other one. Based on the analysis result, a case of putting a cylinder on a rigid surface is selected as the condition of a demonstration drop test. In a basket, bundles of mock-up fuel of which the weight is same as that of real fuel bundles are loaded so that the total weight of a test basket is the same. On the outer surface of a basket, 8 strain gauges and 4 accelerometers are located. Two devices to measure the impact velocity of a basket were invented and the measured velocities are compared and cross-checked. After the drop tests, leakage rates are measured by means of a helium leak test facility. Two performance requirements should be satisfied after the drop tests. The first one is an allowable range for a deformation and the second one is for the leakage rate. These requirements are listed in the Table 1. The first performance requirement shall be satisfied to be able to draw out a basket by a grappeler after a drop accident and the second performance requirement to be able to maintain a primary pressure boundary. The allowable leakage rate of 10^{-5} atm·cm³/sec (He) at a welding region means that there shall be no leakage.

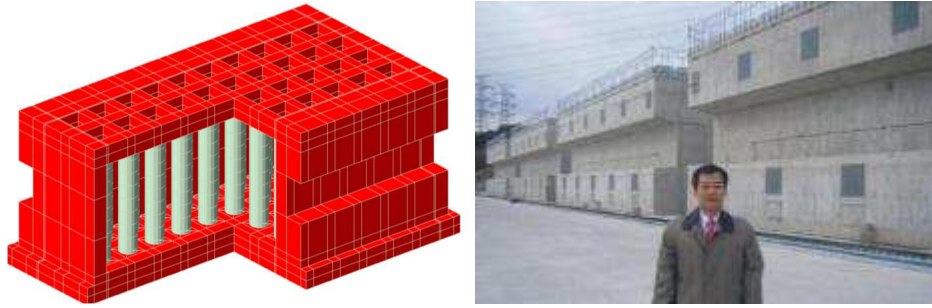


FIG. 1. MACSTOR/KN-400, Wolsung dry interim storage facility.

TABLE 1. PERFORMANCE REQUIREMENT

Performance requirement	Allowable criteria
Deformation	< 1,102 mm (for outer diameter of basket)
leakage rate	< 10^{-5} atm·cm ³ /sec (He)

2. DEMONSTRATION TEST

2.1. Specification of a basket and test facility

The basket test model is the same basket that is now utilized in the Wolsung power plant. In the basket, sixty mock-up fuel bundles which have the same weight as the real CANDU fuel bundles are loaded. After loading fuel bundles, a cover is placed to envelop the basket. The upper meeting part between the cover and the post and the lower part between the cover and the bottom plate are welded by an automatic welding machine. Therefore, the test model is identical to a real basket except that the mock-up fuels with the same weight are loaded. The test facility consists of a cylinder and a tower to support this cylinder. The cylinder is divided into an upper cylinder and a lower drum. These two parts are joined by several bolts. The reason why this cylinder is made with two separable parts is to provide an way to separate the basket from the cylinder when the basket deformation is so large that we can not draw out it in the normal way. In this jammed condition, dismantling the lower drum can retrieve the basket. Two lower drums were fabricated. One was used in the part of a cylinder, and the other as a chamber during leakage test. If the first lower drum became largely deformed in a drop test, it should be replaced with the second one. This drop test facility was established at a KAERI site. Based on the general arrangement and the real size of MACSTOR/KN-400, this facility was fabricated to be able to conduct the drop test at the height of 7.5 m. Preliminary analysis result shows that the case of the cylinder placed on the rigid target induces a larger impact and larger strain and stress due to it than the case of the cylinder hung in the air. This phenomenon is observed especially on the welding part of a basket. So, the test condition is decided based on the analysis result as placing a cylinder on the rigid target. The cylinder is installed with the perpendicularity tolerance of less than 0.01 degree. The basket test model and the drop test facility are shown in Fig. 2 and Fig. 3, respectively.



FIG. 2. A basket test model for the demonstration test.



FIG. 3. A drop test facility consisting of a cylinder and tower.

2.2. Devices to measure an impact velocity

Two devices were invented and installed to measure the impact velocity of a basket onto the cylinder bottom. The first device uses two laser displacement sensors installed with a distance difference from each other. We calculate the time difference between the measured times when the basket passes over each sensor. The distance difference divided by the measured time difference yields the impact velocity of a basket. The first laser displacement sensor was installed at the position above from the cylinder bottom by 30 mm. The second laser displacement sensor was installed at the higher than the first one by 50 mm. At corresponding location of a lower drum, two penetrated holes are prepared. The schematic drawing and the real installed arrangement are represented in Fig. 4 and Fig. 5. To measure the impact velocity when a basket drops on to other basket loaded in the cylinder bottom, two penetrated holes are added in the middle of the lower drum considering the height of a loaded basket. Consequently, four penetrated holes for laser displacement sensors are prepared.

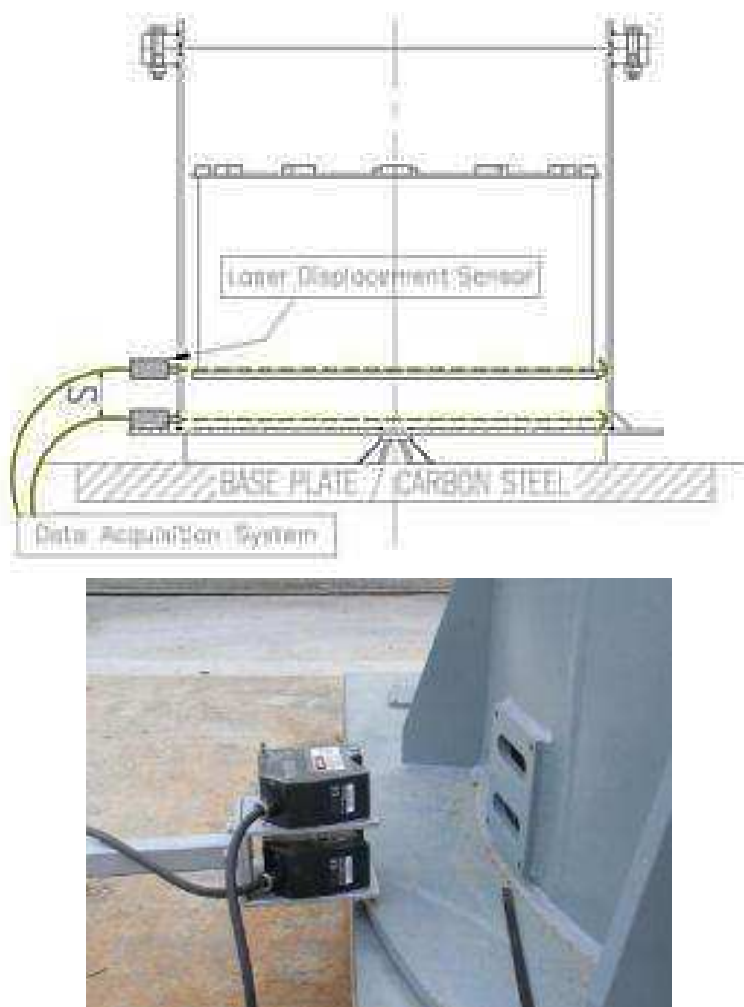


FIG. 4. Schematic drawing and arrangement of two installed laser sensors.

The second device to measure impact velocity uses a fan shaped rotation device and a laser displacement sensor as shown in Figure 5. The invented device is installed above the cylinder. A fishing string is rolled around the circulated object and one end of string is attached to the top of a basket. When the basket starts to drop, the string becomes unfolded and the object starts to circulate. The circulated object has 8 ribs in the radial direction, and a laser sensor is

located in the side of them to acquire the pulse data when it circulates. From this pulse data, the RPM of the circulated object is calculated. Consequently, an impact velocity is calculated from this RPM. The impact velocities by these two different devices are compared to each other and cross-checked.



FIG. 5. An invented device consisting of a circulated object and a laser sensor to measure an impact velocity.

2.3. Accelerometer and strain gauge

Four accelerometers and eight strain gauges are installed on the outer surface of the basket to measure accelerations and strains before and after impact. Four strain gauges are attached to the neighborhood of an upper welded part between the top plate and a post by the space of 90 degrees, and the other four strain gauges are attached to the neighborhood of a lower welded part between the side cylinder and the bottom plate of the basket. Accelerometers are attached to spacer pad blocks. The locations of the sensors are denoted in Fig. 6.

3. TEST RESULTS

For the drop test on to a cylinder bottom, the impact velocity of the basket dropping on to a cylinder bottom calculated by two laser displacement sensors having a distance difference is 9.43 m/s. And the impact velocity measured by the circulated object and a laser sensor is 9.26 m/s. These two values means there was about 23% of a velocity reduction compared to the theoretical impact velocity at the height of 7.5 m that is 12.13 m/s. This velocity reduction is estimated to originate from air damping. The displacement history data from two different device to measure an impact velocity is shown in Fig. 7. The left figure in Fig. 7 represents a protrusion shape of the basket bottom plate and the time difference well. The right figure shows the pulse data measured during the laser sensor detected ribs of circulated object. After the drop test, the dropped basket was withdrawn by a grapppler. This means that the retrievability of a basket for a drop accident was maintained. The measured deformation of a basket satisfied the allowable deformation, which means that the basket satisfied the performance requirement about the deformation.

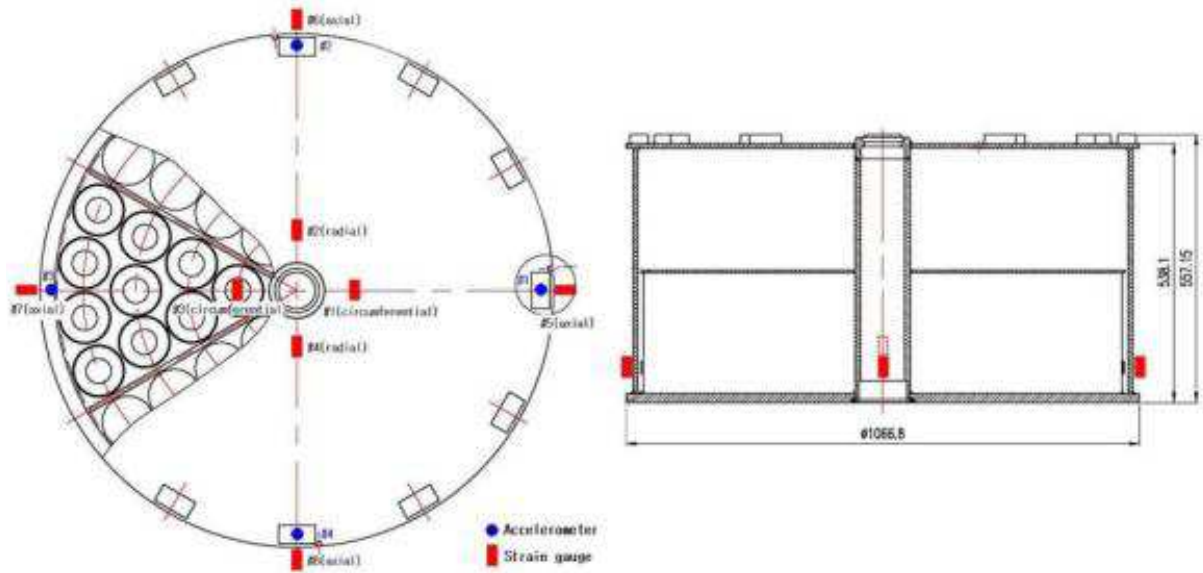


FIG. 6. Location of accelerometer and strain gauge installation.

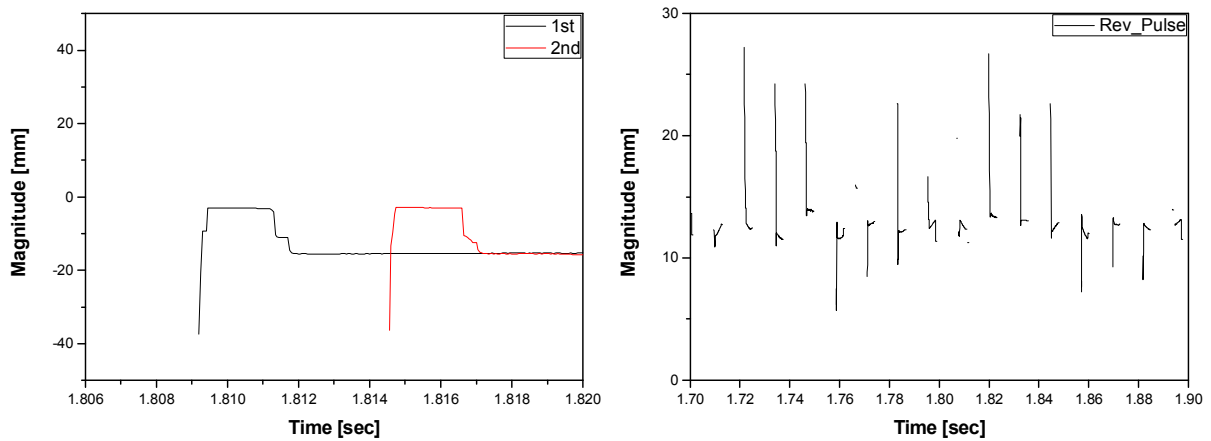


FIG. 7. Result data acquired from both devices to measure impact velocity.

When a basket is loaded in a cylinder, the total drop height reduces. So, the impact velocity in this case is smaller than that in the previous section. The impact velocity of a basket calculated by two laser displacement sensors is 9.152 m/s. And the impact velocity calculated by the RPM of a circulated object is 9.174 m/s. These two values mean there was about 22% of a velocity reduction compared to the theoretical impact velocity at the height of 7.0 m which is 11.72 m/s. This velocity reduction is similar to that in the previous condition. After the drop test, both of the dropped basket and the loaded basket were withdrawn by a grapples. So, for this drop case, the retrievability of both baskets also was maintained. In this second drop test, the measured deformation of both baskets satisfies the performance requirement of the deformation.

The leakage test was performed to measure the leakage rate after the drop test. First, after a basket is charged with helium gas as shown in Fig. 8, a sniffer test is conducted. And then the basket with helium gas is loaded in a chamber and kept for 15 minutes. A leakage rate is measured by the helium mass spectrometer as shown in Fig. 8. In the leakage test after the first drop test, the dropped basket satisfied the leakage rate of 10^{-5} atm·cm³/sec (He). In the

leak test after the second drop test, the dropped basket satisfied the leakage rate. But in the loaded basket, there occurred more leakage than the allowable leakage rate. The PT (Penetrant Test) after the leakage test in Fig. 9 showed that the leakage occurred in the upper welding region between the top plate and the post since the bottom plate of the dropped basket impacted intensively on the post of the loaded basket. So, it is needed to revise the basket design so that the leakage should not occur.



FIG. 8. Basket under charging helium gas and leakage test by helium mass spectrometer.



FIG. 9. Leak happening at upper welding region (PT result).

4. DESIGN ENHANCEMENT

The directions of design enhancement to prevent a leakage on the upper welding region are as follows;

- (1) To enhance the welding performance of welding region itself;
- (2) To afford the deflection of the bottom plate of the dropped basket;
- (3) To increase the bending rigidity of the top plate of the basket;
- (4) To increase the bending rigidity of the bottom plate of the basket.

Based on the directions of design enhancement, six revised designs were generated. The revised candidate designs generated are presented in Fig. 10 and Table 2. Six revised designs

were strictly evaluated by the finite element analyses and specimen tests. The structural evaluation by the finite element analysis on the previous design showed the simulation that the bottom plate of the dropped basket impacted intensively on the post of the loaded basket in Fig. 11. And it also represented that the maximum plastic strain at the upper welding part exceeded the elongation limit.

So, by these structural evaluation for the revised designs, one design was chosen as the final revised design of the basket. The final revised design is the one that makes the largest reduction of plastic strain in the upper welding region. And it also is the one that makes the smallest design change from the existing basket and the one easy to adopt the design change. The final revised design was “design 6” in Table 2, which is decreasing the height of central post. Drop tests and leak tests of the final revised basket were performed and it satisfied all the performance requirements. That means there was not leakage at any basket used in tests. The revised basket was achieved by the minimum structural design. The previous design and the final revised design are represented in Fig. 12.

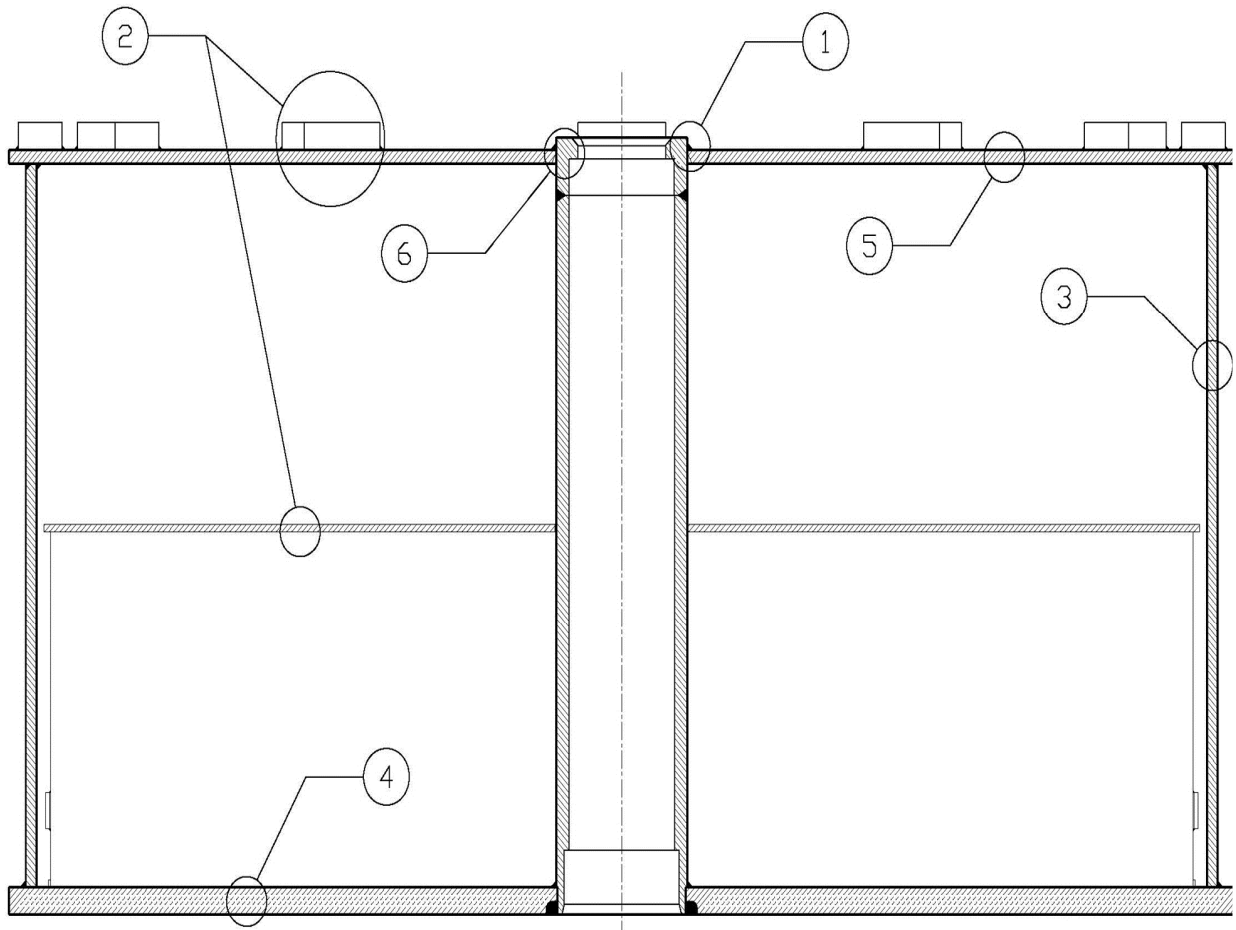


FIG.10. The directions of design enhancement.

TABLE 2. THE REVISED DESIGNS ACCORDING TO THE DIRECTION OF DESIGN ENHANCEMENT

Revised designs	Direction of design enhancement
(1) Increase of the welding thickness at top welding region	(1) To enhance the welding performance of welding region itself
(2) Addition of extra spacer pads and increase of rib height	(2) To afford the deflection of the bottom plate of the dropped basket
(3) Increase of the thickness of side wall	(3) To increase the bending rigidity of the bottom plate of the basket
(4) Increase of the thickness of bottom plate	(4) To increase the bending rigidity of the top plate of the basket
(5) Increase of the thickness of top plate	(5) To increase the bending rigidity of the bottom plate of the basket
(6) Decrease of the height of central post	(6) To afford the deflection of the bottom plate of the dropped basket

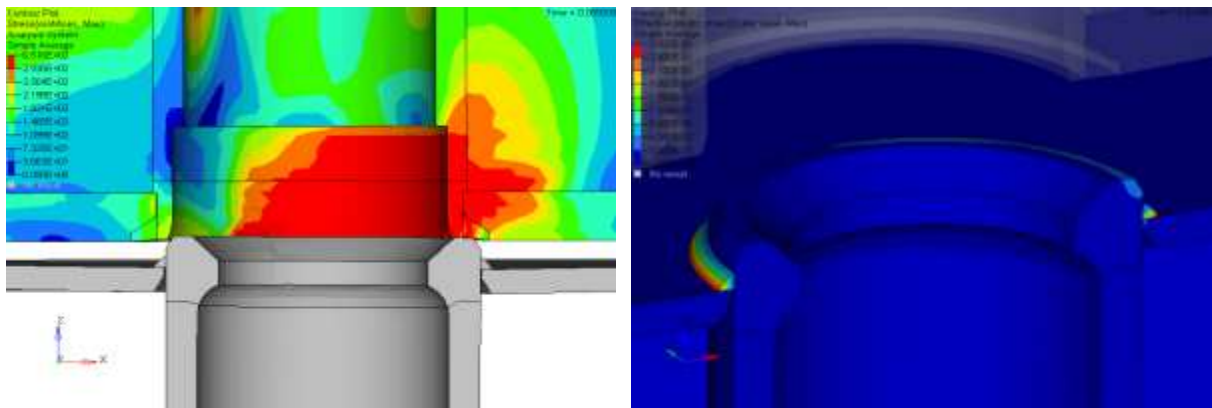


FIG. 11. Drop analysis for the previous basket design.



FIG. 12. The previous and the revised design.

5. CONCLUSIONS

Demonstration tests for the basket used in the MACSTOR/KN-400 in Wolsung Power Plants were performed. Tests were conducted for two cases. One is the case of basket dropping on to the cylinder bottom, and the other is dropping on to the other basket top plate loaded in the cylinder. Impact velocity was calculated by two different devices. There was a velocity reduction by approximately 22% compared to the theoretical impact velocity. Acceleration and strain histories before and after a drop test were acquired. The leakage test after the drop test showed that all the other baskets except the loaded basket satisfied the leakage performance requirement but more leakage than allowable occurred at the loaded basket in the second drop test. A clear understanding of this problem has been done and a basket design revision was made. And drop tests and leak tests of a revised basket were performed and it satisfied all the performance requirements. That means there was not leakage at any basket used in tests. The revised basket was achieved by the minimum structural design change through the evaluation of many FE analysis results and specimen test results.

ACKNOWLEDGEMENTS

This research based on the demonstration test was performed with the financial assistance of Wolsung Power Plant. The authors appreciate the support of Wolsung Power Plant.

REFERENCES

- [1] VIERU, G., "Testing of the CANDU Spent Fuel Storage Basket Package", WM'02 Conference (2002).
- [2] KOREA HYDRO & NUCLEAR POWER CO., "Safety Analysis Report for MACSTOR/KN-400" (2007).

DISTRIBUTIONS OF FISSION PRODUCTS ON PCI IN SPENT PWR FUEL USING EPMA

Y.H. JUNG, Y.B. CHUN, S.B. AHN, W.S. RYU
Korea Atomic Energy Research Institute, Daejeon
Republic of Korea

Abstract

The fuel specimen with 62,000 MWd/tU and the spent failed fuel rod with 53,000 MWd/tU by commercial PWR fuel were examined to compare with oxygen rich & average region at fuel-clad gap. To observe chemical behaviors and distributions of fission products on fuel-clad gap region by EPMA (Electron probe Micro-Analyzer). The results of this study can be used also in the interim storage facilities for spent fuels which were used in the Korea nuclear power plant. In addition, for comparisons of each plant's spent fuel characteristics this data will be used as a basic material. EPMA technique offers the possibility of identifying and analyzing such phases and segregations in spent PWR fuel, although the small amount expected to be present and the background radiation, present a significant analytical challenge. The detailed characterization of spent fuel fuel-clad gap region of fission products before and after its exposure from neutron is an important part of long-term storage of spent fuel. This report presents the results of EPMA examination of a spent fuel specimen with 62,000 MWd/tU performed with the aim of EPMA technique to analyses of fission products on fuel-clad gap region.

1. INTRODUCTION

Several recent studies have been conducted on fuel rod failures involving pellet-clad interaction (PCI) [1]. The results from these studies have established that PCI failures are due to stress corrosion cracking (SCC) of the cladding. A number of fission products (I, Cs, Cd, etc.) involved in the stress corrosion process have been identified. Of these, iodine and cadmium are prime suspects. Spent fuel rods are typically under tensile hoop stress because of internal gas pressure in the rods. In typical PWR fuel rods, the end of life internal pressure can be significant because of the initial helium backfill pressure and added pressure from the release of fission gases. Fuel-cladding interaction and formation of fuel-cladding bonding layers with specified chemical, physical and mechanical properties are important regarding the evolution of thermal conductivity as well as in the context of pellet-clad mechanical interaction PCMI. It is also important in the framework of long-term storage of spent fuel where the phases formed at the fuel-cladding boundary are considered to be the first to be leached in case of cladding failure [2].

This report describes preliminary work performed to examine the application of EPMA a method development. The fuel specimen for examination had a burn up somewhat higher than the normal burn up in Korea commercial nuclear power plants.

2. EXPERIMENTAL

2.1. Sample preparation

A thin diamond wheel was cut off from a PWR fuel rod with the spent failed fuel rod with 53,000 MWd/tU and normal spent fuel rod with 62,000 MWd/tU from nuclear power plant were withdrawn and cooled down for 2 and 4 years respectively. The samples have been embedded in epoxy resin and polished with diamond grinding disks of successively finer

grain size, finishing on cloth with diamond paste of $1\ \mu\text{m}$ as a final stage. Before mounting the sample in the EPMA, the samples were coated with carbon to prevent charging.

The carbon coated specimen was mounted in a holder together with the X-ray standard. The EPMA was performed on a CAMECA SX-60R equipped with two wavelength dispersive X-ray spectrometer shielded with tungsten. The analysis was performed with a beam current of 200 nA at an accelerating voltage 25 kV, in order to give a reasonable peak-to-background ratio for active specimen. Sample preparation schematic drawing shown in Fig. 1. A 4-mm slice was cut from the rod. Those slice mounted samples were shown in Fig. 2 normal spent fuel rod with 62,000 MWd/tU.

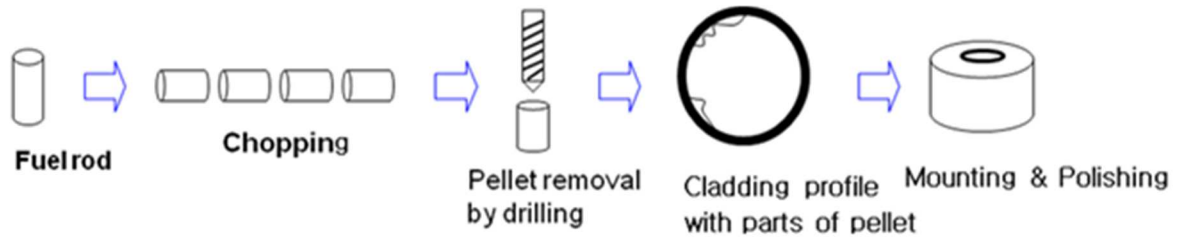


FIG.1. Schematic drawing of sample preparation.

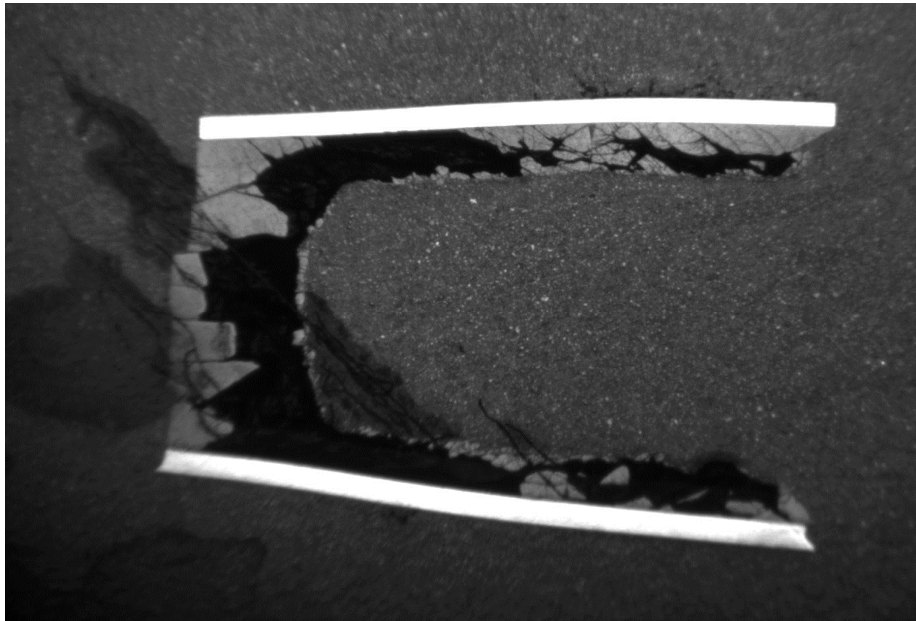


FIG.2. Mounted spent fuel sample 62,000 Wd/tU.

2.2. Results and discussions

A photomicrograph of clad-fuel gap section of the 62,000 MWd/tU fuel rod at an average oxygen region is presented in Fig. 3, which also shows quantitative analysis of O, Zr, U on the fuel-clad gap in the 62,000 MWd/tU on the marked line as shown in Fig. 3. The quantitative line scan data taken from across fuel-clad gap shows stable states at an average oxygen region compare with higher oxygen region as presented in Fig. 4. At a series of radial

positions, points quantitative analysis have been performed covering fuel-clad gap region in order to detect and measure possible local concentration gradients of O, Zr, U within an average oxygen region as shown in Fig. 3 and within a high oxygen region as shown in Fig. 4. Steps of $1\mu\text{m}$ were used to be able to assess the effective concentration gradients and resolution.

The concentration of O, Zr, U illustrate the general trend in fuel-clad gap region as shown in Fig. 3 compare to a high oxygen region as shown in Fig. 4. However, as shown in Fig. 4, the concentration distribution of Zr and U at the higher oxygen region is illustrating the general trend for redistribution in fuel-clad gap region. These results means, even at a high burnup stat in the 62,000 MWd/tU, the fuel-clad gap reliability seems to be appropriated condition.

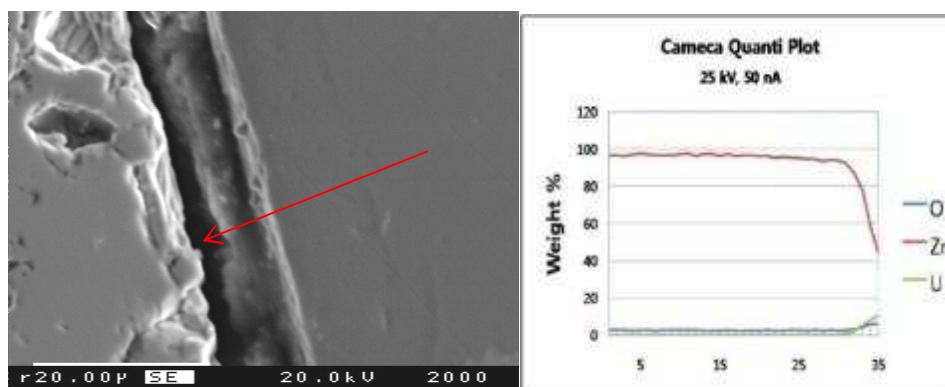


FIG. 3. SEM image and quantitative analysis of O, Zr, U within an average oxygen region.

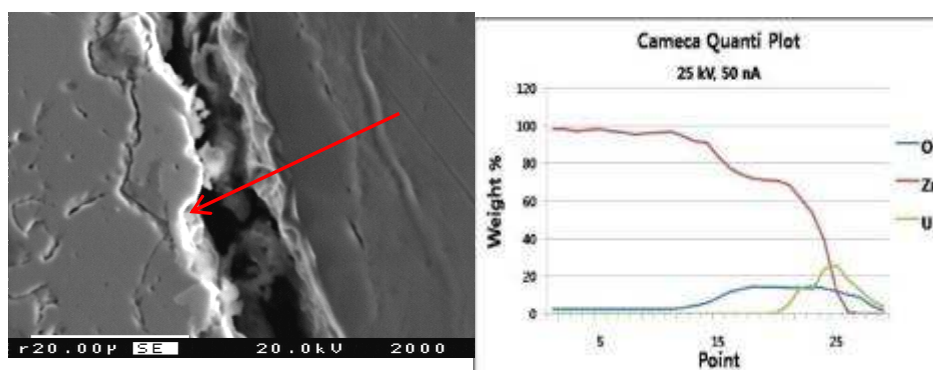


FIG. 4. SEM image and quantitative analysis of O, Zr, U within a high oxygen region.

When using standards for quantitative EPMA, the measurement on the standards can also be a source of error. Two of the major problems encountered here were the lack of suitable standards for Xe and Cs, and in homogeneity porosity in the ceramic standards. The fuel rod experienced appreciable release of the fission gases Kr and Xe, and redistribution of cesium out towards the pellet periphery during the power bump and this is reflected in the radial variation in structure and particularly, the amount and morphology of the porosity.

The specimen used for EPMA examination was unreached to avoid fission product loss on the fuel-clad gap. Xenon and cesium are fission products which are release from the central parts

of the pellet, to the free internal rod volume in the case of xenon and to the cooler outer fuel annulus and the clad in the case of cesium. However, the xenon and oxygen concentration profiles shown in Figs 5–6 illustrate the general trend for release and cesium redistribution in fuel-clad gap region.

The halogens iodine is most volatile fission products, and high release has been reported from early isochronal annealing experiments on irradiated UO₂ at various temperatures [3]. The diffusion coefficient of the halogens in single and polycrystalline UO₂ during irradiation is two orders of magnitude higher than that of xenon.

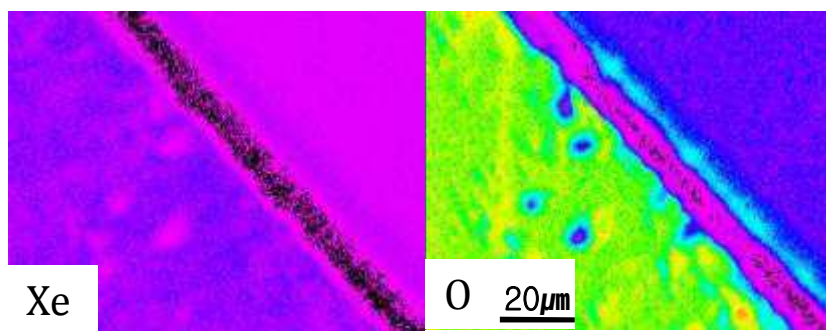


FIG. 5. Image mapping of Xe, O at a fuel-clad gap in the 62,000 MWd/tU. at an average oxygen region.

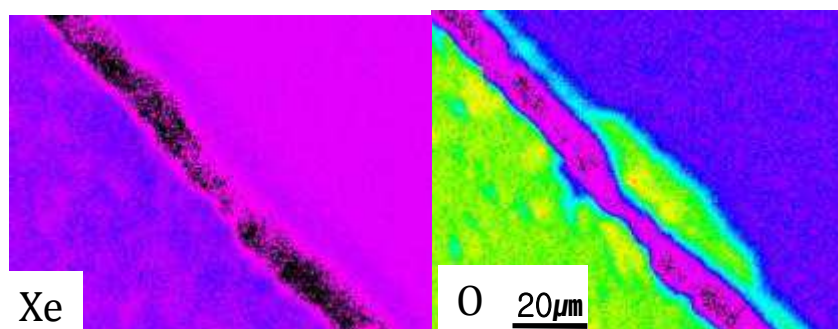


FIG. 6. Image mapping of Xe, O at a fuel-clad gap in the 62,000 MWd/tU. at a high oxygen region.

Figures 7–8 show qualitative concentration profile along the clad-fuel gap obtained by EPMA to conform the reliability of fission products behaviors at high burnup fuel conditions and compare with at an average oxygen region and higher oxygen region of Ce, O. The oxygen and cerium concentration profiles shown in Fig. 7 and 8 illustrate remarkably different trend for oxygen fuel-clad gap region in 84 μm between clad to fuel. Oxygen concentration profile at an average region is about less than 6 μm compare to 20 μm at higher oxygen region between clad to fuel gap as shown Figs 7–8. The chemistry of the alkali metals cesium in irradiated oxide fuels is of high interest because these fission products react with the fuel, with cladding components and with other fission products leading to pin swelling and to cladding corrosion at higher oxygen potentials. Most of redistribution of the fission product nuclide is using the classical methods of micro-sampling.

The chemical state of partly simulated fuel-fission products systems may not represent exactly the in-pile behavior due to the restricted selections of oxygen potential and temperature

influences in the irradiated pin [4]. The noble gas xenon is distributed the general trend for release and redistribution between fuel-clad gap region. X-ray microanalysis of xenon yields qualitative determinations of the unreleased fraction in irradiated fuels. The relative Xe intensities of predominantly intra-granular xenon can be calibrated by the total bonded xenon the fraction.

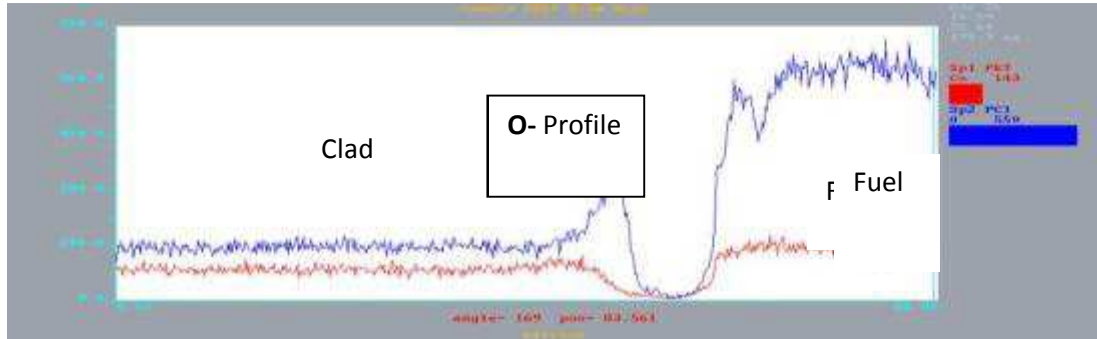


FIG. 7. Qualitative concentration profile of Ce, O along the clad-fuel gap at an average oxygen region.

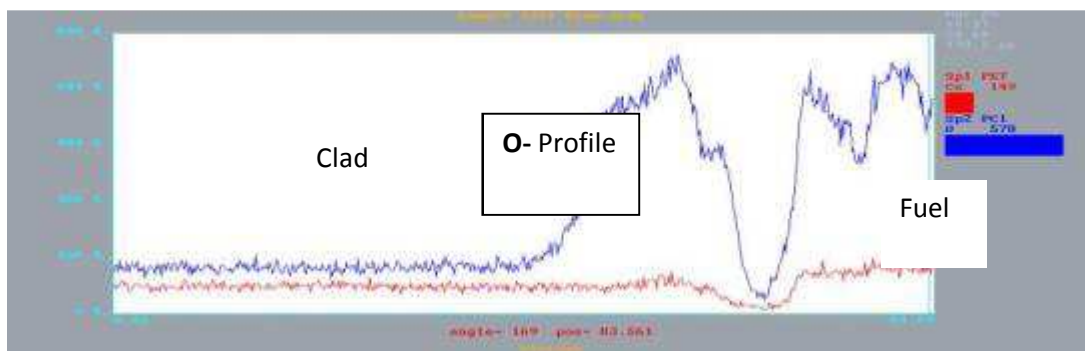


FIG. 8. Qualitative concentration profile of Ce, O along the clad-fuel gap at a high oxygen region.

Zircaloy cladding is known to have a strong affinity for oxygen. In-reactor corrosion of the cladding typically produces a thin outer layer of oxide 8–40 μm in thickness. Under PWR operating conditions, oxidation of Zircaloy is suppressed by the time presence of dissolved hydrogen in the primary coolant. However, oxidation rates in air at temperatures of 400°C can be significantly higher. Thus at a storage temperatures of 400°C, the degradation of cladding due to oxidation is found to be all of Zircaloy cladding will be oxidized.

Activated corrosion products CRUD (Chalk River Unidentified Deposit) from BWR and PWR reactors deposit primarily on the outer surfaces of fuel rods [5]. The generic term ‘crud’ has been applied to particulate material deposits on the surface of fuel rods and assemblies. On these surfaces, the deposits can lead to fuel-rod failures and cladding breaches. During reactor operations, crud deposits on the outer surface of all fuel rods. Also, it can become detached in cooling water and storage systems [6], causing additional radiation exposure to plant workers. These deposits are distinguishable from oxide corrosion products dissolved from structural materials and piping, which are transported into the core from the primary coolant [7].

There is a direct correlation between these fuel attributes and nuclear reactor water chemistry of crud depositing on the fuel rod, and the higher crud loading that has resulted in a number of cases of axial offset anomaly (AOA) in the U.S.A. and overseas, as well as anomalous shutdown chemistry behavior observed at some units. Despite its importance, crud is difficult to characterize by direct analysis, and there are only a few characterization papers in open literature [8]. Also analysis results in accordance with the crud samples collecting techniques of the spent fuel cladding are less studied than other areas.

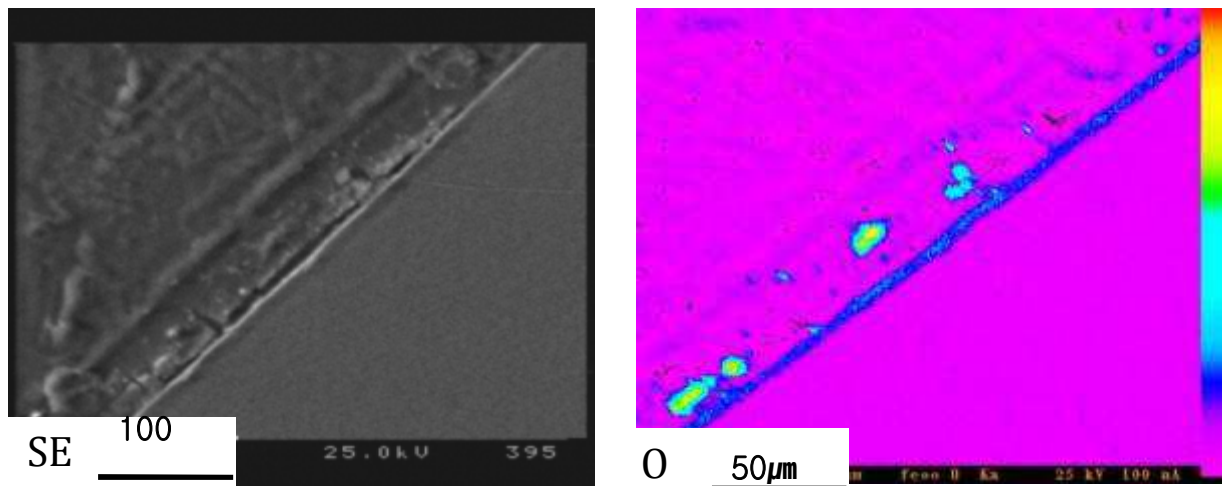


FIG. 9. CRUD sampling from 6,200 MWd/tU using cross-section clad.

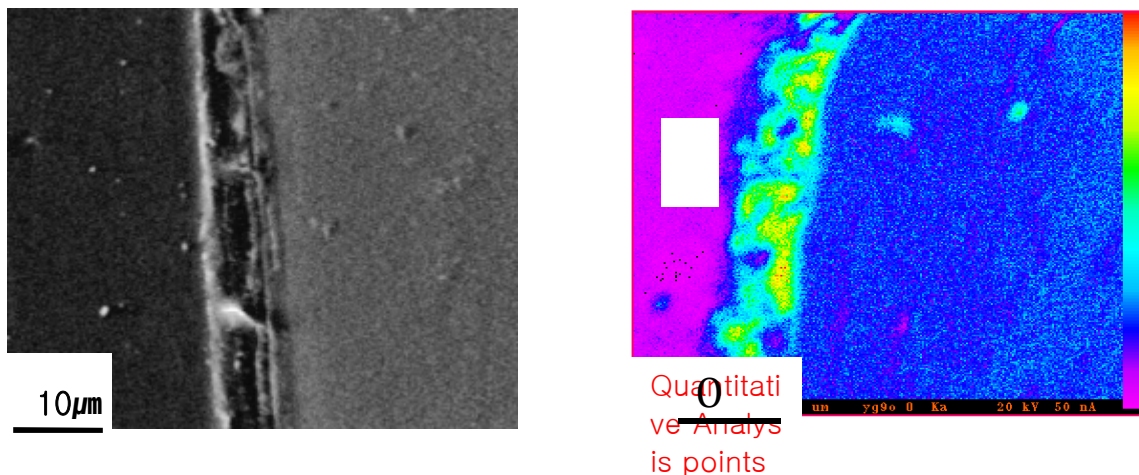


FIG. 10. CRUD sampling from failed fuel 5,300 MWd/tU using cross-section clad.

Figures 9–10 were obtained by analyzing a sample prepared for the process by which the fuel cladding tube was cut by a diamond saw, and inner nuclear fuel was removed. Such samples allow not only the exact investigation of thickness and shape of the portion of crud that is attached to the cross-section of the fuel cladding tube, but also provides an overview of the distribution of the crud. It was found for the figure the thickness and shape were well observed, and the composition gradient was highest according to the location but not with an

equally distributed iron. Not only the result of the analysis about oxygen and nickel on the same location, but also the result of the analysis about chromium, manganese, cobalt, and copper that are potential elements which could be made by corrosion or a corroded product from the primary water used at the common power plant as described in the Figs 9–10.

EPMA quantitative analysis results were executed by dividing part of crud that was 8 μm thick into 16 equal points. Changing the weight ratios of nickel, iron and oxygen, which are known as the main substances of crud, into an atom ratio resulted in a composition comprised of nickel: 16.13 at%, iron: 28.61 at%, and oxygen: 54.01 at%, although this result was similar to Trevorite (NiFe_2O_4). However, it is difficult to meet the sample size conditions required in XRD examinations under the environment that test part and test point are below several μm , so in order to tell exactly whether the crud compound of the test sample was Trevorite, a study is necessary.

3. CONCLUSION

The fuel specimen with 62,000 MWd/tU and the spent failed fuel rod with 53,000 MWd/tU by commercial PWR fuel were examined to compare with oxygen rich and average region at fuel-clad gap were performed to observe chemical behaviors and distributions of fission products on fuel-clad gap region by EPMA. A thin diamond wheel was cut off from a PWR fuel rod with the spent failed fuel rod with 53,000 MWd/tU and normal spent fuel rod with 62,000 MWd/tU from nuclear power plant were withdrawn and cooled down for 2 and 4 years respectively. The surface was ground and polished with 1 μm diamond paint as the final stage. The EPMA was performed on a CAMECA SX-60R equipped with two wavelength dispersive X-ray spectrometer shielded with tungsten. The analysis was performed with a beam current of 200 nA at an accelerating voltage 25 kV, in order to give a reasonable peak-to-background ratio for active specimen.

The concentration of O, Zr, U illustrate the general trend in fuel-clad gap region as shown in Fig. 4 compare to a high oxygen region as shown in Fig. 5. However, as shown in Fig. 5, the concentration distribution of Zr and U at the higher oxygen region is illustrating the general trend for redistribution in fuel-clad gap region. These results means, even at a high burnup stat in the 62,000 MWd/tU, the fuel-clad gap reliability seems to be appropriated condition. The xenon and cesium concentration profiles illustrate the general trend for release and cesium redistribution in fuel-clad gap region in 84 μm between clad to fuel. But, the oxygen and cerium concentration profiles illustrate remarkably different trend for oxygen fuel-clad gap region in 84 μm between clad to fuel. Oxygen concentration profile at an average region is about less than 6 μm compare to 20 μm at higher oxygen region between clad to fuel gap.

REFERENCES

- [1] YAGGEE, F.L., et al. "Characterization of Irradiated Zircalloys: Susceptibility to Stress Corrosion Cracking", EPRI NP-1155 (1979).
- [2] VAN DEN BERGHE, S., LEENAERS, A., Seminar NEA Proceedings on the PCI in Water Reactor Fuels, Aix-en-Provence, France, 266, 9-11 March 2004.
- [3] KLEYKAMP, H., "The Chemical State of the Fission Products in Oxide Fuels", J. Nuclear materials 131 (1985) 228.
- [4] KLEYKAMP, H., "The Chemical State of the Fission Products in Oxide Fuels", J. Nuclear materials 131 (1985) 230.
- [5] OLSEN, C.S., "The Performance of Defected Spent LWR Fuel Rods in Inert and Dry Air Storage Atmospheres," Nuclear Engineering and Design, 89, 51 (1985).

- [6] MIZUNO, T., WADA, K., IWAHORI, T., "Deposition Rate of Suspended Hematite in a Boiling Water System under BWR Conditions" Corrosion-NACE, 38, 1, 15 (1982).
- [7] PASUPATHI, V., STAHI, D., "Expected Performance of Spent LWR Fuel under Dry Storage Conditions" EPRI-Np-2735, 3-4 (1982).
- [8] ZIMA, G.E., "Comments on Fuel Crud as a Safety and Operation Factor of ISFSI". NUREG/CR-0615, 1-2 (1978).

EVALUATION OF CREEP DURING DRY STORAGE IN LOW AND HIGH BURNUP FUELS

F. FERIA, L.E. HERRANZ
Unit of Nuclear Safety Research, CIEMAT
Madrid
Spain

Abstract

There is a general agreement that cladding creep rupture is the most likely and limiting failure mechanism of spent fuel in dry storage compared to other potential mechanisms, like stress corrosion cracking and/or delayed hydride cracking. Nevertheless, occurrence of creep rupture is very improbable since both decay heat and hoop stress decrease along dry storage. In spite of this, the current trend to higher burn up levels has drawn further attention to ensure a safe storage of spent fuel irradiated over 45 GWd/tU. This paper analyses the effect of burnup on creep evolution during dry storage. To do this, the FRAPCON-3.3 code capabilities have been extended to model fuel rod creep under dry storage conditions. Two postulated representative scenarios of Zircaloy-4 fuel rods irradiated to 45 GWd/tU and 63 GWd/tU have been simulated and the results obtained have been analyzed and compared. According to this study, creep is substantially affected by burnup. As a consequence, safety assessments of fuel rod integrity under dry storage conditions need to be extended to encompass anticipated fuel rod burnups in upcoming years.

1. INTRODUCTION

Several potential threats are postulated to can jeopardize cladding integrity over the projected dry storage life of nuclear fuel: creep-driven clad deformations and subsequent rupture and loss of cladding integrity due to mechanisms as delayed hydride cracking (DHC) and/or stress corrosion cracking (SCC). Several studies [1–2] have shown that the combined effect of decay heat and cladding hoop stress increase from internal pressurization, turn creep rupture into the most likely fuel failure mechanism. Despite its very low probability, new cladding materials (i.e., ZIRLO, M5), conditions under reactor operation and high burnup, recommend creep studies to be updated to confirm the expected sound behaviour of nuclear fuel cladding under dry storage conditions.

“In reactor” conditions are so different from dry storage ones that an extrapolation of “in-reactor” studies is not allowed, at least without a thorough validation. Dry storage conditions entail cooling periods that extend at least for a few decades, which makes prototypical testing not straightforward. However, some data have been obtained from tests as representative as possible and creep laws have been derived for the current available zirconium alloys [3–5]. Implementation of these laws into fuel performance codes may enable these tools to deal with these new challenging scenarios while benefiting from the extensive modelling effort done previously. Nevertheless, such extensions will require a detailed analysis of the results as well as a data-predicition comparison whenever feasible.

In this work two postulated scenarios are simulated and compared to assess the effect of burnup on the fuel rod response to a similar history of dry storage. An adaptation to dry storage of the FRAPCON-3.3 code has been used to model the behaviour of a 45 GWd/tU and 63 GWd/tU Zircaloy-4 fuel rods under a 1-year cooling within fuel storage pool followed by a 1-day heat-up during the fuel rod drying process and up to 2-year dry storage. As the FRAPCON-3.3 adaptation to dry storage conditions has been presented elsewhere [6], here a mere short description will be done to make the paper self-consistent.

2. EXTENSION OF CREEP LAW

2.1. In-FRAPCON modelling

The FRAPCON-3.3 mechanical model considers three contributions to cladding deformation: elastic and plastic deformations (ε^e and ε^p , respectively) and thermal expansion (ε^T). Therefore, deformation components along each space direction (i.e., radial, axial and azimuthal) may be generally expressed as:

$$\varepsilon_i = \varepsilon_i^e + \varepsilon_i^p + d\varepsilon_i^p + \varepsilon_i^T \quad i = \theta, z, r \quad (1)$$

It is worth to note that the plastic strain is calculated in an incremental way [7], and it is in the calculation of that increment ($d\varepsilon_i^p$) where creep ($\dot{\varepsilon}_c$) is considered as a source of plastic deformation:

$$d\varepsilon^p = dt \cdot \dot{\varepsilon}_c \quad (2)$$

Based on data taken from fuel rods under reactor operation conditions [8,9,10], the creep strain rate is calculated through a function in which the hoop stress, temperature and flux effects are factorized,

$$\dot{\varepsilon}_c = \frac{4}{\varepsilon_c} (f_1(\sigma_\theta) \cdot f_2(T) \cdot f_3(\phi))^2 \quad (3)$$

In this equation ε_c is the total accumulated creep strain and functions f_1 , f_2 and f_3 correlate fast neutron flux, temperature and hoop stress dependencies, as follows,

$$f_1(\sigma_\theta) = \sigma_\theta + 725.2 \exp(4.967 \cdot 10^{-8} \sigma_\theta) \quad (4)$$

$$f_2(T) = \exp(-10000 / RT) \quad (5)$$

$$f_3(\phi) = 5.129 \cdot 10^{-29} \phi \quad (6)$$

where ϕ is the fast neutron flux ($\text{n/m}^2\text{s}$), T is the cladding average temperature (K), R is the universal gas constant ($\text{cal/mol} \cdot \text{K}$) and σ_θ is the hoop stress (Pa).

This expression applies to Zircaloy-2 and its validity domain range is defined by the following intervals: $\phi = 0-3.1 \cdot 10^{17} \text{ n/m}^2\text{s}$, $T = 260-300^\circ\text{C}$, $\sigma_\theta = 100-300 \text{ MPa}$. Strictly speaking, its application should be restricted to “in-reactor” conditions. Therefore, the extension of the FRAPCON-3.3 mechanical model with a suitable creep model for dry storage is indispensable if the code use is to be enlarged to the dry storage domain.

2.2. Database and correlation

As said above, the development of a creep law for dry storage is based on experimental results obtained from tests as representative as possible. A literature review shows several significant data sources of the mechanical response of current zirconium alloys (Zircaloy-4, Zircaloy-2, ZIRLO) to creep tests under internal pressure [5,11–13]. Given the large database gathered by

EDF for SRA Zircaloy-4 and its comprehensive reporting [5], it has been adopted as a basis to extend the creep law within the FRAPCON-3 code. The test conditions of all those experiments are shown in Table 1.

TABLE 1. EDF CREEP TEST CONDITIONS

	As-received	Irradiated
Hoop stress (MPa)	55-200	121-225
Temperature (°C)	350-420	380-420
Fast fluence (n/cm ²)	0	(1.8-9) × 10 ²¹
Duration (hours)	0-16000	0-1000

In order to fit these experimental data, the Zircaloy creep strain can be expressed through a generic expression like,

$$\varepsilon^c = \varepsilon_p^c + \varepsilon_s^c \quad (7)$$

where ε_p^c is the primary creep and ε_s^c is the secondary creep. These two contributions can be generically factored in individual terms of a few key variables like hoop stress, σ_θ , temperature, T, fast neutron fluence, ϕt , and time, t:

$$\varepsilon_i^c = f_{1i}(\sigma_\theta) \cdot f_{2i}(T) \cdot f_{3i}(\phi t) \cdot f_{4i}(t) \quad i = p, s \quad (8)$$

In the absence of fast neutron flux in the case of dry storage, the effect of prior irradiation hardening is supposed to be embeded within the other individual functions (f_{1i} , f_{2i} and f_{4i}).

2.3. CIEMAT creep law

With the aim to reduce the complexity and parameterization of creep laws in the literature [5] and keep at the same time a reasonable accuracy and a robust behavior [6], a creep law of a similar structure to the one within the FRAPCON-3.3 code for in-reactor conditions is proposed:

$$\varepsilon_\theta = f_1(\sigma_\theta) \cdot f_2(T) \cdot f_3(\phi t) \cdot t^{-0.5} \quad (9)$$

where

$$f_1(\sigma_0) = \frac{a}{2} \sigma_0^b \quad (10)$$

$$f_2(T) = \exp\left(\frac{-c}{T + 273}\right) \quad (11)$$

$$f_3(\phi t) = \exp(-d \cdot \phi t) \quad (12)$$

According to the database available, the parameters' fitting was done separately for as-received and irradiated material. Table 2 shows the values of the parameters associated to the best fitting of the equations (10–12). Accuracy of the resulting expressions has already been demonstrated in [6].

TABLE 2. PARAMETERS OF CIEMAT CREEP LAW

Parameter	As-received	Irradiated
a	$6 \cdot 10^4$	300
b	1.84	2.95
c	15000	15000
d	0	$2.8 \cdot 10^{-22}$

2.4. Implementation

The equation (9) has been implemented in the FRAPCON-3.3 mechanical model together with a suitable logic that allows choosing between the “in-reactor” equation and the dry storage equation implemented, according to the prevailing conditions at the calculation time. Depending on the databases used, the dry storage equation has been implemented within FRAPCON-3.3 split in two hoop stress ranges:

- $\sigma_0 \geq 121$ MPa, where equation (9) parameters have been derived based on information from irradiated claddings;
- $\sigma_0 < 121$ MPa, where equation (9) parameters have been derived from as-received material data (no experimental data is available with irradiated material under low hoop stress).

3. CREEP ASSESSMENT

3.1. Postulated scenarios

In order to illustrate fuel rod response under dry storage conditions, the FRAPCON-3.3 adapted version has been used to simulate two postulated scenarios:

- (a) A Zircaloy-4 fuel rod irradiated to 45 GWd/tU;

(b) A Zircaloy-4 fuel rod irradiated to 63 GWd/tU.

All the fuel rods history has been simulated, from the in-reactor irradiation to dry storage cooling (2 years), going through a 1 year cooling in the fuel storage pool and even the anticipated heat-up during the 1 day dry out process. The average linear power imposed in each case and the normalized temperature decay with respect to the dry out highest temperature are represented in Figs 1–3, respectively.

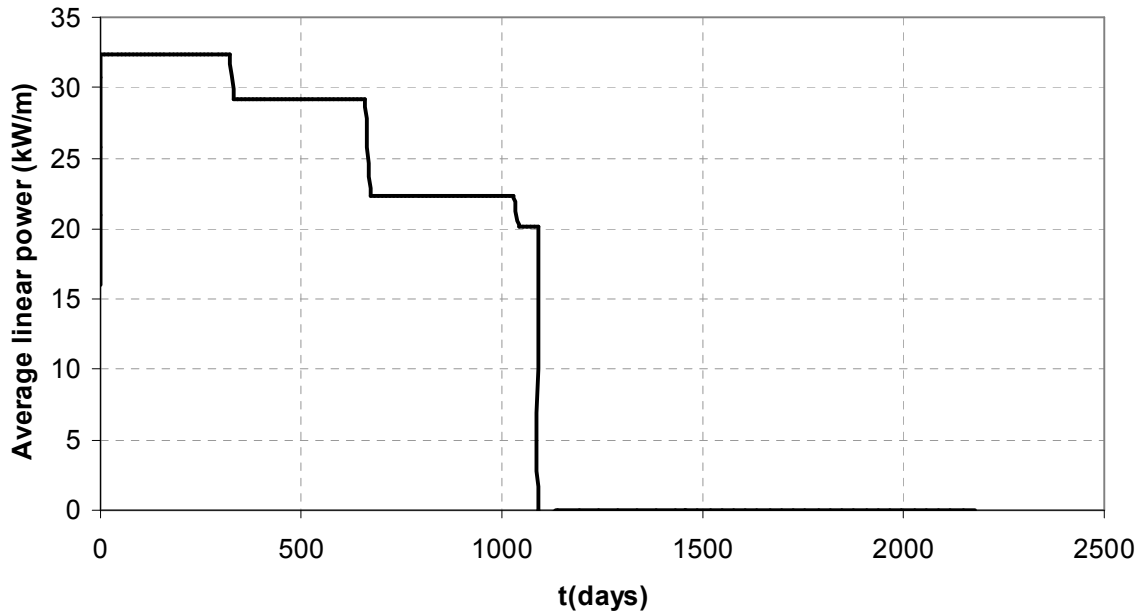


FIG. 1. Average linear power vs time for scenario a).

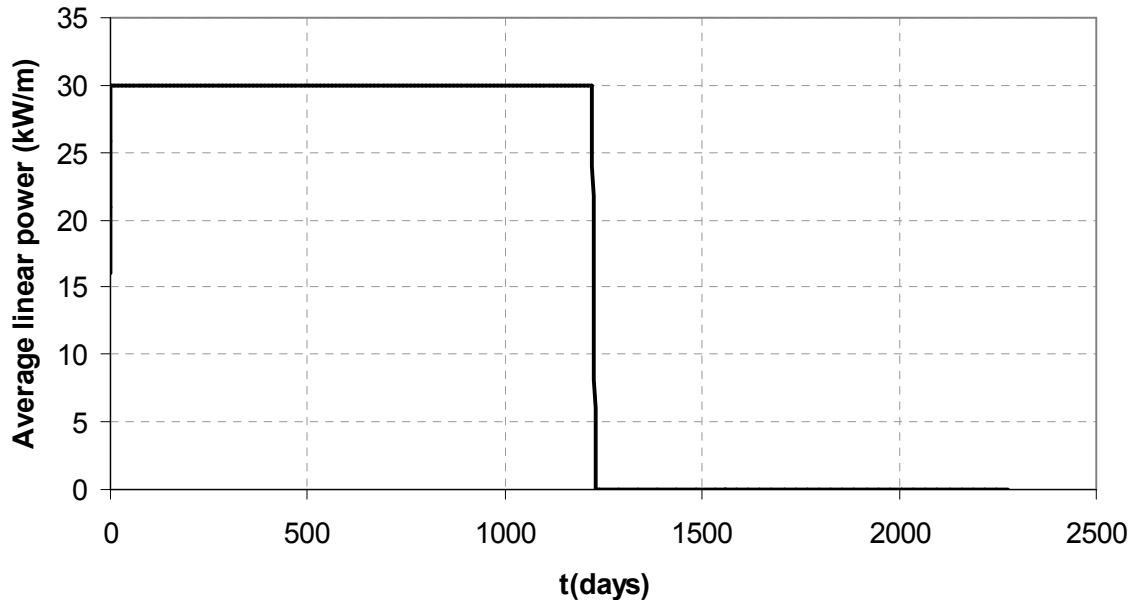


FIG. 2. Average linear power vs time for scenario b).

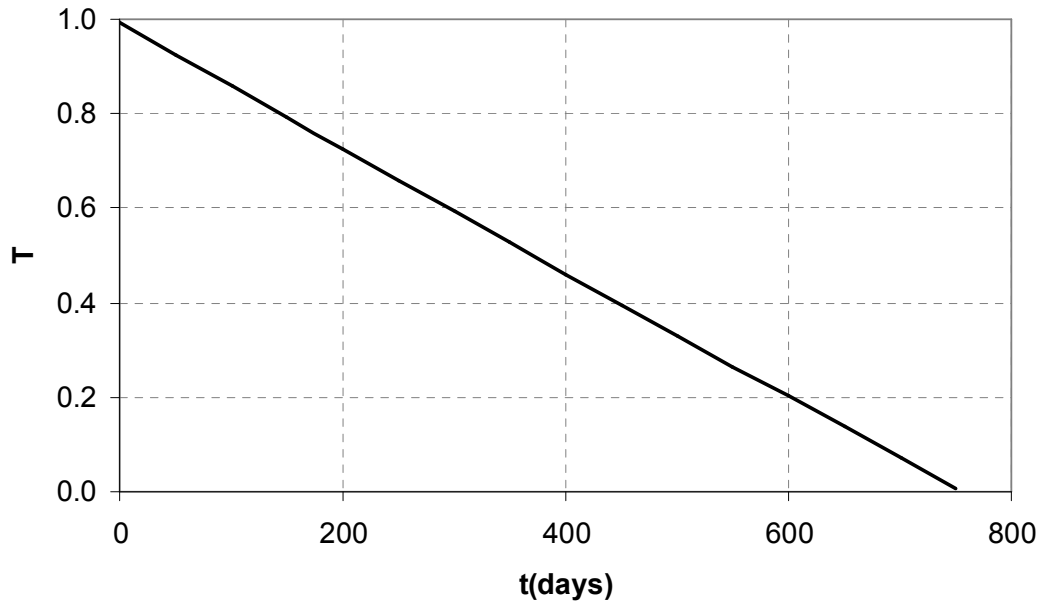


FIG. 3. Normalized temperature decay during dry storage period.

3.2. Results and discussion

The results obtained have been presented in Figs 4–5 in terms of hoop strain evolution. It is shown that once dry storage starts hoop stress causes a positive plastic deformation rate that causes a creep-out situation. This increase of hoop strain is maintained, although at different rates, all over the calculated time.

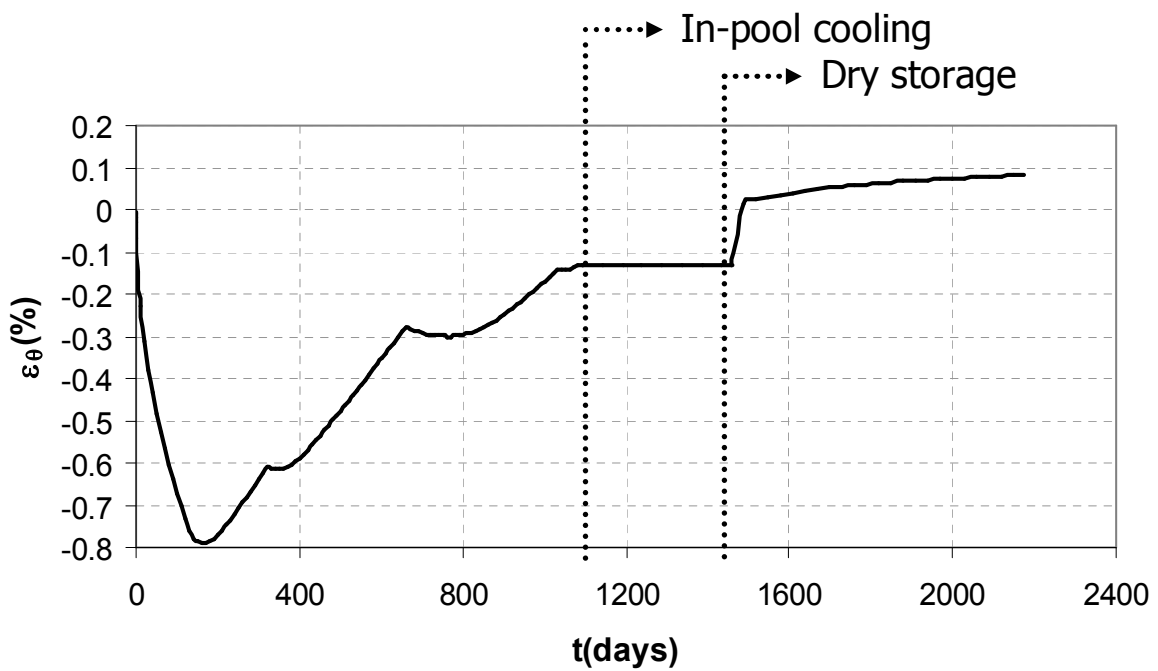


FIG. 4. Creep hoop strain vs time for scenario a).

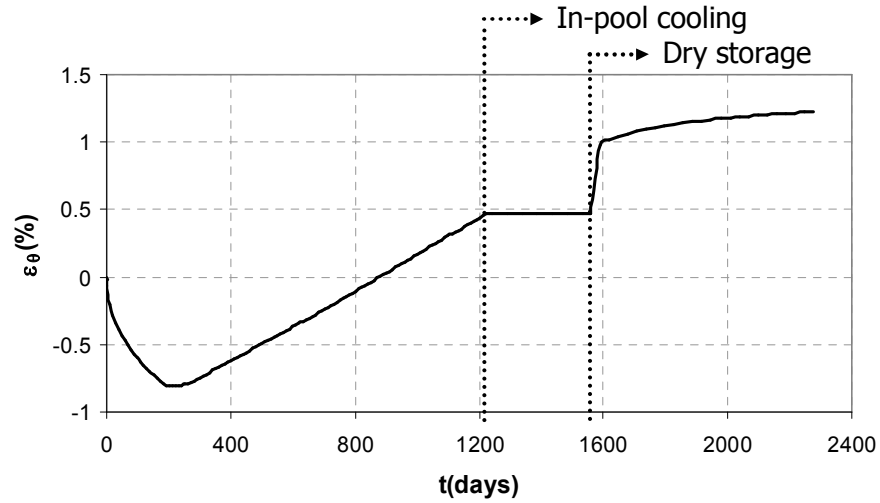


FIG. 5. Creep hoop strain vs time for scenario b).

In Fig. 6 it is represented the hoop creep strain evolution along the dry storage period for the two postulated scenarios. It is observed that the main impact of creep would take place during the first years of dry storage, as expected. As a matter of fact, the highest contribution to the final dry storage creep is reached in both scenarios in less than about two months since the drying process. Furthermore, even in the most challenging scenario investigated (63 GWd/tU), the hoop strain is far from 2% (strain limit [14]) in the period calculated. This together with the asymptotic trend allows stating that fuel rod integrity would not be jeopardized by creep during dry storage.

Finally, it is worth to note that in Fig. 6 the creep associated to the simulation of the scenario a is lower than the one associated to the scenario b (nearly 4 times higher hoop strain as burnup is increased by 40%). This result makes sense from the point of view of the hoop stress applied in each case: around 40 MPa in a and 90 MPa in b. It is worth noting that these hoop stresses entail that the FRAPCON-3.3 adapted version took the equation (9) based on non-irradiated material, so that the relaxing effect of irradiation on hoop stress is not considered. Hence, those results would have a conservative nature.

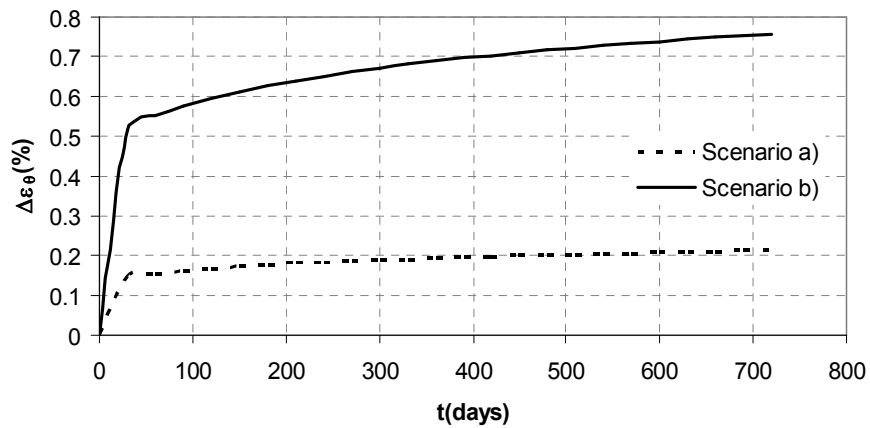


FIG. 6. Creep evolution during dry storage.

4. CONCLUSIONS

In this study it is shown that high burnup effect seems substantial and causes major differences in the nuclear fuel response in terms of creep. The results obtained could change by consider the irradiation hardening effect but it is not included in the CIEMAT creep law at low hoop stresses because of the lack of experimental data.

Therefore, further work is foreseen to keep on extending CIEMAT creep law to irradiated fuel rods submitted to low stresses. Moreover, it would be interesting to extend this study up to 100 years, so that the final creep asymptotic value can be estimated.

ACKNOWLEDGEMENTS

The authors wish to thank ENRESA, particularly P. Zuloaga and F.J. Fernández, for their technical contributions and, no less important, for their financial support.

REFERENCES

- [1] CUNNINGHAM, M.E., SIMONEN, E.P., ALLEMANN, R.T., LEVY, I.S., HAZOLTON, R.F., PNL 6364 (1987).
- [2] PEEHS, M., GARZAROLLI, F., GOLL, W., IAEA-TECDOC-1089, p. 313, Vienna (1999).
- [3] GRAS, J. M., Entreposage Des Combustibles Usés. BILAN DU PPRD T4-97-07, EDF, Janvier (2000).
- [4] LIMON, R., CAPPELAERE, C., BREDEL, T., A Formulation of the Spent Fuel Cladding Creep Behavior for Long Term Storage. LWR Fuel Performance Meeting, Park City, Utah, April 10–13 (2000).
- [5] BOUFFIOUX, P., Transportation and interim dry storage of PWR's spent fuel. EDF report, HT25-C2005-192/PBF (2005).
- [6] HERRANZ, L.E., FERIA, F., Extension of the FRAPCON-3.3 creep model to dry storage conditions. Progress in Nuclear Energy. In press (2010).
- [7] BERNA, G. A., BEYER, C. E., DAVIS, K. L., LANNING, D. D., FRAPCON-3: A computer code for the calculation of steady-state, thermal- mechanical behavior of oxide fuel rods for high burnup. NUREG/CR-6534, Vol. 2 (1997).
- [8] ROSS-ROSS, P.A. AND HUNT, C.E.L., The in-reactor creep of cold-worked Zircaloy-2 and Zirconium-2.5 wt% Niobium pressure tubes. Journal of Nuclear Materials, **26**, 2-17 (1968).
- [9] IBRAHIM, E.F., In-Reactor tubular creep of Zircaloy-2 at 260–300°C. Journal of nuclear Materials, **43**, 169-182 (1973).
- [10] FIDLERIS, V., Summary of experimental results on in-reactor creep and radiation growth of zirconium alloys. Atomic Energy Review, **13**, 1, 51-80 (1976).
- [11] ITO, K., KAMIMURA, K., TSUKUDA, Y., Evaluation of irradiation effect on spent fuel cladding creep properties. Proceedings of the 2004 International Meeting on LWR Fuel Performance - Orlando, Florida, September 19-22 (2004).
- [12] TSAI, H. AND BILLONE, M.C., Thermal creep of irradiated Zircaloy-4 cladding. ASTM-STP 1467 – pp. 632–650 (2006).
- [13] QUECEDO, M., LLORET, M., CONDE, J.M., ALEJANO, C., GAGO, J.A., FERNÁNDEZ, F.J., Results of thermal creep test on highly irradiated ZIRLO. Proceedings of the International LWR Fuel Performance Meeting, Seoul, Paper 8063 (2008).
- [14] GOLL, W., SPILKER, H., TOSCANO, E., Short-time creep and rupture tests on high burnup fuel rod cladding. Journal of Nuclear Materials, **289** (3), 247-253 (2001).

MATERIALS PERFORMANCE AND AGING CONSIDERATIONS FOR POWER AND RESEARCH REACTOR SPENT NUCLEAR FUEL IN STORAGE SYSTEMS

R.L. SINDELAR, N.C. IYER, T.M. ADAMS, G.T. CHANDLER
Savannah River National Laboratory
Aiken, SC
USA

Abstract

The primary aging consideration in the management of spent nuclear fuel⁴ is to limit its degradation throughout the storage period. Excessive degradation of the spent nuclear fuel can impact the functions important to safety including thermal performance, radiological protection, confinement, sub-criticality, and retrievability that are explicit in regulatory requirements for storage. The aging phenomena that can cause degradation of power reactor (PR) fuel clad with zirconium alloys in water pool storage and in dry storage systems are summarized and compared to those phenomena important to cause degradation of research reactor (RR) fuel clad with aluminum alloys. Limits to additional degradation of spent nuclear fuel in storage to maintain safety are achieved through controls to the environments of storage. Corrosion, with its various modes of attack, is the primary concern for RR spent nuclear fuel in water pool storage. Water quality is controlled (for RR fuel) to avoid corrosion degradation and enable many decades of safe water pool storage. There are several degradation phenomena at normal and off-normal storage conditions that could lead to a large failure of the fuel in dry storage or post-storage handling. These include creep (of PR and RR fuel), corrosion (of PR and RR fuel), hydrogen-related phenomena, including embrittlement and delayed hydride cracking (of PR fuel), and oxidation of fuel pellet (of PR fuel). A storage system design to limit the fuel storage temperature and minimize amount of corrosive species, including water and air, would allow only minimal additional fuel degradation from its initial post-reactor condition, and thereby avoid cladding degradation leading to rupture. Limits to the environmental parameters for dry storage are dependent on the initial materials' condition of the fuel including composition, microstructure, and wastage (loss of net section) of the cladding as a result of its in-reactor operation and post-reactor handling history.

1. INTRODUCTION

Spent nuclear fuel discharged from both power reactors (PR) and research reactors (RR) is cooled in a water pool and may continue to be stored in the pool. In the U.S., power reactor fuel was originally intended to be stored in the water pool several years prior to reprocessing. However, the U.S. has followed a "once-through" nuclear fuel cycle strategy since the late 1970s, and this has led to interim storage in full pools or soon-to-be full pools at most of the U.S. reactor sites, and the design and deployment of dry storage systems licensed by the U.S. Nuclear Regulatory Commission (NRC) to continue to store PR fuel. Furthermore, at present, the U.S. is in the process of re-evaluating its fuel cycle strategy, and the need for continued storage is apparent.

The U.S. Department of Energy's Environmental Management (DOE-EM) Program is responsible for the receipt and storage pending disposition of spent nuclear fuel that was used in research and test reactors worldwide, and that contains U.S. origin and certain non-U.S.

⁴ Used Nuclear Fuel or Used Fuel (UF) is the term recently adopted by U.S. Department of Energy - Office of Nuclear Energy to reflect that additional energy in the form of enriched uranium and plutonium remain in fuel presently discharged from commercial power reactors, and would be available to be recovered through reprocessing. Fuel that has little or no energy value would be termed "spent". It is recognized that the present body of information including international publications and regulations use the term "spent nuclear fuel" for discharged fuel, regardless of its energy value, and this term is used in this report.

origin enriched uranium. The foreign and domestic RR fuel is primarily aluminium-based, aluminium-clad fuel that is being stored in L-basin, a water basin or pool at the Savannah River Site (SRS). Additionally, aluminium fuel, the majority of which originated from the Advanced Test Reactor, is in both wet and dry storage in the CPP-666 basin and the Irradiated Fuel Storage Facility (IFSF), respectively, at the Idaho Nuclear Technology and Engineering Center (INTEC) at the Idaho National Laboratory.

Figure 1 shows pictorially the options of wet storage and dry storage common to RR and PR spent nuclear fuel.

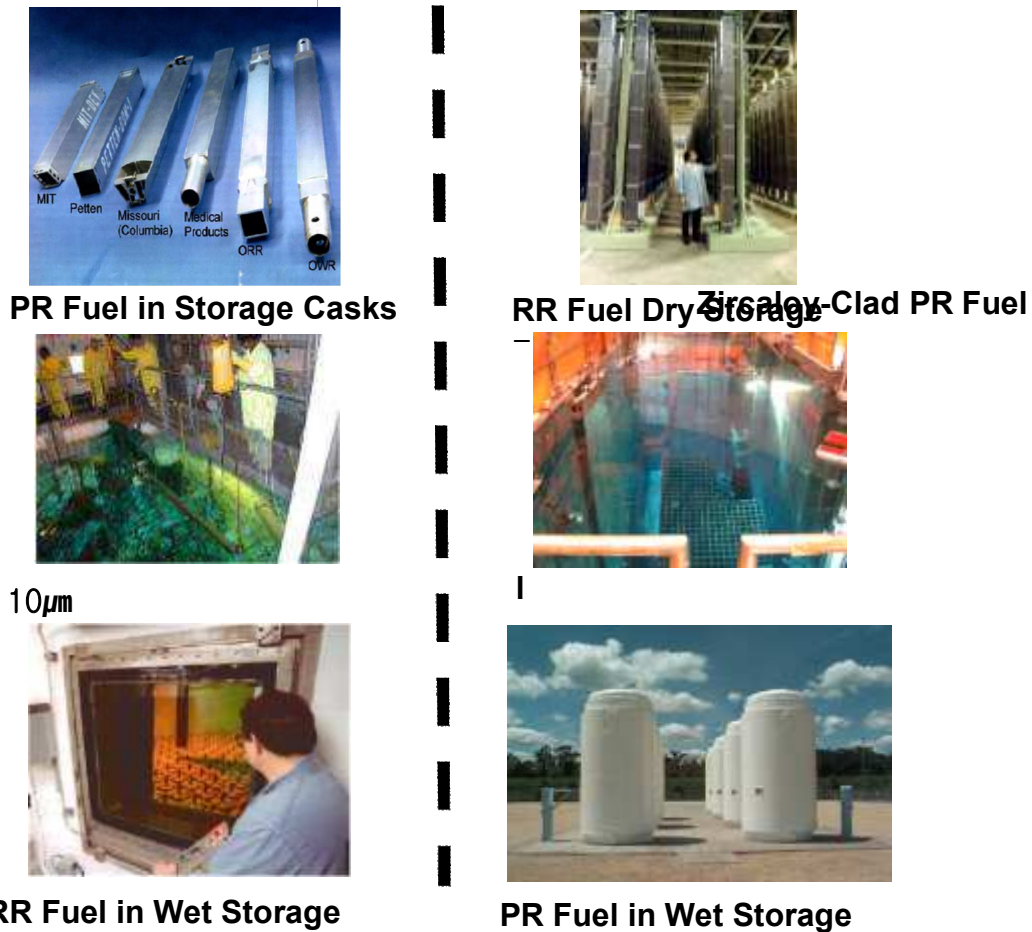


FIG. 1. Interim storage options for research reactor (RR) fuel and power reactor (PR) fuel are wet pool storage and dry storage [photographs from open web sites].

Technical bases for the demonstration that the fuel storage systems would continue to satisfy the safety-related requirements by regulatory authorities for PR fuel, and maintain safe storage as expected by the U.S. DOE for RR fuel, are predicated upon the satisfactory performance of materials in consideration of the effects of time, temperature, radiation field, and environmental conditions of normal service and off-normal design basis events. This paper summarizes the degradation phenomena that can impact zirconium and aluminium cladding alloys in wet and dry environments of storage for spent nuclear fuel.

2. WATER POOL STORAGE

Both PR and RR fuel claddings are degraded to an extent as a result of reactor operation. Zirconium alloys are susceptible to oxidation and hydride formation in water at PR temperatures that can lead to embrittlement and cracking. Loss of ductility is also incurred from radiation damage of the cladding. The extent of oxidation, hydride formation, and the loss of mechanical stability of the fuel cladding with burnup are important considerations for further degradation in storage. Once hydrogen has been incorporated into the metal, Delayed Hydride Cracking (DHC) can produce structural failure of zirconium alloy components even down to room temperature. Nevertheless, for storage of zirconium alloys at low temperatures in the water pool, the water quality does not require stringent controls to avoid attack. Many years of pool storage experience in the U.S. alone of nearly 200,000 assemblies of PR spent nuclear fuel with no reported failures is a strong service record that there is no significant degradation of PR spent nuclear fuel in water pools [1]; however detailed examination of the fuel following extended low temperature water exposure to check for additional degradation has not been performed.

Similar to the feature of passive film (ZrO_2) formation on zirconium alloy cladding on PR fuel in reactor operation, an adherent, passive film of Boehmite ($\gamma\text{-AlO(OH)}$ or $\text{Al}_2\text{O}_3 \cdot \text{H}_2\text{O}$) is formed on the aluminium alloy cladding on RR fuel [2]. In contrast to zirconium-alloy-clad PR fuel, however, specifications for water quality⁵ are needed for storage of aluminium-clad RR fuel in water to avoid aggressive corrosion attack [2]. Where water quality is poor, the aluminium alloys are subject to localized corrosion (pitting, crevice) and galvanic attack sufficient to cause through-clad breaches within months of exposure. Where the water chemistry has been well controlled, aluminium alloys show few, if any, signs of either localized or general corrosion, even after more than 40 years of exposure to pool water.

Section 2.1 is a summary of the degradation phenomena for wet storage of PR fuel clad with zirconium alloys, and section 2.2 is a summary of the degradation phenomena for wet storage of RR fuel clad with aluminium alloys.

2.1. Zirconium cladding alloys in water

Zirconium cladding alloys are subject to oxidation and hydride formation, which essentially happen in water only at power reactor operating temperatures. The extent of oxidation and hydride formation depends on metallurgical characteristics, such as alloy composition, thermo-mechanical treatments, microstructure, texture, welds, and residual stresses. Fig. 2 shows a cladding microstructure with circumferentially-oriented hydrides produced during reactor operation.

Once hydrogen has been incorporated into the metal, a process called delayed hydride cracking (DHC) can produce structural failure of zirconium alloys components in a wide temperature range, if the right conditions (hydrogen content and susceptible material) are present [4]. Crack propagation is even possible at room temperature with the marginal amount of hydrogen incorporated during fabrication. Nevertheless, keeping the conductivity and water temperature low in pool storage will minimize the intensity of electrochemical reactions which could generate additional hydrogen in the cladding as part of the metal oxidation process [5].

⁵ Water quality is defined by a set of parameters that are used to characterize the water physical and chemical conditions. It includes pH; conductivity; dissolved impurity species; undissolved solids; colloids; organic substances; biological organisms; and temperature

There are typically no technical specifications or requirements for water chemistry to mitigate corrosion of zirconium alloys in pool storage due to the relatively innocuous environment of low temperature water exposure vis-à-vis reactor operation that causes corrosion attack and hydrogen ingress. Water control is required in pool storage, however, to limit water radioactivity levels [6].

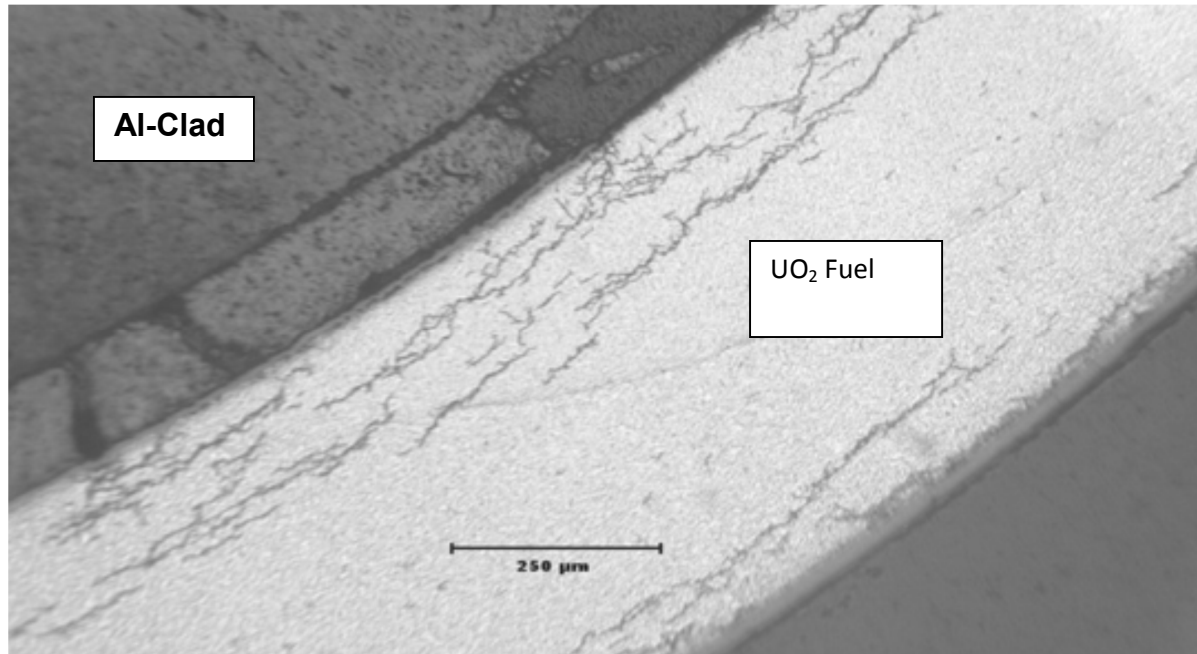


FIG. 2. PR fuel clad cross section showing circumferential hydride microstructure in zircaloy cladding on spent nuclear fuel (from Ref. 3).

2.2. Aluminium cladding alloys in water

Aluminium cladding alloys in water pool storage are susceptible to rapid corrosion attack if the water is of poor quality. Fig. 3 shows an example of the corrosion attack on two Materials Test Reactor design (multiple fuel plates in a “box” assembly) assemblies that had been stored for between 12–26 years in poor quality water.

The following is a list of potential corrosion modes of attack, and, except for stress corrosion cracking and erosion-corrosion, have been observed in aluminium alloy cladding of RR fuel as a result of water storage in poor water quality conditions [2]:

- (1) General corrosion;
- (2) Pitting corrosion;
- (3) Crevice corrosion;
- (4) Galvanic corrosion;
- (5) Intergranular corrosion
- (6) End-grain attack
- (7) Blister formation;
- (8) Microbial corrosion,
- (9) Sediment-induced corrosion;
- (10) Stress corrosion cracking
- (11) Erosion-corrosion.

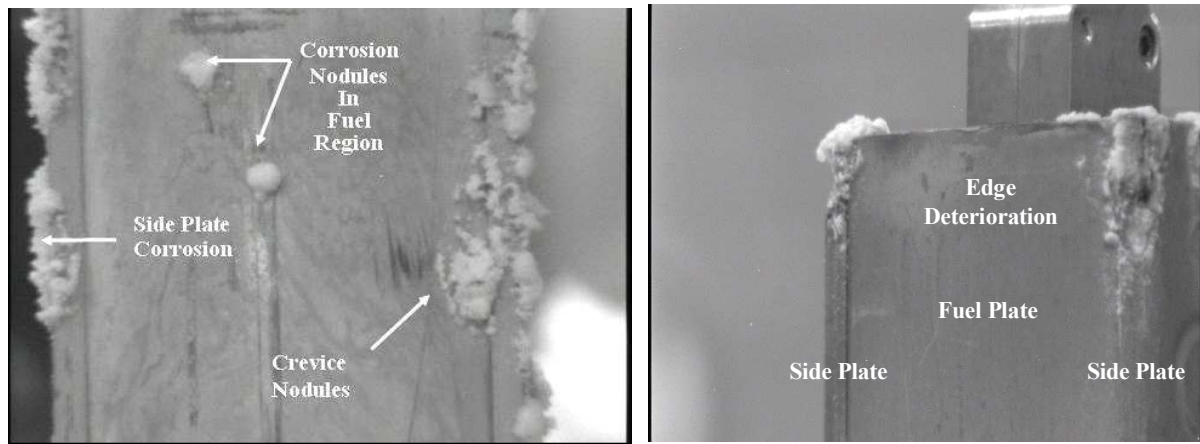


FIG. 3. Aluminum-based, aluminum-clad spent nuclear fuel in moderately degraded condition post-irradiation and storage in a basin with poor water quality (~ 80 – 170 $\mu\text{S}/\text{cm}$ during storage) storage conditions. The photographs show (a) corrosion product evidence of pitting corrosion attack and crevice corrosion attack; and (b) evidence of galvanic attack with the two different aluminum alloys coupled at the location of the fuel plate and side structural plate (SRNL photographs).

TABLE 1. RECOMMENDED PHYSICAL-CHEMICAL PARAMETERS, LIMITS, AND MONITORING FREQUENCIES FOR WATER IN FUEL DECAY AND STORAGE BASINS (FROM REFERENCE 2)

PARAMETER	VALUE (LIMIT)	MONITORING FREQUENCY
pH	4.5–7	Weekly
Conductivity	< 10 $\mu\text{S}/\text{cm}$	Weekly
Solids	< 5 mg/l	Every 6 months
Cu Concentration	< 0.1 mg/l	Every 6 months
Cl Concentration	< 0.1 mg/l	Every 6 months
Nitrate (NO_3^-), mg/l	< 10 mg/l	Every 6 months
Sulphate (SO_4^{2-}), mg/l	< 10 mg/l	Every 6 months
Fe Concentration	< 1.0 mg/l	Every 6 months
Al Concentration	< 1.0 mg/l	Every 6 months
Temperature	$< 45^\circ\text{C}$	Monthly
Radioactivity level (*)	(see note below)	Weekly
Turbidity (**)	(see note below)	

(*) Water Radioactivity level and the presence of radioisotope species should be measured each time a water sample is drawn or one time per week. A gamma scan is recommended to measure the presence of radioisotopes that would have come from failed fuel (e.g., Cs-137). No specific limits are set. The presence of radioisotope species should be evaluated on case-by-case basis. Measurement of the activity from filters and resin columns should be performed to detect the presence of leaking fuel.

(**) Turbidity should be reduced, as necessary, to provide visual clarity in the water system.

A recent publication by the IAEA [2] contains recommended practices for water quality management in RR systems and describes the above corrosion modes in detail for aluminium alloys. Table 1 below, reproduced from Reference 2, is a list of the water quality parameter limits for aluminium clad fuel in water pool storage to avoid corrosion. Reference 2 also includes case studies of research reactor fuel storage experience, and recommended protocols for corrosion surveillance programs in research reactor water systems including primary and secondary reactor cooling circuits.

3. DRY STORAGE

An important first step to minimize degradation in a dry storage system is the drying of the spent nuclear fuel before it is placed in a sealed canister with an inert cover gas for storage. Zirconium cladding alloys are resistant to corrosion in storage pool water and water vapor, with a low corrosion rate. Further, there are no hydrated zirconium oxides on cladding alloys, and therefore no chemically-bound water challenges the drying of the fuel. It is important however that the drying protocol for PR fuel be performed so as to avoid redistribution of hydrides from circumferential orientation to a radial orientation that would cause a brittle structure with a potential to split the cladding [7]. Qualitatively, existing hydrides would tend to dissolve in cladding brought to very high temperatures during drying, and radially-oriented hydrides would form under a slow cool with high hoop stresses.

Drying of aluminum alloy clad RR fuel is more challenging than PR fuel. As stated above, bound water as a result of reactor operation is present on the fuel. If water remains with the fuel/canister configuration, material interactions may result in fuel corrosion damage, fuel container corrosion damage, criticality safety issues, generation of flammable gases (hydrogen), or formation of pyrophoric species (uranium hydride).

To mitigate these issues in dry storage of PR and RR spent nuclear fuel, it is important to remove the water from the fuel and canister system to the extent practicable. The total amount of water associated with a spent fuel and canister system are from three basic sources. These are: 1) free water that includes water in pits in the cladding, crevices, etc.; 2) waters of hydration on existing oxyhydroxides (chemisorbed water); and 3) adsorbed waters on oxyhydroxides and on aluminium metal and other materials in the system (physisorbed water). Material-specific considerations and general guidelines for drying of spent nuclear fuel for various cladding alloys have been developed [8].

A time-temperature recipe for use in a drying system for a specific fuel, for example RR plate fuel, is highly dependent on the following factors:

- Fuel configuration (e.g., plate fuel with crevices);
- Fuel condition (e.g., fuel with various oxyhydroxides of various thickness containing chemically-bound and adsorbed waters, and with debris on fuel); and
- Configuration of the fuel-in-canister system to be dried (e.g., large canister).

Decomposition of Boehmite to release its water is not practical since a temperature of approximately 500°C would be required [8]. Free water removal to avoid extensive corrosion (e.g., that would occur if aluminium fuel were to be in a canister with bulk free water) is the primary concern.

A fuel drying station has been developed [9] and is in use at INTEC for aluminium spent fuel to remove free water from the plate fuel [10]. The aluminium fuel being stored at INTEC in the Irradiated Fuel Storage Facility in CPP-603 is in a vented (non-sealed) dry storage system to mitigate the potential issue of hydrogen generation from corrosion or radiolytic reactions with the bound water in the oxyhydroxides. Aluminium spent fuel has also been dry stored in other countries including Canada and Australia [11].

Section 3.1 is a summary of the degradation phenomena for dry storage of PR clad with zirconium alloys, and section 3.2 is a summary of the degradation phenomena for dry storage of RR fuel clad with aluminium alloys.

3.1. Zirconium-alloy-clad PR fuel in dry storage

Dry storage of PR fuel in the U.S. is subject to NRC regulations that include explicit consideration of degradation of the fuel and systems, structures, and components (SSCs) of the dry storage system throughout the storage period. Design criteria [12] and licensing/regulatory requirements [13] for dry storage facilities and with extended operation [14–15] include safety-related consideration of the effects of time, temperature, radiation field, and environmental conditions of normal and off-normal service. Standard Review Plans have been provided by the U.S. NRC for initial license application [16] and license renewal [17] to demonstrate that the safety functions of the regulatory requirements are met by the materials of a dry storage system.

To date, the body of information to support safe dry storage of PR fuel was established in the context of relatively short term tests and experience and would support ~60 years storage of low burnup (< 45 GWd/MtU) fuel [3]. As PRs increase fuel burnup, and national program uncertainties continue to delay fuel disposition, the regulations and the compliance methods used to grant licenses may require additional investigation. Quantification of degradation, including predictive models that are well-accepted by consensus bodies, is important to obtain NRC approval of extended dry storage systems.

Dry storage of the PR fuel is challenging due to elevated temperatures when removed from cooling water pools and initially placed in storage systems with fuel compacted in canisters and placed in shielded casks or other systems. Elevated temperatures effectively pressurize the pins and stress the cladding. Creep of the cladding is the primary mechanism that can lead to failure of zirconium alloy cladding early in the dry storage period, and temperatures for storage have been established to preclude creep cladding rupture by limiting creep-induced strain. Other postulated mechanisms include hydrogen embrittlement and delayed hydride cracking (DHC) in dry storage.

In off-normal environmental conditions, breached fuel in contact with air at elevated temperature can lead to deleterious volume expansion of the oxide fuel and loading of the cladding to worsen the breach. Remaining water in the dry storage system and/or presence of air can cause additional corrosion and radiolytic reactions that evolve hydrogen.

The following sections summarize degradation mechanisms for the PR fuel clad with zirconium alloys. The information is heavily drawn from several key review publications and guides on this topic [7, 18–19].

3.1.1. Creep

Creep causes dimensional changes in the fuel pin diameter and length, and can be observed in the microstructure of the cladding (for example, triple-point cavities). Creep rupture or creep strain to failure is the concern. Two principal physical factors in the creep behaviour of irradiated cladding are the hoop stress and the temperature. The hoop stress results from the rod internal pressure, a combination of the original fill gas and the fission gas release during service, and the temperature results from the decay heat of the fuel assemblies. At low temperatures and stresses, the creep strain is negligible; at high temperatures and stresses the strain can be sufficient to cause creep rupture. For typical fuel cladding hoop stresses, strain may be detected at temperatures above about 300°C, although significant strain (for zirconium alloy cladding) is not expected to occur until the temperature is well in excess of 350°C. Over long storage times, both the pressure and the temperature decrease and, thus, the strain rate approaches zero.

The creep strain rate and strain-at-failure of spent nuclear fuel cladding are affected by material parameters like alloy composition, fabrication steps (for example, cold work, solution anneal, recrystallization anneal), hydride content, and radiation fluence. At temperatures of the drying, transportation, and initial storage operations, there may be significant recovery of mechanical and irradiation damage, which will affect the creep behaviour. In creep tests at temperatures between 250–400°C with Zircaloy cladding irradiated up to a burnup of 64 GWd/MtU, no failures have been observed below 2% strain [20–21]. The strain predicted to occur in storage must be less than the creep strain to failure. The environmental control would be to limit the temperature of the fuel in the dry storage system.

3.1.2. *Hydrogen mechanisms*

Zirconium alloys absorb hydrogen during corrosion with water. The quantity of hydrogen absorbed into the matrix depends primarily on the environmental conditions and the composition of the alloy. The quantity of hydrogen absorbed, determined as a fraction of the total hydrogen generated via corrosion, is known as the hydrogen pick-up fraction. For Zircaloy in either BWR or PWR service this fraction is typically in the range of 10%, or equivalent to less than about 500 ppm. The solubility of hydrogen in zirconium alloys increases with increasing temperature in the unirradiated condition [22–24]; irradiation does not appear to have a significant impact on this temperature dependence. The solubility of hydrogen in Zircaloy at room temperature is significantly less than 1 ppm. At 400°C, the calculated solubility is in the 170–300 ppm range. As a result of corrosion during irradiation, the hydrogen concentration can increase to values in excess of 300 ppm (for higher burnup fuels, the concentrations may be considerably higher) and, hence, result in hydride formation and precipitation. The zirconium hydrides formed can impact the mechanical properties of the Zircaloy, generally increasing the strength and decreasing the ductility (hydride embrittlement). DHC, a subcritical environmental cracking phenomenon, may also occur [25–28].

3.1.3. *Stress-corrosion cracking*

Another subcritical environmental cracking phenomenon is stress-corrosion cracking (SCC). This mechanism involves chemical corrosion of a crack tip with crack extension being driven by a stress on the cladding. This mechanism would be plausible for incomplete drying. A review of the testing done on SCC of irradiated Zircaloy determined that under conditions expected for dry storage failure would not occur by this mechanism [29]. Even under conditions of higher than expected stress (270 MPa), only pinhole breaches were observed. Under normal storage conditions, the release of gas and/or volatile fission products from the fuel pellets to the gap of an intact rod should be negligible. Therefore, the gas pressure loading stress on the cladding is highest at the start of storage and decreases with storage time due to a decreasing temperature. In addition, it is expected that no corrosive fission products will be released from the fuel pellets to the cladding gap during the storage period. Therefore, if the unexpected SCC is going to occur in a particular fuel rod, it would likely occur early in storage, when stress is highest, not later during the extension period (> 20 years of storage).

3.1.4. *Diffusion-controlled cavity growth*

Diffusion related phenomena manifest themselves as voids formation and migration, ion migration, grain boundary alteration and enrichment in chemical species, and formation and migration of reaction products from the site of generation. The kinetics of diffusion processes generally follow an Arrhenius rate law. A temperature threshold typically exists below which

the kinetics of the process may be too slow to be of any concern even for a dry storage period of up to 100+ years. Diffusion-controlled cavity growth is a potential mechanism for mechanical degradation, but it has never been observed in spent nuclear fuel cladding.

3.1.5. *Off-normal condition degradation phenomena*

If the inert cover gas environment and/or temperature controls are not maintained throughout the storage period, the zirconium alloy cladding materials may be subject to rapid degradation. Ingress of air and/or water into the storage environment of the fuel could cause additional degradation.

Excessive oxidation of the cladding combined with an internal stress can potentially overload the cladding. Oxidation of the Zircaloy [30] is a thermally-induced process. Above 300°C, significant oxidation of the cladding may occur during the storage period, depending on the temperature and amount of air ingress.

Oxidation of the fuel, UO_2 , is possible if the fuel is exposed directly to air in the dry storage cask system. A comprehensive review of the mechanisms and kinetics of fuel oxidation is provided in reference 31. Oxidation of UO_2 would occur by first forming either U_3O_7 or U_4O_9 , phases that are denser than the original UO_2 . This first transition is accompanied by a net contraction of the fuel, relieving mechanical stress on the cladding. Upon further exposure to air, the fuel is oxidized to U_3O_8 , a phase which is approximately 36% less dense than the original fuel. The swelling of the fuel as U_3O_8 forms has been shown to supply sufficient mechanical stress to split the cladding [32–33]. Water ingress and formation of hydrated phases of uranium oxides would exacerbate the fuel swelling and oxidation kinetics [34].

Water ingress may raise the potential for degradation of the cladding due to the creation of a humid atmosphere. Possible effects of the humid atmosphere include: radiolysis of the moisture to create highly oxidizing radicals, corrosion of the cladding and hydrogen ingress into the cladding.

3.2. Aluminum-alloy-clad RR fuel in dry storage

To achieve limited, acceptable additional degradation to the initial condition of the fuel cladding, dry storage systems need to maintain controls for a storage environment, analogous to water quality controls for wet storage. Controls of the storage environment would provide estimation of degradation of the fuel to a limited, acceptable level during the drying and storage period to ensure criticality safety, radionuclide confinement by the fuel/clad system, post-storage handle ability, and a full range of ultimate disposal options.

Maintaining changes to the fuel condition within acceptable degradation is consistent with the requirements for dry storage of commercial spent nuclear fuel given in Title 10 of the U.S. Code of Federal Regulations, Part 72, paragraph h [13] which allow no large breach of the cladding during storage and subsequent handling. Limits for acceptable degradation of aluminium fuel during fuel drying and a dry storage period of 50 years were identified in early work [35].

An evaluation of degradation mechanisms that could impact aluminium fuel for a range of storage environments as technical background for development of acceptable degradation of aluminium-clad fuels for dry storage for a 50-year period was also reported [35–36]. Mechanisms which could cause the following degradation modes were evaluated:

- A loss in net section of cladding through cracking, pitting, or general thinning;

- Embrittlement of the cladding;
- Distortion (slumping) of the fuel; and
- Diffusion of fuel or fission products through the cladding or through the fuel matrix only (in fuel with breached cladding).

Limits were identified for the environmental storage conditions to limit degradation to an acceptable level for a 50-year storage period [35]. A key limit, based on creep analysis, is a temperature limit of 200°C of the cladding to avoid creep-induced slump of a plate of 0.1 inches (2.54 mm) which would be the most limiting mechanism in the absence of corrosion for aluminium alloy clad RR fuel.

3.2.1. Creep

In contrast to creep rupture for PR fuel cladding, RR fuel cladding is not subject to rupture, but the aluminium fuel is subject to significant dimensional changes and slumping due to creep. An analysis was performed [37] to evaluate slump of RR plate fuel under self-weight loading. Fig. 4 shows the analytical model and the results as a function of fuel temperature and grain size for a 50-year period. Coble creep, which involves grain boundary diffusion and sliding, was considered the predominant steady-state creep mechanism for the low stresses, small grain size, and low temperatures of the material [38]. The wealth of literature test data for creep of aluminium is almost exclusively at higher stress levels, or higher temperature or both compared to dry storage conditions assumed. One data set that is close to the low stress, low temperature condition is in reference [39]. Test data is reported at 250°C and 200 psi applied stress for up to 3,200 hours. The grain size was reported to be 0.09 mm. A good match of the test data using Coble creep in an analytical model to the test data was found [37].

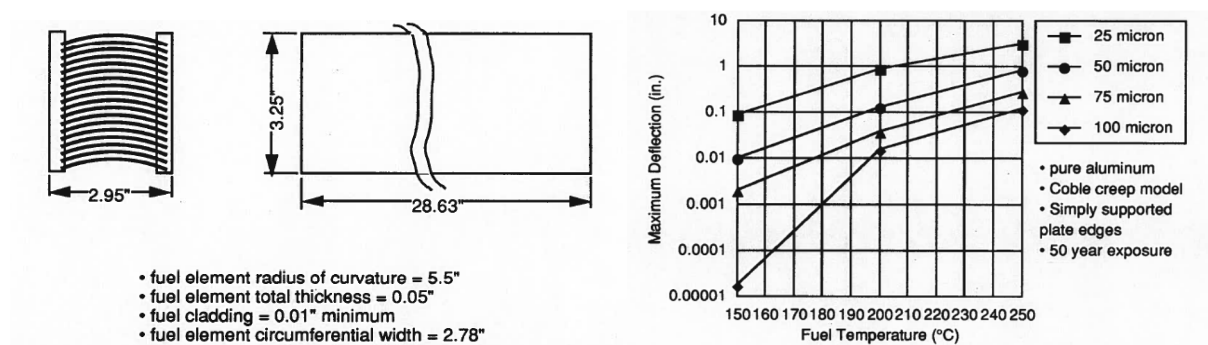


FIG. 4. Materials test reactor fuel model and analysis of fuel plate slump under creep (from Ref. 37).

3.2.2. Off-normal condition degradation phenomena

The approach to avoid excessive degradation in a sealed system is to dry the contents of water remaining in the fuel/container to-be-sealed, for both free and bound waters, to a level such that if the water is consumed by corrosion of the fuel, acceptable degradation of the fuel is maintained; and also that the production of hydrogen does not adversely impact the pressure capacity of the canister or retrieval of its contents. Gases produced may overpressure containers, embrittle materials, reach flammable concentrations, accelerate corrosion, or form pyrophoric species that would impact safe post-storage retrieval.

Aluminium cladding alloys are subject to vapor corrosion, and an extensive test program was performed [40] to evaluate this degradation phenomenon for various test conditions of alloy type, temperature, air, water, and gamma radiation to simulate the attendant radiation of the fuel. In laboratory tests in which aluminium cladding alloys were placed in a sealed capsule with air and water and placed in a gamma cell, rapid corrosion occurred compared to no-radiation cases as indicated in Figure 5. In addition, corrosion occurred at all relative humidity conditions in contrast to the case with no radiation with a threshold of approximately 20% RH [40]. The cause of the rapid attack was attributed to a lowering of the pH of the water by radiolysis of the air [40–41].

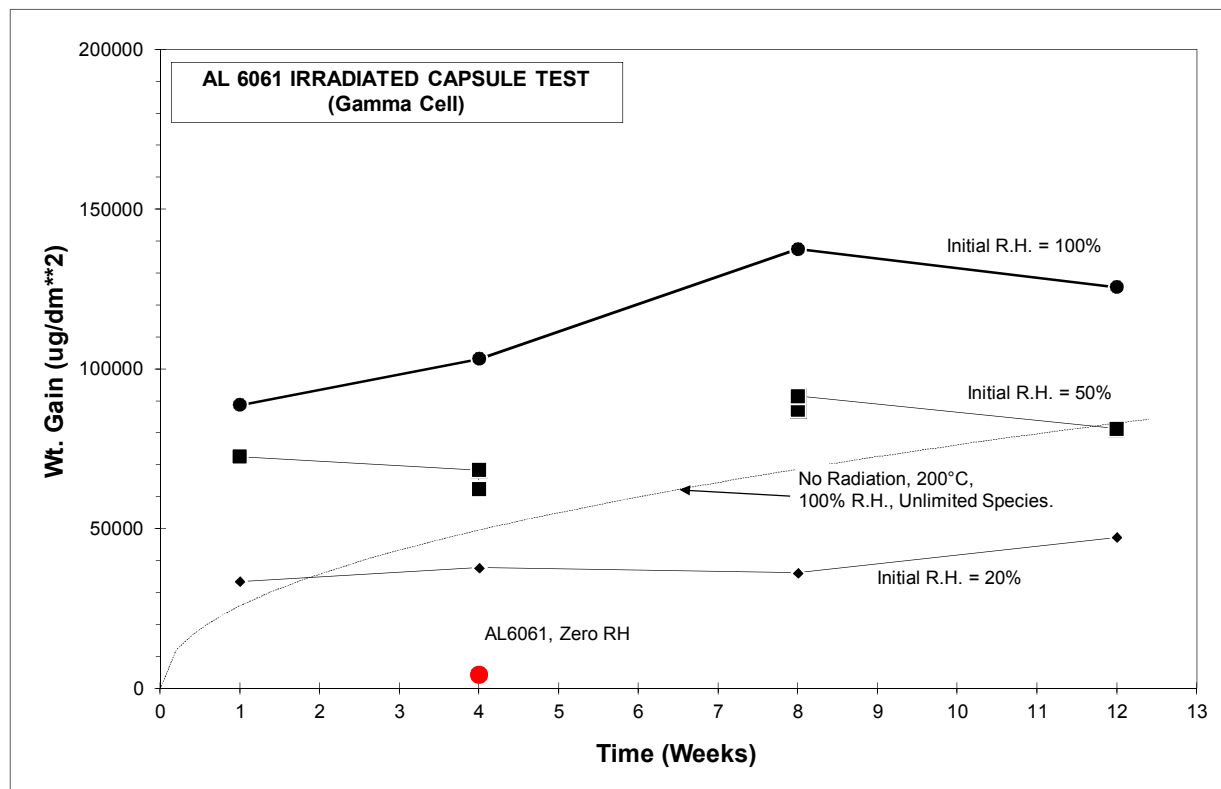


FIG. 5. Vapor corrosion of aluminum alloys under air and water vapor exposure with effect of Gamma (Co60) radiation at $1E4$ Gy/hr. The total available water is consumed in approximately one week for all relative humidity conditions in the irradiation capsules (reproduced from Ref 40).

Another phenomenon that is expected to occur is radiolysis of aluminium oxyhydroxides to generate hydrogen gas. Exposure of oxyhydroxides of aluminium, present on spent fuel, to gamma irradiation can produce radiolytic hydrogen gas [unpublished work of the author]. This phenomenon should be better characterized for a sealed storage system with aluminium fuel.

A recent IAEA workshop showed examples of wet and dry storage practices that resulted in maintaining RR fuel with minimal degradation, and those that caused significant degradation. A guide for practices for wet and dry storage systems from this workshop is also being developed by the IAEA to facilitate technology transfer among member nations [11], and will supplement the existing information base for safe dry storage of aluminium-alloy clad RR fuel.

4. CONCLUSIONS

The imperative for interim storage of spent nuclear fuel is to limit its degradation to maintain functions important to safety throughout storage and post-storage handling. The fuel cladding is a critical confinement barrier and structural material for fuel integrity for the storage period and also for safe fuel retrieval and handling pending final disposition. The vast body of literature, with several critical reviews of zirconium alloys for PR fuel cladding, shows there is a firm technical basis to demonstrate safe storage of PR fuel in both water pool (with minimal water quality controls) and dry systems (with environmental controls) for at least many decades.

The aluminium fuel storage experience to date, supported by the understanding of the effects of environmental variables on materials performance, also shows that storage systems that minimize degradation and provide full retrievability of the RR fuel up to several decades can be achieved in wet storage (with strict water quality controls) and vented or non-sealed dry storage systems.

The specific response of the PR and RR fuel to storage environments is dependent on the initial materials' condition including composition, microstructure, and wastage as a result of reactor operation.

Continued storage that provides full retrievability for 100+ years may require establishment of new environmental limits with firm technical bases for the fuel with vigilance in maintaining those environmental limits of acceptable storage considering, too, degradation of the storage system materials. A fuel temperature limit for dry storage would not be challenged with storage time since the fuel would cool substantially in the first decades of storage.

Verification of predicted degradation for 100+ years of extended storage can be addressed through lead surveillance of fuel and storage system materials at extreme or bounding environmental conditions of storage, and also periodic monitoring (inspection) of these materials.

ACKNOWLEDGEMENTS

The present work was supported through Contract DE-AC09-08SR 22470 with the U.S. Department of Energy. The views and opinions of the authors expressed herein do not necessarily state or reflect those of the United States Government or any agency thereof.

REFERENCES

- [1] LAMBERT, J.D.B., LAMBERT, R., "An Overview of Spent Fuel Storage at Commercial Reactors in the United States," in *Safety Related Issues of Spent Nuclear Fuel Storage, NATO Security through Science Series*, J.D.B. Lambert and K.K. Kadyrzhanov, eds, Springer, 2007, pp. 55-70.
- [2] INTERNATIONAL ATOMIC ENERGY AGENCY, "Recommended practices for water quality management in research reactors & spent fuel storage facilities," IAEA Nuclear Energy Series, to be published 2010.
- [3] ELECTRIC POWER RESEARCH INSTITUTE, presentation by John Kessler,

- June 2009, <http://www.nwtrb.gov/meetings/2009/june/kessler.pdf>
- [4] COLEMAN, C.E., “Cracking of Hydride Forming Metals and Alloys”, in *Comprehensive Structural Integrity*, vol 6, ISBN-0-08-44153-X, 103-162 (2003).
 - [5] INTERNATIONAL ATOMIC ENERGY AGENCY, “Effects of radiation and environmental factors on the durability of materials in spent fuel storage and disposal,” IAEA-TECDOC-1316, IAEA, Vienna (2002).
 - [6] U.S. NUCLEAR REGULATORY COMMISSION, Regulatory Guide 1.13, “Spent Fuel Storage Facility Design Basis,” Revision 2, March 2007.
 - [7] EINZIGER, R.E., BROWN, C.L., HORNSETH, G.P., INTERRANTE, C.G., “Data Needs for Storage and Transportation of High-Burnup Fuel,” *Radwaste Solutions*, March/April 2005, pp. 44-57.
 - [8] AMERICAN SOCIETY FOR TESTING AND MATERIALS, ASTM C1553-08, Standard Guide for Drying Behavior of Spent Nuclear Fuel, ASTM International, 2008.
 - [9] SDD-45. System Design Description, INTEC IFSF Fuel Conditioning Station, 11/21/05.
 - [10] EDF-5063, Intact Aluminium Plate Fuel Drying Characteristics, INL, 6/7/06.
 - [11] INTERNATIONAL ATOMIC ENERGY AGENCY, Presentations at IAEA Technical Meeting “Guideline of Good Practice for the Management and Storage of Research Reactor Spent Fuel,” October 19—23 2009, Dounreay, Thurso, U.K., Mr Lubi Dimitrovski, Australian Nuclear Science and Technology Organisation (ANSTO) Manager, Waste Operations, Mr Jim Z.W. Lian, Research Reactor Fuel Development, Station E5, AECL — Chalk River Laboratories; Guidelines for Wet and Dry Storage of Research Reactor Fuel, IAEA, (to be published in 2011).
 - [12] AMERICAN NATIONAL STANDARDS INSTITUTE/AMERICAN NUCLEAR SOCIETY ANSI/ANS-57.9-1992; R2000, Design Criteria for an Independent Spent Fuel Storage Installation (Dry Type).
 - [13] Title 10 of U.S. Code of Federal Regulations, Part 72, Licensing Requirements for the Independent Storage Of Spent Nuclear Fuel, High-Level Radioactive Waste, and Reactor-Related Greater Than Class C Waste.
 - [14] Title 10 of U.S. Code of Federal Regulations, Part 51, Environmental Protection Regulations For Domestic Licensing And Related Regulatory Functions.
 - [15] Title 10 of U.S. Code of Federal Regulations, Part 54, Requirements For Renewal Of Operating Licenses For Nuclear Power Plants.
 - [16] U.S. NUCLEAR REGULATORY COMMISSION, NUREG-1536, Standard Review Plan for Spent Fuel Dry Storage Systems at a General License Facility — Draft Report for Comment (NUREG-1536, Revision 1A), March 2009.
 - [17] U.S. NUCLEAR REGULATORY COMMISSION, NUREG-1927, Standard Review Plan for Renewal of Independent Spent Fuel Storage Installation Licenses and Dry Cask Storage System Certificates of Compliance, Draft Report for Comment, September 2009.
 - [18] AMERICAN SOCIETY FOR TESTING AND MATERIALS, ASTM C1562-03, Standard Guide for Evaluation of Materials Used in Extended Service of Interim Spent Nuclear Fuel Dry Storage Systems, ASTM International, 2003.
 - [19] KESSLER, J., EINZIGER, R.E., “Technical Bases for Extended Dry Storage of Spent Nuclear Fuel,” ELECTRIC POWER RESEARCH INSTITUTE report TR-1003416, December 2002.
 - [20] SPIKER, H., PEEHS, M., DYCK, H.P., KASPER, G., AND NISSEN, K., “SNF Dry Storage in Large Transport Casks After Extended Burnup,” *J. Nucl. Mater.* **250** (1997) 63-74.
 - [21] GOLL, W., SPIKER, H., TOSCANO, E., “Short-time Creep and Rupture Tests

- on High Burnup Fuel Rod Cladding,” *J. Nucl. Mater.* **289** (2001) 247-253.
- [22] KEARNS, J.J., “Terminal Solubility and Partitioning of Hydrogen in the Alpha Phase of Zirconium, Zircaloy-2 and Zircaloy-4,” *J. Nucl. Mater.* **22** (1967) 292-303
- [23] SAWATZKY, A., WILKINS, B.J.S., “Hydrogen Solubility in Zirconium Alloys Determined by Thermal Diffusion,” *J. Nucl. Mater.* **22** (1967) 304-310.
- [24] McMINN, A. DARBY, E.C., SCHOFIELD, J.S., “The Terminal Solid Solubility of Hydrogen in Zirconium Alloys,” *Zirc. Nucl. Ind.: 12th Inter. Symp.*, ASTM STP 1354, West Conshohocken, PA, 2000, pp. 173-195
- [25] HUANG, J.H., HUANG, S.P., “Effect of Hydrogen Contents on the Mechanical Properties of Zircaloy-4,” *J. Nucl. Mater.* **208** (1994) 166-179.
- [26] NORTHWOOD, D.O., KOSASIH, U., “Hydrides and Delayed Hydrogen Cracking in Zirconium and Its Alloys,” *Inter.Met. Rev.*, **28** (1983) 92-121.
- [27] SIMPSON, L.A., CANN, C.D., “Fracture Toughness of Zirconium Hydride and Its Influence on the Crack Resistance of Zirconium Alloys,” *J. Nucl. Mater.* **87** (1979) 303-316.
- [28] SIMPSON, L.A., PULS, M.P., “The Effects of Stress, Temperature and Hydrogen Content on Hydride-Induced Crack Growth in Zr-2.5 pct. Nb,” *Metallurgical Transactions*, **Vol. 10A** (1979) 1093.
- [29] PESCATORE, C., COWGILL, M., “Temperature Limit Determination for the Inert Dry Storage of Spent Nuclear Fuel,” ELECTRIC POWER RESEARCH INSTITUTE report TR-103949, May 1994.
- [30] ROTHMAN, A.J., “Potential Corrosion and Degradation Mechanisms of Zircaloy Cladding on Spent Nuclear Fuel in a Tuff Repository,” Report Attachment 10 to MRB-0418, JUDIC-20172, Contract W-7405-Eng-48, Lawrence Livermore National Laboratory, 1984.
- [31] McEACHERN, R.J., TAYLOR, P., “A Review of the Oxidation of Uranium Dioxide at Temperatures Below 400°C,” *J. Nucl. Mater.* **254** (1998) 87-121.
- [32] EINZIGER, R.E., COOK, J.A., “Behaviour of Breached Light Water Reactor Spent Fuel Rods in Air and Inert Atmospheres at 229°C,” *Nuclear Technology* **69** (1985) 55-71.
- [33] EINZIGER, R.E., STRAIN, R.V., “Behaviour of Breached Pressurized Water Reactor Spent Fuel Rods in an Air Atmosphere Between 250 and 360°C,” *Nuclear Technology* **75** (1990).
- [34] McEACHERN, R.J., TAYLOR, P., “A Review of the Oxidation of Uranium Dioxide at Temperatures Below 400°C,” *J. Nucl. Mater.* **254** (1998) 87-121.
- [35] SINDELAR, R.L., PEACOCK, H.B., LAM, P-S., IYER, N.C., AND LOUTHAN, JR., M.R. Acceptance Criteria for Interim Dry Storage of Aluminium-Alloy Clad Spent Nuclear Fuels (U) Fuels, Westinghouse Savannah River Company Report WSRC-TR-95-0347, March 1996.
- [36] SINDELAR, R.L., PEACOCK, JR., H.B., LAM, P-S., IYER, N.C., LOUTHAN, JR., M.R., MURPHY, J.R., “Scientific Basis for Storage Criteria for Interim Dry Storage of Aluminium-Clad Fuels,” Symposium V, Scientific Basis for Nuclear Waste Management XIX, published by the Materials Research Society, 1996, ISBN 1558993150.
- [37] MILLER, R.F., SINDELAR, R.L., “Creep Analysis for Materials Test Reactor (MTR) Fuel Assemblies in Dry Storage,” WSRC-TR-95-0121, Westinghouse Savannah River Co., April 1995.
- [38] LANGDON, T. G., MOHARNED, F. A., “A New Type of Deformation Mechanism Map for High-temperature Creep,” *Materials Science and Engineering*, **32** (1978) 103-112.

- [39] McKEOWN, J., EBORALL, R., LUSHEY, R.D.S., The Creep Properties of 99.8% Purity Aluminium at 20–80°C and at 250°C and 450°C,” *Metallurgia*, July 1954, 13-15.
- [40] LAM, P-S., SINDELAR, R.L., and PEACOCK, Jr., H.B., “Vapor Corrosion of Aluminium Cladding Alloys and Aluminium-Uranium Fuel Materials in Storage Environments,” WSRC-TR-97-0120, April 1997, Savannah River Site
- [41] SINDELAR, R.L., LAM, P.-S., LOUTHAN, JR., M.R., IYER, N.C., “Corrosion of Metals and Alloys in High Radiation Fields,” *Materials Characterization*, **43** (1999) 147-157.

TESTING OF METAL CASK AND CONCRETE CASK

K. SHIRAI*, M. WATARU*, H. TAKEDA*, J. TANI**, T. ARAI**, T. SAEGUSA**

* Civil Engineering Laboratory, Central Research Institute of Electric Power
Abiko-shi

** Materials Science Laboratory, Central Research Institute of Electric Power Industry
Abiko-shi
Japan

Abstract

In Japan, the first interim spent fuel storage facility (ISF) outside of nuclear power plant site in use of dual-purpose metal cask is being planned to start its commercial operation in 2012 in Mutsu city, Aomori prefecture. The CRIEPI (Central Research Institute of Electric Power Industry) has executed several study programs on demonstrative testing for interim storage of spent fuel, mainly related to metal cask and concrete cask storage technology to reflect in Japanese safety requirements for dry casks issued by NISA/METI (Nuclear and Industrial Safety Agency, Ministry of Economy and Trade Industry). On top of that, the Japan Nuclear Energy Safety Organization (JNES) has executed study programs on spent fuel integrity, etc. This paper introduces the summary of these research programs.

1. INTRODUCTION

At the end of 2007, 55 commercial nuclear power units are operating in Japan, with a total electric generation capacity of 49,467 MWe. Nuclear power generation is 30.5% of total electric power generation, with two power plants currently under construction and eleven plants in preparation for construction. All sixteen nuclear power plant sites have storage pools for spent fuel. The total amount of spent fuel stored at these sites was approximately 12,140 tHM as of September 2007, compared to a capacity of 19,000 tHM.

The “Framework for Nuclear Energy Policy” [1] was issued by the Atomic Energy Commission on October, 2005. According to this framework, spent fuel will be reprocessed, and the surplus amount exceeding the capacity will be stored intermediately. Construction of spent fuel interim storage facilities at NPP site or outside of NPP site is expected to be early realized.

On safety technical requirements for spent fuel interim storage facility using dry cask, NISA issued the technical requirements on interim spent fuel storage facility (ISF) using dry metal cask and concrete cask on April 2006 [2–3]. In Japan, the first ISF outside of NPP site in use of dual-purpose metal cask as shown in Figure 1 is being planned to start its commercial operation in 2012 in Mutsu city, Aomori prefecture.

TESTING OF METAL CASK AND CONCRETE CASK

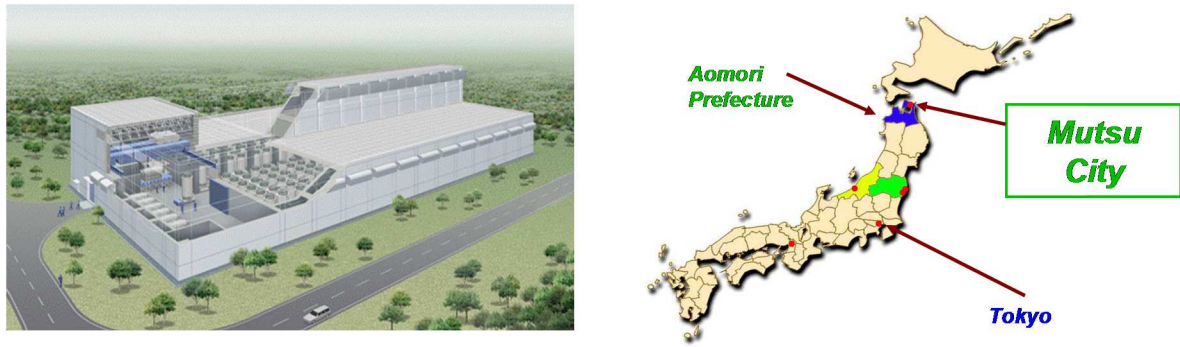


FIG. 1. First interim storage facility outside of NPP site in Japan (3,000 tU).

In parallel with those regulatory and promoting activities on ISF, CRIEPI has performed supportive research studies for the regulation and early realization of ISF. Key issues of these studies include safety requirements in operation and maintenance during spent fuel storage and unloading/loading for transportation, long-term integrity of metal canister and concrete materials, etc. From 1997, CRIEPI completed the research program of the demonstration test for interim storage of spent fuel, mainly involving concrete cask storage technologies, to reflect in the technical requirements issued by NISA. Moreover, a new research program for the verification testing of cask integrity under long-term dry storage conditions has been started. The schedule for these test programs is shown in Table 1. On top of that, the JNES has executed research on spent fuel integrity as shown in Table 2. This paper summarizes these research programs.

TABLE 1. TEST PROGRAMS FOR STORAGE CASK IN CRIEPI

Program Item	2000	2001	2002	2003	2004	2005	2006	2007	2008
<i>Concrete cask performance test:</i>									
a. Basic design;									
b. Fabrication of full-scale concrete cask;									
c. Demonstration tests - Heat removal;									
- MPC drop;									
- Seismic;									
d. SCC evaluation test;									
<i>Containment performance test of metal cask:</i>									
a. Drop test without impact limiter;									
b. Aircraft crash test;									
c. Long-term confinement test of lid structure.									

* Horizontal Test:
2/5Scale
* Vertical Test:
Full-Scale

TESTING OF METAL CASK AND CONCRETE CASK

TABLE 2. TEST PROGRAMS ON SPENT FUEL INTEGRITY IN JNES

Program item	2000	2001	2002	2003	2004	2005	2006
Survey and planning							
Creep test			PWR 48 GWd/t, BWR 50 GWd/t			PWR 55 GWd/t, BWR 55 GWd/t	
Creep rupture test			PWR 48GWd/t, BWR 50 GWd/t				
Hydride reorientation test						PWR 48 GWd/t, PWR 55 GWd/t	
Hydride effects evaluation test						BWR 50 GWd/t, BWR 55 GWd/t	
Mechanical property test							
Irradiation hardening recovery test			PWR 48 GWd/t, BWR 50 GWd/t				
			330–420°C				<330°C

2. CONCRETE CASK PERFORMANCE TEST WITH FULL-SCALE CASK

2.1. Demonstration test

Concrete cask performance tests with the full-scale cask including heat removal tests, drop test and seismic tests have been successfully finished. To perform heat removal tests and drop tests with full-scale test bodies efficiently, the demonstration test facility as shown in Fig. 2 was constructed in the Akagi Test Center of CRIEPI. In this facility, there are heat removal test area and drop test area. In the drop test area, a steel plate is fixed on the base concrete. Size of the steel plate is 7.5 m long, 4.5 m wide and 50 mm thick. Thickness and weight of the base concrete are 2 m and 550 t, respectively.

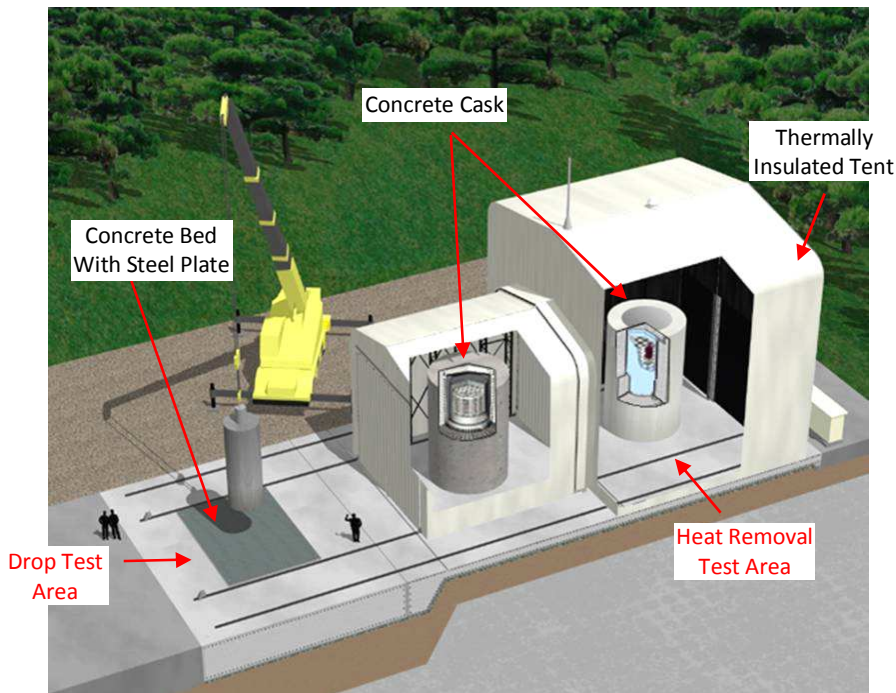


FIG. 2. Demonstration test facility.

TABLE 3. DESIGN OF CONCRETE CASK

Design storage period	40–60 years
Fuel type	17 × 17 array for PWR
Enrichment (wt% U ²³⁵)	4.9%
Burnup (Max)	55 MWd/kgHM
Cooling time	10 years
Environmental temperature	33°C
Storage cell	21
Total heat load (max)	22.6 kW

Preliminary design parameters are shown in Table 3. The concrete cask was assumed to be for indoor use. Two types of concrete cask, a reinforced-concrete cask (RC cask) and concrete-filled-steel cask (CFS cask) to store the high burnup spent fuel, were designed. Preliminary designs for two types of cask, RC cask and CFS cask were employed as the basic structure as shown in Fig. 3. Two types of the concrete casks have been constructed in the test facility as shown in Fig. 5 [4–5].

2.2. Heat removal test

Fig. 5 shows the temperature distribution of the concrete inside for the test case of the initial storage stage with 22.6 kW with RC cask. The maximum value in the vicinity of the outlet duct was 91°C, and exceeded the allowable temperature limit value for the long-term; i.e., 90°C [6]. In both casks, the canister surface temperature was below 100°C in the tests case of the final storage stage with 10.0 kW, which may be susceptible to the atmospheric stress corrosion cracking of the stainless steel in a salty air environment.

Considering the accident condition, the tests were performed under the condition of blockage of two inlets of four inlets. In the RC cask, the air is uniformly distributed to the annulus gap from the bottom cavity. On the other hand, in the CFS cask, the air flows to the annulus gap directly as shown in Fig. 6. In both casks, the maximum temperatures in the concrete container were under the allowable temperature limit value for the short-term, i.e., 175°C [6] within 24 hours.

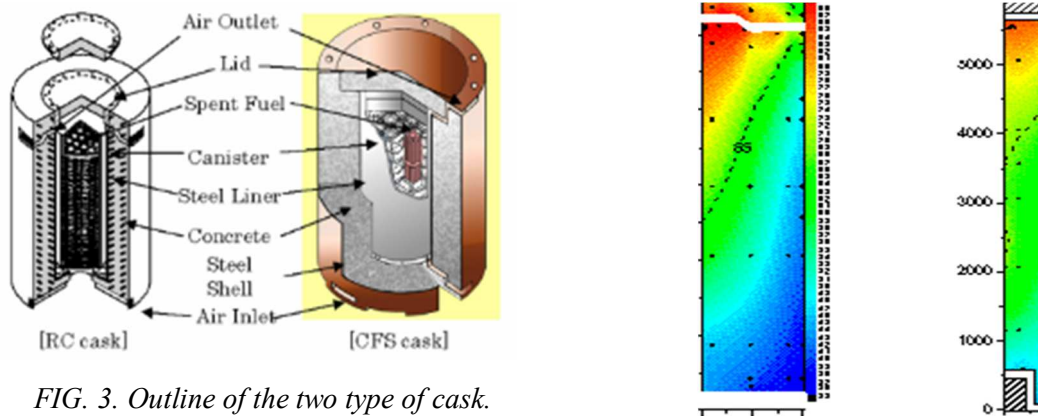


FIG. 3. Outline of the two type of cask.

FIG. 4. Temperature distributions of the concrete inside in normal conditions.



FIG. 5. Construction of full-scale casks.

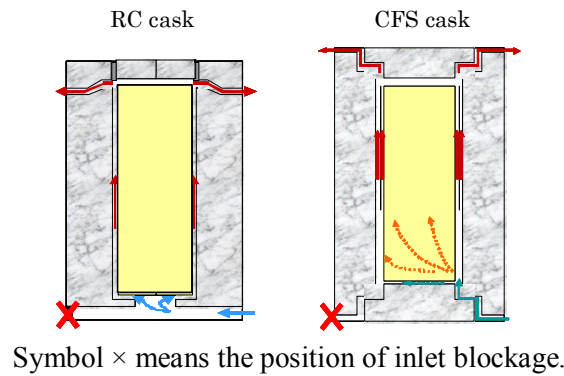


FIG. 6. Flow patterns under 50% blockage of the inlet ducts.

2.3. Canister drop test

Table 4 shows drop test conditions for the full-scale MPCs. Two drop tests in horizontal and vertical orientations were conducted considering non-mechanistic drop or impact events during handling, and the drop heights were 1m and 6m, respectively. Regarding contents of MPC, dummy steel structures equal to the total weights of the spent fuels (14.7 t) were used.

TABLE 4. DROP TEST CONDITIONS

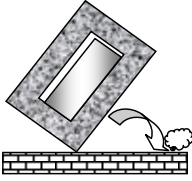
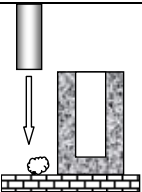
Non-mechanical drop or impact events during handling	Tipping-over Event: Equivalent drop height for rotational velocity caused by tipping-over from height of GC		Drop Event: Drop height from cask height	
Orientation	Horizontal		Vertical	
Height	1m		6m	
MPC	RC Cask Type		CFS Cask Type	

Figure 7 shows photographs of the test MPC before and after the horizontal drop test. The test MPC was slightly deformed near the impacted area. He leak tests were performed before and

after the drop tests to confirm the integrity of leak-tightness of the test MPCs (especially welded lids) against impact loads. Measured leakage rates shows the integrity of leak-tightness at lids and MPC shell, as all values are under $1.0 \times 10^{-9} \text{ Pa} \cdot \text{m}^3/\text{s}$.

Figure 8 shows a photograph of the test MPC in the vertical drop test. According to the He leak tests performed before and after the drop tests, measured leakage rates shows the integrity of leak-tightness at lids and MPC shell, as all values are under $1.0 \times 10^{-9} \text{ Pa} \cdot \text{m}^3/\text{s}$. From these results, it seems that the crack initiation may be avoided in the drop events with the vertical orientation even if the impact load over 1000 G was applied.



FIG. 7. Horizontal drop test.

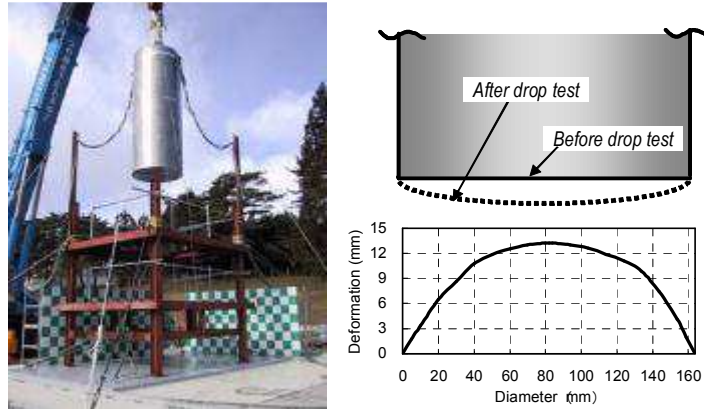


FIG. 8. vertical drop test.

2.4. Seismic test

For vertically free-standing concrete cask on the floor pad in the cask storage facility, its tip-over and sliding behavior and the integrity of the spent fuel during strong seismic motions are still the technical key issues to guarantee its safe performance.

The full-scale concrete cask and the storage house floor were set on a three-dimensional shaking table in 3-D full-scale earthquake testing facility “E-Defense “ designed and constructed by National Research Institute for Earth science and Disaster prevention as shown in Fig. 9. As for spent fuel structures, one full-scale PWR fuel (17×17) and 20 dummy PWR fuel assemblies, which modal deformation was equivalent to the full-scale one, were used.

According to the seismic excitation test results, it is found that the tip-over of the full-scale cask did not occur at the acceleration level which exceeds the input level one-and-a-half times as strong as the uplifting limit level, but the special attention should be paid for the sliding or jumping behavior of the cask under the strong earthquake motion, even if the friction coefficient is still large. Nevertheless, it seems that the integrity of spent fuel might be maintained under the Japanese typical design seismic loads.

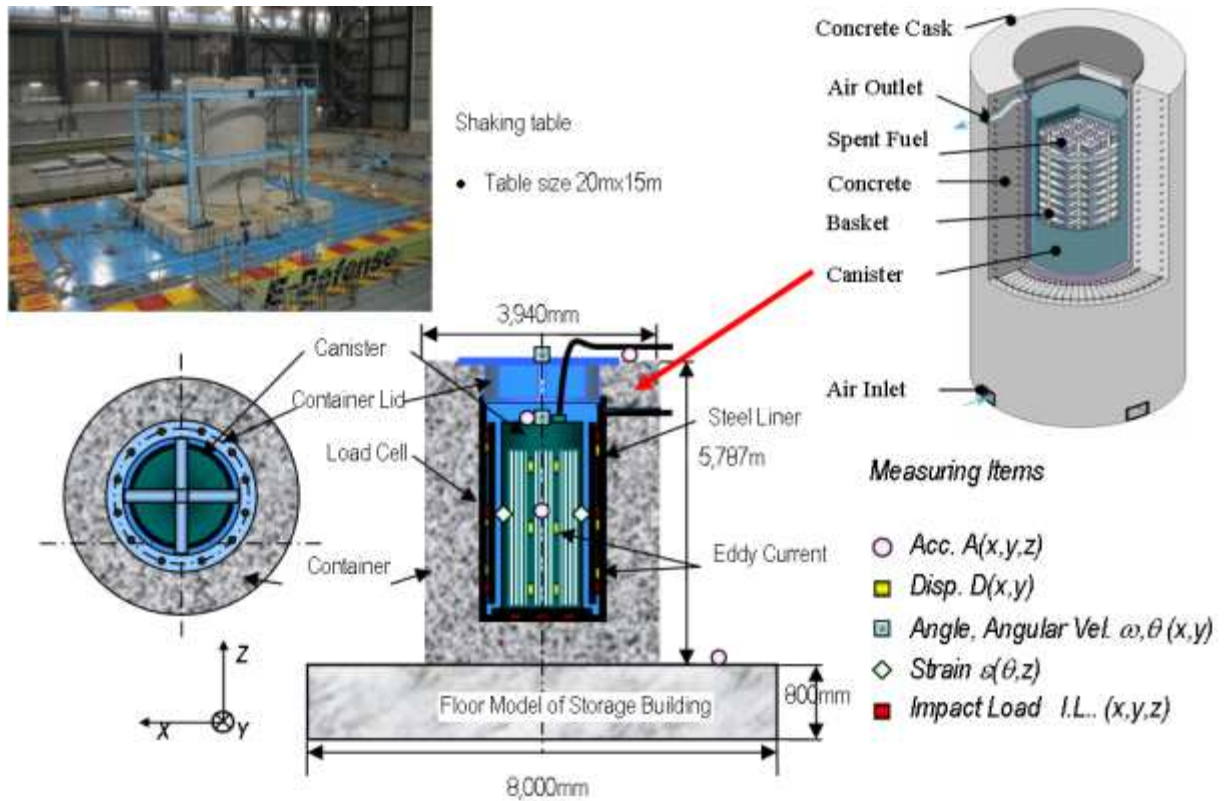


FIG. 9. 3D earthquake testing with full-scale concrete cask and concrete floor.

2.5. SCC evaluation test

ISF in Japan will be likely installed at coastal sites. Temperature decreases during storage period and salt condensation increases on the metal canister surface. Key issue for realization of the metal canister storage technology should be “Long-term integrity of canisters”, considering deterioration of metal canister in a salt water environment.

Austenitic stainless steels are susceptible to stress corrosion cracking (SCC) in certain environments under a tensile stress. The type of SCC induced by sea salt particles, chlorides, for example, is called as external SCC (ESCC) or atmospheric SCC since the cracking starts from out side of the equipment in air as shown in Fig. 10.

The storage canister has several welding lines in the wall and lid which probably have high residual tensile stresses. Contamination by sea salt particles also is well expected during the long service life of MPCs as mentioned previously. Thus, to prevent penetration through the wall thickness, susceptibility to ESCC should be evaluated carefully for candidate MPC materials [10]. Therefore, since 2004, CRIEPI has started SCC evaluation tests to clarify basic deterioration mechanism.

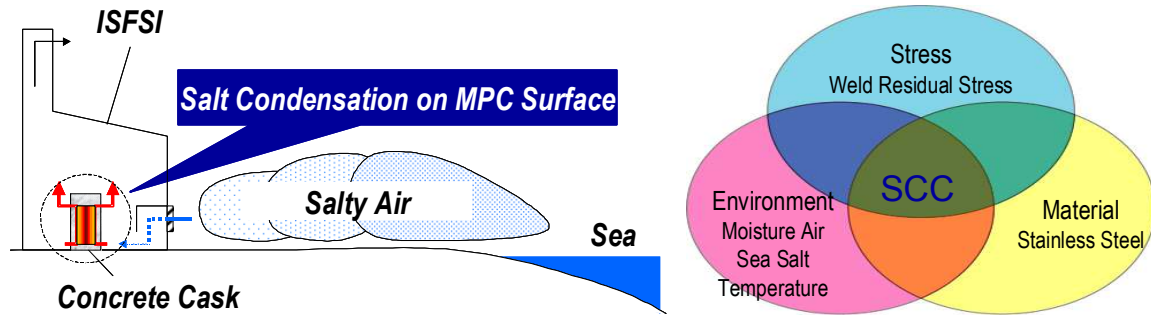


FIG. 10. Deterioration of metal canister in a salt water environment.

2.5.1. Corrosion and crack growth test

Tensile specimens were attached to a loading apparatus that uses a spring to apply a constant stress as shown in Fig. 11. Applied stress ranged from $1.1\sigma_y$ to $1.5\sigma_y$ of the SS (where σ_y : 0.2% proof stress). After corrosion crack growth tests, the surface of some specimens was observed by scanning electron microscopy (SEM) to determine corrosion morphologies or cracking.

CT specimens with chloride deposition were also attached to a loading apparatus as shown in Fig. 12 was placed in constant temperature and humidity chambers kept at temperatures of 323K with RH=35%, 333K with RH=25%, 343K and 353K with RH=15%, which condition was set considering the canister surface condition in the actual storage. The range of K value was between 10 and $30\text{MPa}\cdot\text{m}^{0.5}$. It seems that the candidate materials have the crack growth rate highly larger than the reference material. Therefore, both the candidate materials showed a superior ESCC resistance.

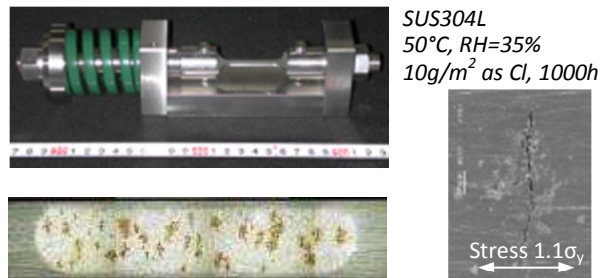


FIG. 11. Corrosion test with UNS S30403 SS.



FIG. 12. Crack growth test.

2.5.2. Chloride deposition velocity test

To measure the chloride accumulation transported by the cooling air on the metal canister surface, two kinds of test (laboratory test and field test) using the wind tunnel in the vertical position were performed. Laboratory test showed that the chloride deposition velocity was higher when the air velocity was high and the temperature of the specimen was low.

According to the field test, the chloride deposition velocity was also made clear as a function of time.

2.5.3. Salt particle collection test

The salt particle collection performance test has been started from 2007 to evaluate the effectiveness of the salt particle collection device designed by CRIEPI as shown in Fig. 14. The device might be attached at the inlet for natural cooling of the cask storage facility and consist of the multiple layered trays with a certain amount of water. When the air including sea salt particles goes through the trays, a part of sea salt particles in the cooling air might be trapped by collision with the water trays. The top surface of each tray has projections to make the air collide with the water surface effectively. The salted water is discharged out of the facilities by overflowing these trays.

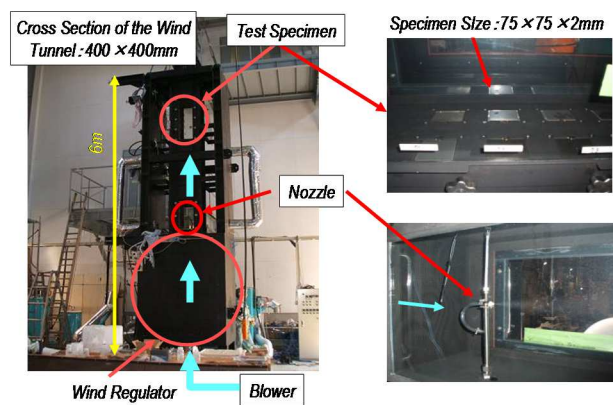


FIG.13. Chloride deposition velocity test.

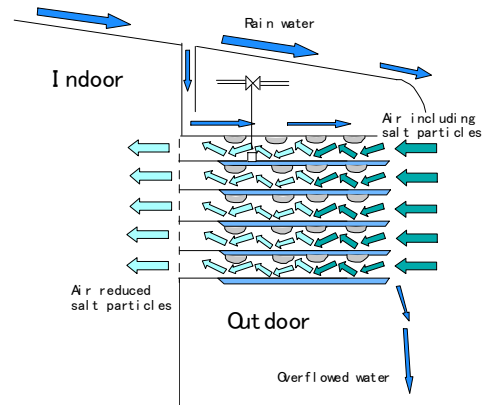


FIG.14. Salt particle collection device.

2.6. MPC surface inspection test

Inspection of canister surface was carried out using an optical camera inserted from the air outlet through the annulus of a concrete cask (VSC-17). The VSC-17 has been storing spent nuclear fuel for over 15 years as part of a dry cask storage demonstration project at Idaho National Laboratory (INL) for more than 15 years as shown in Fig. 15.

Figure 16 shows the photographs of the surface of the MPC. They were snapped by an optical camera inserted from the air outlet through the annulus of a concrete cask. According to the visual inspections, since there is some surface rust present but no large scale flaking, it seems that no gross corrosion, pitting, or general attack, and all coatings appear to be intact. Moreover, there is no considerable indication that the MPC support beams have undergone any structural degradation.

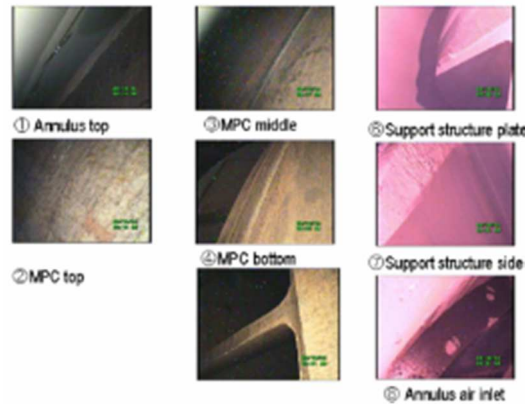
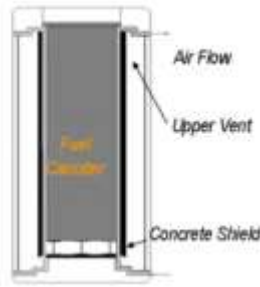


FIG. 15. VSC-17 at INL.

FIG. 16. Photographs of the surface of the MPC.

CONTAINEMENT PERFORMANCE TEST OF METAL CASK

3.1. Drop test without impact limiters under accident

In an interim storage facility of spent fuel, metal casks will be handled without impact limiters. Therefore, leak tests were performed using a full-scale metal cask without impact limiters considering drop accidents during handling in a storage facility. Instantaneous leak rate was quantitatively measured at the drop tests [11].

Figure 17 shows overview of a full-scale metal cask model for impact analysis. This model has been designed as metal cask for dry storage and transportation installing 21 PWR-type fuel assemblies. Fig. 18 shows drop test conditions. A series of impact tests using the full-scale cask described above (a horizontal drop test from a 1m height and a rotational impact test around an axis of a lower trunnion of the cask from the horizontal orientation at a 1m height) were conducted onto the reinforced concrete slab simulating the floor structure of the facility. The main measurement items are the sliding and opening displacements of the primary and secondary lids, leak rates, and inner pressure in the volume between two lids. In the drop test, non-degraded (fresh) metal gaskets were used. During drop tests, although the leak rate value from the secondary lid increased by two orders of magnitude during the impact immediately, the leak rate recovered the background level value 20 minutes later after the drop test. Moreover, the change of the inner pressure between two lids was negligible.

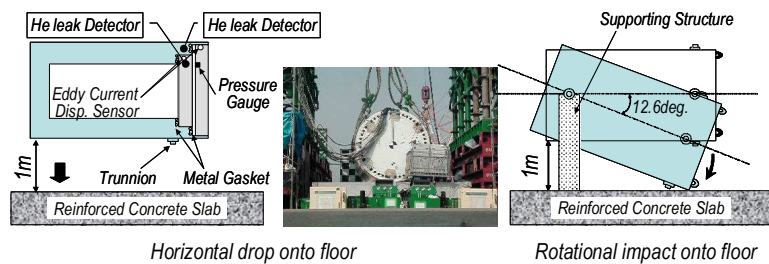


FIG. 17. Full-Size metal cask.

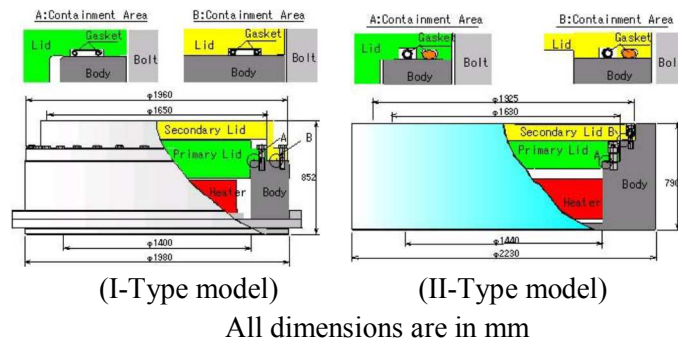
FIG. 18. Drop test conditions with full-scale metal cask.

3.2. Long-term containment performance test of metal cask

The containment function is secured by inserting gaskets between the cask body and the lid, and then bolting them together. Metal gaskets are used for long-term durability. Therefore, it is very important to clarify the influence of the stress relaxation of the gaskets on the containment performance of the metallic gaskets for a long-term usage.

Fig.19 shows the two kinds of tested lids that are parts of full-scale model casks. In the I-type model, the cask body and lid are made of forged carbon steel. The sealing surface is overlaid with stainless steel welding (SUS304), and a double metal gasket (enveloped with aluminium) is installed. In the II-type model, the cask body is made of ductile cast iron, and the lid is made of stainless steel. The sealing surface of the body is plated with nickel. In this model, an inner metal gasket (enveloped with silver), and an outer rubber gasket (silicone rubber) were installed. In both models, the test temperature (130–140°C at the secondary lid) was maintained with the electrical heaters installed in the cask cavities.

Containment of the secondary lid has been tested using a helium leak detector about twice a month for more than 19 years under a constant temperature. The very reliable containment performance has been demonstrated and confirmed to be as low as a leakage of 10^{-9} Pa·m³/s. Moreover, by applying the Larson-Miller Parameter, the results indicate that the containment will be maintained for more than 60 years, taking account of the decay heat of the nuclear spent fuel [12]. Moreover, after the heating degradation test, at the beginning of 2010, tested lids were opened and the aging inspection of the lid components (such as metal gaskets, tightening bolts and so on) were executed as shown in Fig. 20.



(Metal and elastomer gaskets)



FIG. 19. Long-term containment test models.



(Tightening bolt)

FIG. 20. Example of aging inspection.

3.3. Aircraft crash test

To investigate of the integrity of the lid structure of the metal cask during the extreme impact loads due to aircraft crash, two impact scenarios for aircraft engine crash onto the metal cask without impact limiters are considered for both, a vertical impact onto the lid structure and a horizontal impact hitting the cask, as shown in Fig. 21. The horizontal impact test using scale model engine of aircraft has been executed and leak rate from the metallic gasket in the cask also measured at the impact in the test. The vertical impact onto the head of the full-scale metal cask has been also executed.

The test cask was mounted on a supporting frame structure by the specific panel. The reaction forces were measured by six load cells installed between the panel and the supporting frame. At the impact in the test, the leak rate, inner pressure between the lids and displacement of the lids were measured. From these experimental results, it seems that the loss of the inner pressure of the cask cavity may be avoided in the impact event with the horizontal and vertical orientation even if the severe impact load was applied on to the metal cask due to aircraft engine crash.

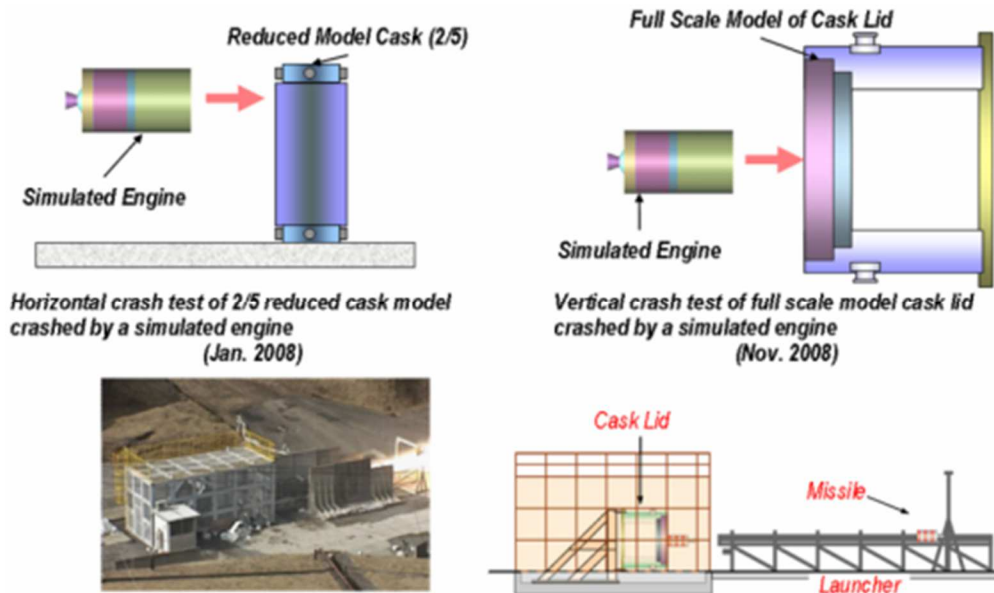


FIG. 21. Outline of aircraft engine crash test.

4. SPENT FUEL INTEGRITY

The Japan Nuclear Energy Safety Organization (JNES) had investigated the technical subjects to be considered for keeping integrity of spent fuel during long term storage and the test plans were established [14–16]. The factors which may affect the fuel integrity under dry storage condition are as follows:

- (a) Thermal creep;
- (b) Hydrogen effect in the cladding(hydrogen solution, hydride precipitate, hydride re-orientation, hydrogen migration according to temperature gradient);
- (c) Irradiation damage recovery;
- (d) Stress corrosion cracking;

- (e) Cladding oxidation;
- (f) Heat generation according to alpha-decay;
- (g) Change of pellet characterization.

The factors of (d) - (g) are not adequately studied, since the spent fuel was stored in an inert atmosphere environment and there may not be a significant change in the chemical condition in a fuel rod, so those were omitted from the scope of the project. On the other hand, the creep behavior of fuel cladding was regarded as the most important issue for spent fuel integrity based on the references. On the subjects of (a) and (b), it was judged that obtaining creep data of spent fuel cladding is necessary as well as evaluating hydrogen effects (solution, precipitation, re-orientation). Moreover, preparation of the basic data for evaluating the cladding strength change during long-term dry storage due to the irradiation damage recovery would be important for subject of (c).

The JNES tests were composed of hydride effect evaluation testing, irradiation hardening recovery testing, and creep testing. In hydride effect evaluation testing, hydride reorientation testing has been performed in order to evaluate the correlation between hydride reorientation behavior and conditions such as hoop stress, temperature, and cooling rate for BWR and PWR irradiated cladding tubes. As for creep behaviour, JNES had already established the creep equation based mainly on secondary creep rate evaluation for 50GWd/t type BWR and 48GWd/t type PWR fuel cladding tube until 2003. The creep rupture behaviour had been evaluated for the same type of cladding tubes. The creep property of both BWR and PWR 55GWd/t type fuel cladding tubes was evaluated by 2006.

5. CONCLUSIONS

In Japan, utilities are planning to commence the operation of the first ISF in 2012. Regulatory authority correspondingly modified the reactor regulation law and has been settling the relevant safety rules to operate the interim storage facility. To prepare the safety requirements and promote the rational reviewing procedure for the application of ISF establishment license, CRIEPI is steadily performing the key research studies, which includes degradation of cask component materials, leakage from the lid at accidents during the subsequent transportation after storage. The JNES showed supportive study on spent fuel

ACKNOWLEDGMENTS

These works have been carried out under the contract from NISA/METI.

REFERENCES

- [1] ATOMIC ENERGY COMMISSION, "Framework for Nuclear Energy Policy" (2005).
- [2] NUCLEAR AND INDUSTRIAL SAFETY AGENCY, "Technical Requirements on Interim Spent Fuel Storage Facility Using Dry Metal Cask", NISA-314c-06-02, (in Japanese) (2006).
- [3] NUCLEAR AND INDUSTRIAL SAFETY AGENCY, "Technical Requirements on Interim Spent Fuel Storage Facility Using Dry Concrete Cask" NISA-314c-06-01 (in Japanese), (2006).

- [4] TAKEDA, H., et. al., "Heat Removal Verification Tests Using Concrete Casks under Normal Condition", NED 238, pp.1196-1205 (2008).
- [5] WATARU, M., et. al., " Heat Removal Verification Tests of Full-Scale Concrete Casks under Accident Conditions ", NED 238, pp.1206-1212 (2008).
- [6] JAPAN SOCIETY OF MECHANICAL ENGINEERS, "Code for Construction of Spent Nuclear Fuel Storage Facilities –Rule on Concrete Casks, Canister Transfer Machines and Canister Transport Casks for Spent Nuclear Fuel –“, JSME S FB1-2003 (2003).
- [7] SHIRAI, K., et. al., "Demonstrative Drop Tests of Transport and Storage Full-Scale MPCs with High Corrosion-resistant material”, NED 238, pp.1241-1249 (2008).
- [8] SHIRAI, K., et al., Experimental Studies of Free-Standing Spent Fuel Storage Cask subjected to Strong Earthquake, Proc. of the 15th Int. Symposium on the Packaging and Transportation of Radioactive Materials, PATRAM 2007, Miami, Florida, USA (2007).
- [9] NUCLEAR SAFETY COMMISSION, "Regulatory Guide for Reviewing Seismic Design of Nuclear Power Reactor Facilities", (Sep. 2006).
- [10] MAYUZUMI, M., et. al., " Chloride Induced Stress Corrosion Cracking of Candidate Canister Materials for Dry Storage of Spent Fuel”, NED 238, pp.1241-1249 (2008).
- [11] TAKEDA, H., et.al., " Leakage Evaluation of Metal Cask during Drop Test ", Proc. of GLOBAL 2005, No.575, Tsukuba, Japan (2005).
- [12] ITOH, C., et al., Long Term Containment Performance Test for Spent Fuel Transport/Storage Casks, Trans. At. Energy Soc. Japan, Vol.2, No.2, pp.158-162 (in Japanese) (2003).
- [13] SHIRAI, K., et al., Safety Analysis of Dual Purpose Metal Cask Subjected to Impulsive Loads due to Aircraft Engine Crash, Proc. of ICONE16, Int. Conference on Nuclear Engineering, Orland, Florida, USA (2008).
- [14] ITOOKA, S., et al., "Supporting Study of Regulation for Interim Storage Facility for Spent Fuel in Japan".
Proc. ICONE 13-50617, Beijing, China, May 16-20, 2005.
- [15] ITO, K, KAMIMURA, K., TSUKUDA, Y., "Evaluation of Irradiation Effect on Spent Fuel Cladding Creep Properties", Proc. 2004 Int'l Mtg on LWR Fuel Performance, Orlando, Florida, Sept.19-22, 2004, Paper 1117.
- [16] AOMI, M., et al, "Evaluation of Hydride Reorientation Behavior and Mechanical Properties for High Burnup Fuel Cladding Tubes in Interim Dry Storage ", Journal of ASTM international (2008).